UNIVERSIDADE FEDERAL DO PARANÁ

JULIANE CARLOTTO

POLISSACARÍDEOS E METABÓLITOS SECUNDÁRIOS DOS IPÊS ROXO E AMARELO: CARACTERIZAÇÃO ESTRUTURAL E ATIVIDADES BIOLÓGICAS

CURITIBA
2019

JULIANE CARLOTTO

POLISSACARÍDEOS E METABÓLITOS SECUNDÁRIOS DOS IPÊS ROXO E AMARELO: CARACTERIZAÇÃO ESTRUTURAL E ATIVIDADES BIOLÓGICAS

Tese apresentada como requisito parcial à obtenção do grau de Doutora em Ciências – Bioquímica, no Curso de Pós-Graduação em Ciências – Bioquímica, Departamento de Bioquímica e Biologia Molecular, Setor de Ciências Biológicas, Universidade Federal do Paraná.

Orientador: Prof. Dr. Thales Ricardo Cipriani

Coorientador: Prof. Dr. Lauro Mera de Souza

CURITIBA

2019

Universidade Federal do Paraná. Sistema de Bibliotecas.
Biblioteca de Ciências Biológicas.
(Dulce Maria Bieniara – CRB/9-931)

Carlotto, Juliane
Polissacarídeos e metabólitos secundários dos ipês roxo e amarelo: caracterização estrutural e atividades biológicas. / Juliane Carlotto. – Curitiba, 2019.
131 p.: il.
Orientador: Thales Ricardo Cipriani
Coorientador: Lauro Mera de Souza

Tese (doutorado) - Universidade Federal do Paraná, Setor de Ciências Biológicas. Programa de Pós-Graduação em Ciências - Bioquímica.

1. Tabebuia 2. Polissacarídeos 3. Compostos orgânicos I. Título II. Cipriani, Thales Ricardo III. Souza, Lauro Mera de IV. Universidade Federal do Paraná. Setor de Ciências Biológicas. Programa de Pós-Graduação em Ciências - Bioquímica.

CDD (20. ed.) 582.16

MINISTÉRIO DA EDUCAÇÃO
SETOR DE CIENCIAS BIOLOGICAS
UNIVERSIDADE FEDERAL DO PARANÁ
PRÓ-REITORIA DE PESQUISA E PÓS-GRADUAÇÃO
PROGRAMA DE PÓS-GRADUAÇÃO CIÊNCIAS
(BIOQUÍMICA) - 40001016003P2

TERMO DE APROVAÇÃO

Os membros da Banca Examinadora designada pelo Colegiado do Programa de Pós-Graduação em CIÊNCIAS (BIOQUÍMICA) da Universidade Federal do Paraná foram convocados para realizar a arguição da tese de Doutorado de **JULIANE CARLOTTO** intitulada: **Polissacarídeos e metabólitos secundários dos ipês roxo e amarelo: caracterização estrutural e atividades biológicas**, sob orientação do Prof. Dr. THALES RICARDO CIPRIANI, que após terem inquirido a aluna e realizada a avaliação do trabalho, são de parecer pela sua APROVAÇÃO no rito de defesa.

A outorga do título de doutor está sujeita à homologação pelo colegiado, ao atendimento de todas as indicações e correções solicitadas pela banca e ao pleno atendimento das demandas regimentais do Programa de Pós-Graduação.

CURITIBA, 06 de Dezembro de 2019.

THALES RICARDO CIPRIANI
Presidente da Banca Examinadora (UNIVERSIDADE FEDERAL DO PARANÁ)

LUCIMARA MACH CORTES CORDEIRO
Avaliador Interno (UNIVERSIDADE FEDERAL DO PARANÁ)

FERNANDA FOGAGNOLI SIMAS
Avaliador Externo (UNIVERSIDADE FEDERAL DO PARANÁ)

CAROLINE MELLINGER SILVA
Avaliador Externo (EMPRESA BRASILEIRA DE PESQUISA AGROPECUÁRIA)

RESUMO

Handroanthus heptaphyllus e *Handroanthus albus*, conhecidos popularmente como “ipê roxo” e “ipê amarelo”, são duas espécies de árvores nativas do Brasil que têm sido utilizadas na medicina popular no combate ao câncer, diabetes, alergias, artrite, gastrite, feridas, inflamações em geral e outras enfermidades. Neste trabalho foram realizados processos de extração, purificação e caracterização estrutural de polissacarídeos de cascas (HHBSF e HABSF) e folhas (HHSF e HASP) de ambas as espécies, bem como avaliação das atividades gastroprotetora, anti-inflamatória e citotóxica das frações. Além disso, foi realizado o fracionamento de metabólitos secundários extraídos das cascas de *H. heptaphyllus* bioguiado por atividade citotóxica contra células tumorais, bem como a purificação do composto ativo. Análise de metilação e de RMN indicaram a presença de frações polissacarídicas complexas, constituídas majoritariamente por arabinogalactana do tipo II, arabinana e ramnogalacturonana do tipo I, além de glucomanana em HHBSF e HABSF. HHSF apresentou efeito anti-úlcera gástrica, enquanto HASP demonstrou ação anti-inflamatória e analgésica. HABSF e HHBSF foram testadas quanto ao efeito citotóxico nas linhagens Caco-2 (cólon) e MCF-7 (mama), mas apenas a primeira fração mostrou-se ativa. Em relação aos metabólitos secundários, extratos orgânicos promoveram efeito citotóxico dose-dependente em células Caco-2 e MCF-7, com baixa toxicidade para células normais (Vero). A fração clorofórmica HHE-C concentrou os compostos responsáveis pelo efeito citotóxico, e apresentou-se constituída principalmente por triterpenoides, ácidos graxos saturados de cadeia longa, ácido 4-metoxibenzoico, ácido 3,4-dimetoxibenzoico e lignanas. Os compostos da fração foram purificados por cromatografia semi-preparativa e identificou-se como composto ativo o ácido 4-metoxibenzoico. Portanto, este trabalho mostrou a caracterização estrutural de biomoléculas *H. heptaphyllus* e *H. albus* e a sua potencial aplicação farmacêutica, que pode ser melhor explorada em trabalhos futuros.

Palavras-chave: Handroanthus heptaphyllus. Handroanthus albus. Polissacarídeos. Ácido 4-metoxibenzoico. Atividade gastroprotetora. Atividade anti-inflamatória. Atividade citotóxica.

ABSTRACT

Handroanthus heptaphyllus and *Handroanthus albus*, popularly known as “ipê roxo” and “ipê amarelo”, are two native Brazilian tree species which has been traditionally used for the treatment of cancer, diabetes, allergies, arthritis, digestive disorders, inflammations, and other diseases. Thus, in the present investigation, we performed the extraction, purification and structural characterization of polysaccharides obtained from barks (HHBSF and HABSF) and leaves (HHSF and HASP) of both species, as well as evaluation of gastroprotective, anti-inflammatory and cytotoxic activity of these fractions. Furthermore, it was developed a bioguided fractionation from secondary metabolites of *H. heptaphyllus* barks based on the cytotoxic activity against tumor cells, along with the purification of the active compound. Methylation and NMR analysis indicated the presence of complex polysaccharide fractions, mainly constituted by type II arabinogalactan, arabinan and type I rhamnogalacturonan, as well as glucomannan in HHBSF and HABSF. HHSF showed a gastric anti-ulcer effect, whereas HASP anti-inflammatory and analgesic effects. HABSF and HHBSF were assayed for cytotoxic effect on Caco-2 (colon) and MCF-7 (breast) human tumor cells, but only the first fraction was active. Regarding the secondary metabolites, organic extracts promoted cytotoxic effect in a dose-dependent manner on Caco-2 and MCF-7 cells, with low toxicity on non-tumor cells (Vero). The chloroform fraction (HHE-C) concentrated the cytotoxic compounds, being composed by triterpenoids, long-chain saturated fatty acids, 4-methoxybenzoic acid, 3,4-dimethoxybenzoic acid, and lignans. The compounds of this fraction were purified by semi-preparative chromatography and the active compound was identified as being the 4-methoxybenzoic acid. Therefore, this work showed the structural characterization of *H. heptaphyllus* and *H. albus* biomolecules and their potential pharmaceutical application, which can be further better explored.

Keywords: *Handroanthus heptaphyllus*. *Handroanthus albus*. Polysaccharides. 4-Methoxybenzoic acid. Gastroprotective activity. Anti-inflammatory activity. Cytotoxic activity.

LISTA DE FIGURAS

SUMÁRIO

1 INTRODUÇÃO

O Brasil, país detentor de rica biodiversidade, possui de 15% a 20% do número total de espécies e a mais diversa flora do mundo, além de contar com alguns dos biomas mais ricos do planeta em número de espécies vegetais, como a Amazônia, a Mata Atlântica e o Cerrado (MMA, 2011). Apesar dessa riqueza e do potencial que ela representa, a biodiversidade brasileira é ainda pouco conhecida e sua utilização tem sido negligenciada. Portanto, é fundamental que o país intensifique investimentos e implemente programas de pesquisa na busca de um melhor aproveitamento sustentável desse imenso patrimônio natural.

Nesse contexto, o Ministério do Meio Ambiente lançou o livro “Espécies Nativas da Flora Brasileira de Valor Econômico Atual ou Potencial: Plantas para o Futuro - Região Sul”, que contempla uma lista com as espécies de plantas nativas de importância atual e potencial presentes na região Sul do Brasil. Dentre as espécies descritas encontra-se a *Handroanthus heptaphyllus*, árvore conhecida popularmente como “ipê roxo”, que desperta especial interesse, tendo em vista que sua casca possui uso medicinal em tratamento de doenças tumorais (MMA, 2011). Na região Sul do Brasil também pode-se encontrar com facilidade outra espécie de ipê, *Handroanthus albus*, conhecida popularemente como “ipê-amarelo” (Flora do Brasil 2020, 2019).

Os ipês pertencem ao gênero *Handroanthus* (família Bignoniaceae), que compreende cerca de 100 espécies e tem ampla distribuição, desde o México e Antilhas até o Norte da Argentina (MAEDA; MATTHES, 1984). A parte mais utilizada do ipê na medicina popular é a casca, embora folhas e flores também apresentem uso medicinal. As cascas são utilizadas no combate ao diabetes, leucemia, excesso de peso, tumores sólidos, alergias de todos os tipos, anemia, artrite, bronquite, cistite, colite, corrimento vaginal, doenças parasitárias em geral, gastrite, feridas, inflamações em geral, psoríase, etc. As partes desta planta são consumidas na forma de infuso, decocto ou extrato etanólico (CARVALHO, 1994).

Os estudos fitoquímicos realizados com madeira e cascas de *H. heptaphyllus* relataram o isolamento e a identificação dos seguintes metabólitos secundários: naftoquinonas, lignanas, triterpenos, esteroides, ácidos fenólicos, iridoides e aldeídos ciclopentenos (GARCEZ et al., 2007; SCHMEDA-HIRSCHMANNA; PAPASTERGIOU, 2003). Na literatura ainda não foram reportados estudos sobre a caracterização fitoquímica de *H. albus*.

As propriedades biológicas de ipês estão relacionadas principalmente à presença de naftoquinonas, dentre elas lapachol e lapachona, que apresentam potente atividade antiproliferativa (BALASSIANO et al., 2005; FIORITO et al., 2014; PINK; PLANCHON; et al., 2000; PINK; WUERZBERGER-DAVIS et al., 2000; PLANCHON et al., 2001; RAO; MCBRIDE; OLESON, 1968; SUNASSEE et al., 2013). Os metabólitos secundários sempre foram o foco principal das investigações realizadas no gênero *Handroanthus*, mas por meio de infusões e decocções também são extraídos produtos de metabolismo primário, incluindo os polissacarídeos. Não foram evidenciados na literatura estudos sobre a caracterização desta classe de compostos no gênero *Handroanthus.*

Os polissacarídeos formam uma importante classe de compostos naturais bioativos (SIMÕES et al., 2007). Dentre as diferentes atividades biológicas relacionadas aos polissacarídeos, destacam-se o seu efeito antitumoral (MENG et al., 2016; SU et al., 2016; TAMIELLO et al., 2018; WU et al., 2015; ZHU et al., 2016), anti-inflamatório (CARBONERO et al., 2008; CARLOTTO et al., 2016; LIU et al., 2015; MZOUGHI et al., 2018; OVODOVA et al., 2009; SMIDERLE et al., 2008) e antiúlcera gástrica (CIPRIANI et al., 2006, 2008; NASCIMENTO et al., 2013, 2017; SCOPARO et al., 2014; SIMAS-TOSIN et al., 2014).

Desta forma, considerando a importância de espécies de ipê como potencial fonte de novos princípios ativos de interesse medicinal, este trabalho tem por objetivo caracterizar estruturalmente e avaliar a atividade citotóxica, antiúlcera gástrica e anti-inflamatória de polissacarídeos de cascas e folhas de *H. heptaphyllus* e *H. albus*, bem como realizar um fracionamento bioguiado por atividade citotóxica dos metabólitos secundários extraídos das cascas de *H. heptaphyllus*.

2 REVISÃO BIBLIOGRÁFICA

2.1 DESCRIÇÃO BOTÂNICA

Handroanthus heptaphyllus (FIGURA 1) é uma árvore caducifólia, terrícola e hermafrodita (Laboratório de Manejo Florestal Unicentro, 2018). Ela pote atingir até 30 m de altura e o tronco 90 cm de diâmetro. Seus ramos dicotômicos, tortuosos e grossos formam uma copa moderadamente ampla e globosa. O tronco, mais ou menos reto e cilíndrico, possui casca pouco espessa, escura, de coloração pardo-

cinzenta, fissurada longitudinalmente e descorticante em placas grandes. Suas raízes são vigorosas e profundas (IPEF, 2018a).

FIGURA 1 – *Handroanthus heptaphyllus.*

FONTE: https://sites.unicentro.br/wp/manejoflorestal/10503-2/.

As folhas, de coloração verde-escura, são opostas, compostas, digitadas e com os bordos serrilhados. Cada folha é composta por 5 a 7 folíolos, glabros, com ápice agudo. A flor, roxo-violácea, é pouco pilosa. São muito abundantes, nascendo nos ramos ainda sem folhas, com lenho adulto. O cálice é pequeno, campanulado e a corola campanulada-afunilada (IPEF, 2018a). O fruto, seco e deiscente, é linear ou sinuoso, estriado, muito longo, podendo atingir até mais de 50 cm, de coloração preta. As sementes aparecem em grande quantidade e são grandes e aladas. Medem de 2.5 a 3 cm de comprimento e cerca de 6 a 7 mm de largura. São acastanhadas e membranáceas (LONGHI, 1995).

Esta espécie ocorre nas regiões Nordeste (Bahia, Ceará, Pernambuco), Centro-Oeste (Mato Grosso do Sul, Mato Grosso), Sudeste (Espírito Santo, Minas Gerais, Rio de Janeiro, São Paulo) e Sul (Paraná, Rio Grande do Sul, Santa Catarina), no Cerrado e Mata Atlântica. Trata-se de uma espécie nativa, porém não endêmica do Brasil (Flora do Brasil 2020, 2019).

Handroanthus albus (FIGURA 2) é uma árvore caducifólia, terrícola e hermafrodita, que possui cerca de 30 metros de altura. O tronco é reto ou levemente tortuoso, com fuste de 5 a 8 m de altura. A casca externa é grisáceo-grossa, possuindo fissuras longitudinais esparsas e profundas. A coloração desta é cinza-rosa intenso, com camadas fibrosas, muito resistentes e finas, porém bem distintas. Com ramos grossos, tortuosos e compridos, o ipê amarelo possui copa alongada e alargada na base. As raízes de sustentação e absorção são vigorosas e profundas (IPEF, 2018b).

As folhas, deciduais, são opostas, digitadas e compostas. A face superior destas folhas é verde-escura, e, a face inferior, acinzentada, sendo ambas as faces tomentosas. Os pecíolos das folhas medem de 2.5 a 10 cm de comprimento. Os folíolos, geralmente, apresentam-se em número de 5 a 7, possuindo de 7 a 18 cm de comprimento por 2 a 6 cm de largura. Quando jovem estes folíolos são densamente pilosos em ambas as faces. O ápice destes é pontiagudo, com base arredondada e margem serreada (IPEF, 2018b).

FIGURA 2– *Handroanthus albus.*

FONTE: http://www.ufrgs.br/fitoecologia/florars/index.php?pag=buscar_mini.php.

As flores, grandes e lanceoladas, são de coloração amarelo-ouro. Possuem em média 8 x 15 cm. Quanto aos frutos, estes possuem forma de cápsula bivalvar e são secos e deiscentes. Medem de 15 a 30 cm de comprimento por 1.5 a 2.5 cm de largura. Possuem grande quantidade de sementes. As sementes são membranáceas

brilhantes e esbranquiçadas, de coloração marrom. Possuem de 2 a 3 cm de comprimento por 7 a 9 mm de largura e são aladas (IPEF, 2018b).

Esta espécie ocorre nas regiões Sudeste (Minas Gerais, Rio de Janeiro, São Paulo) e Sul (Paraná, Rio Grande do Sul, Santa Catarina) do Brasil, na Mata Atlântica. Trata-se de espécie nativa, mas não endêmica do Brasil (Flora do Brasil 2020, 2019).

2.2 METABOLISMO VEGETAL

As moléculas produzidas pelos vegetais podem ser divididas em dois grandes grupos: metabólitos primários e secundários. Os primeiros são moléculas essenciais a todos os seres vivos. Nesse grupo estão incluídos os lipídeos, proteínas e carboidratos. Muitos produtos do metabolismo primário, por meio de rotas sintéticas diversas, podem originar o segundo grupo de compostos químicos – os metabólitos secundários – que geralmente apresentam estrutura complexa, baixa massa molar, marcante atividade biológica e, diferentemente daqueles do metabolismo primário, são encontrados em concentrações relativamente baixas e grande diversidade entre os diferentes grupos de plantas, além de serem necessários para a sobrevivência e preservação das plantas, atuando primeiramente na defesa vegetal, bem como nas interações planta/planta (alelopatia), nas quais um vegetal compete com outro, possivelmente para assegurar o fornecimento de água, luz e nutrientes (SIMÕES et al., 2007).

2.3 CARBOIDRATOS DE PLANTAS

Nas plantas, os carboidratos existem como monossacarídeos, oligossacarídeos, polissacarídeos e seus derivados, tais como glicosídeos cianogênicos e fenólicos, flavonóides glicosilados e glicoproteínas (AVIGAD, 1997).

Depois da água, os carboidratos estruturais são os principais constituintes químicos em tecidos de plantas e células vegetais, uma vez que formam a parede celular, a qual fornece o suporte estrutural para a célula vegetal (REID, 1997).

2.3.1 Parede celular

A parede celular é uma complexa estrutura macromolecular que envolve e protege a célula, e é essencial para a sobrevivência das plantas. A estrutura da parede celular é continuamente modificada para acomodar o estágio de desenvolvimento da planta e se adaptar às condições ambientais às quais ela está submetida (CAFFALL; MOHNEN, 2009).

Durante o crescimento inicial e expansão da célula são formadas a lamela média e a parede celular primária. Na fase de diferenciação celular, muitas células elaboram dentro da parede primária uma parede celular secundária, que é mais espessa e reforçada (BUCHANAN; GRUISSEM; JONES, 2000). A parede primária contribui para a integridade estrutural da célula, adesão celular e transdução de sinal, e é caracterizada por uma quantidade relativamente menor de celulose e maior de pectina comparada à parede secundária (CARPITA; GIBEAUT, 1993).

A parede celular vegetal apresenta uma composição altamente organizada de diferentes polissacarídeos, proteínas e compostos aromáticos. A composição molecular e o arranjo dos polímeros na parede diferem entre as espécies, entre tecidos de uma única espécie, entre células individuais e entre regiões da própria parede (BUCHANAN; GRUISSEM; JONES, 2000).

Estudo realizado por Carpita e Gibeaut (1993) descreve dois modelos distintos de parede celular primária para angiospermas. As dicotiledôneas e monocotiledôneas, com exceção das gramíneas, apresentam paredes ricas em pectina e hemicelulose, denominadas paredes tipo I. A parede primária das gramíneas, chamadas tipo II, contém pouca pectina e proporcionalmente mais hemicelulose. Na parede celular primária tipo I (FIGURA 3), microfibrilas de celulose estão entrelaçadas por xiloglucanas e esta estrutura está embutida numa matriz de polissacarídeos pécticos, homogalacturonanas e ramnogalacturonanas, sendo que estas últimas podem estar substituídas por pequenos grupos laterais de arabinana, galactana e arabinogalactana. Na parede tipo II, as microfibrilas de celulose são entrelaçadas por glucuronoarabinoxilanas e apenas uma pequena quantidade de pectina está presente.

FIGURA 3– MODELO DE PAREDE CELULAR PRIMÁRIA TIPO I

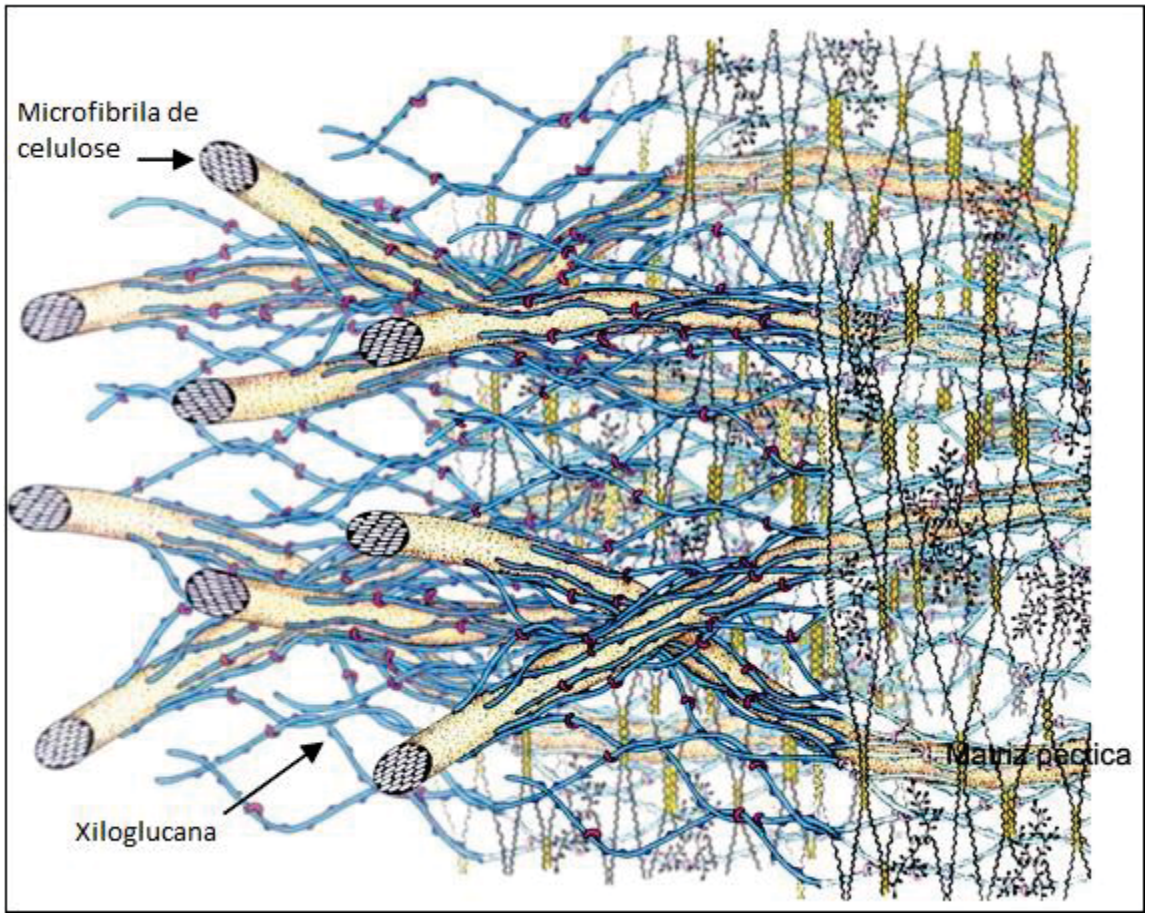

FONTE: Adaptado de CARPITA e GIBEAUT (1993).

2.3.2 Pectinas

As pectinas apresentam em sua composição grande quantidade de ácido galacturônico (GalA) com ligações glicosídicas do tipo α-(1→4) (MOHNEN, 2008). Os polissacarídeos pécticos compõem 35% da parede primária de dicotiledôneas e monocotiledôneas não-gramíneas, e de 2 a 10% de gramíneas e outras comelinóides (RIDLEY; NEILL; MOHNEN, 2001).

As principais classes estruturais dos polissacarídeos pécticos são: homogalacturonana (HG), xilogalacturonana (XGA), ramnogalacturonana tipo II (RGII), ramnogalacturonana tipo I (RGI), arabinana, galactana e arabinogalactanas (AGs) tipo I e II (BUCHANAN; GRUISSEM; JONES, 2000). As últimas três classes de polímeros descritas constituem as substâncias pécticas neutras.

Homogalacturonana é um polímero linear de unidades de α-D-Gal*p*A unidas por ligação (1→4), que compreende mais de 60% da quantidade de polissacarídeos

pécticos da parede celular vegetal. Resíduos de ácido galacturônico podem ser metil-esterificados na carboxila C-6, e podem ser *O*-acetilados nas posições O-2 ou O-3. O padrão de esterificação ou metilação varia para cada tipo vegetal. Xilogalacturonana é um polímero de (1→4)-α-D-Gal*p*A substituído na cadeia principal por resíduos de D-xilose na posição O-3 (RIDLEY; NEILL; MOHNEN, 2001).

RGII é o polissacarídeo péctico estruturalmente mais complexo. Sua estrutura altamente conservada consiste de uma cadeia principal de unidades de α-D-GalA unidos por ligação (1→4), com cadeias laterais constituídas de doze tipos diferentes de açúcar, ligados por vinte diferentes tipos de ligação. Entre os diversos tipos de açúcares, estão inclusos apiose, ácido acérico (3-*C*-carboxi-5-deoxi-L-xilose), 2-*O*-metil-fucose, 2-*O*-metil-xilose e outros (CAFFALL; MOHNEN, 2009).

RGI representa 20-35% dos polissacarídeos pécticos (MOHNEN, 2008). É um heteropolímero constituído por repetições do grupo dissacarídico [→4)-α-D-Gal*p*A-(1→2)-α-L-Rha*p*-(1→] (CARPITA; GIBEAUT, 1993). As RGI também podem ser constituídas por longos segmentos de [→4)-α-D-Gal*p*A-(1→], eventualmente interrompidos por unidades de [→2)-α-L-Rha*p*-(1→]. Elas podem ser ramificadas por arabinanas, galactanas ou arabinogalactanas, na posição *O*-4 de algumas unidades de ramnose (FIGURA 4) (BUCHANAN; GRUISSEM; JONES, 2000). Em geral, quase metade das unidades de ramnose apresenta cadeias laterais, mas isto pode variar de acordo com o tipo celular e o estado fisiológico. Além disso, unidades de ácido galacturônico podem ser acetiladas nas posições O-2 e/ou O-3 e podem ser metil-esterificados na carboxila C-6 (MOHNEN, 2008).

Arabinanas e galactanas puras estão presentes na parede celular de plantas em quantidade muito baixa. As arabinanas são polímeros de (1→5)-α-L-arabinose com algum grau de ramificação nas posições O-2, O-3 ou em ambas. Galactanas são polímeros lineares com ligações β-(1→4), que podem possuir um pequeno número de resíduos ligados na posição O-6 (REID, 1997).

As arabinogalactanas podem ser classificadas em dois tipos, de acordo com as diferenças nas ligações químicas envolvidas na formação da cadeia principal destas macromoléculas. O tipo I é caracterizado por uma cadeia principal de (1→4)-β-D-galactana. Enquanto que o tipo II é caracterizado por uma cadeia principal formada por (1→3) e (1→6)-β-D-galactana (ASPINALL, 1973).

FIGURA 4 – ESTRUTURA BÁSICA DE RAMNOGALACTURONANA TIPO I (RGI) COM CADEIAS LATERAIS DE (1→4)-β-D-GALACTANA, (1→5)-α-L-ARABINANA E ARABINOGALATANA TIPO I (AGI)

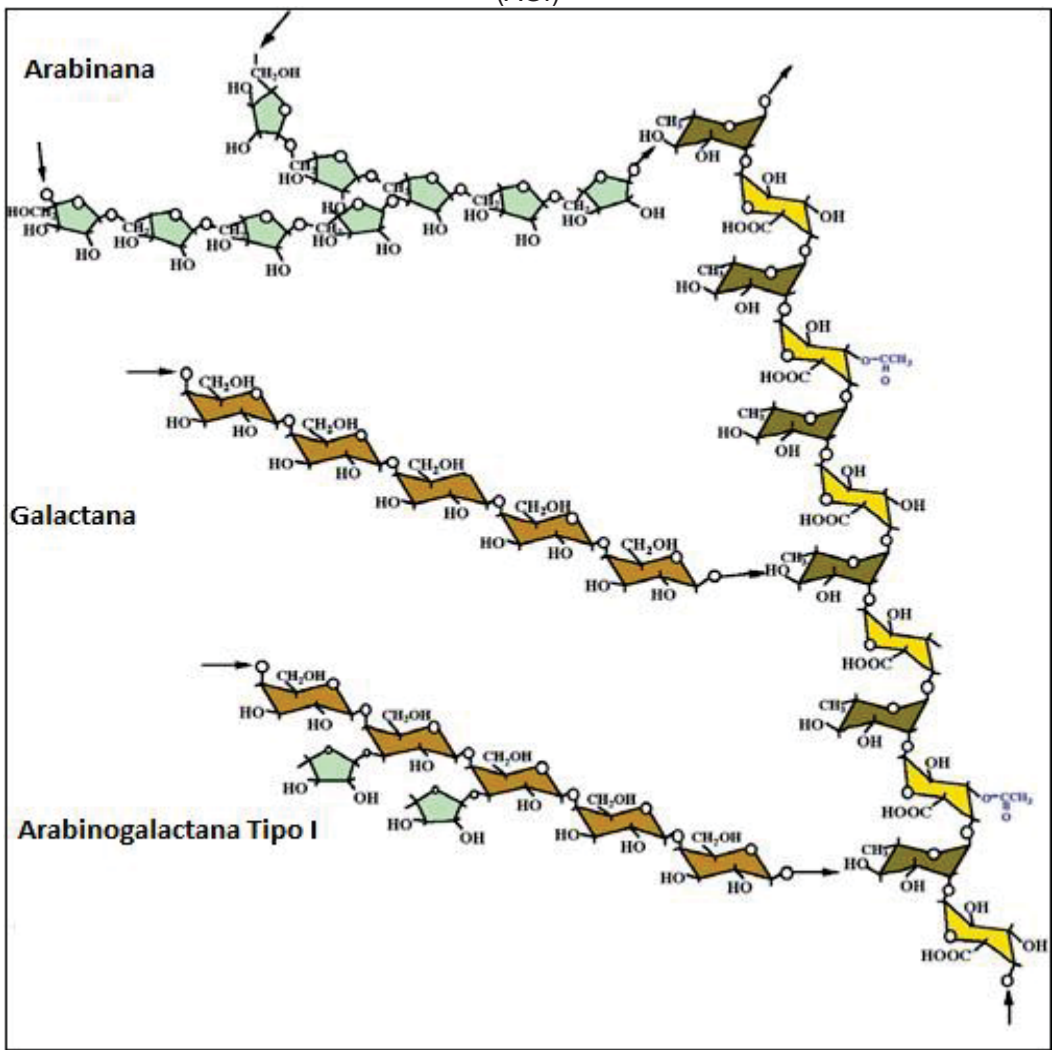

FONTE: Adaptado de BUCHANAN et al. (2000).

As arabinogalactanas tipo I são encontradas somente em frações pécticas, geralmente associadas às ramnogalacturonanas tipo I. Elas apresentam, na maioria das vezes, unidades de arabinose ligadas na posição O-3 dos resíduos de galactose (CARPITA; GIBEAUT, 1993)

As arabinogalactanas tipo II (FIGURA 5) estão presentes na parede celular vegetal, ramificando ou não as ramnogalacturonanas. Elas podem também estar ligadas a proteínas, constituindo uma classe de proteoglicanas denominadas arabinogalactanas-proteínas (AGPs) (BUCHANAN; GRUISSEM; JONES, 2000).

As arabinogalactanas tipo II apresentam uma estrutura fina que varia muito entre as espécies. Estes polissacarídeos apresentam a maior parte das unidades de galactose com as posições O-3 e O-6, que não estão envolvidas na ligação da cadeia

principal, substituídas com resíduos de arabinose. Também podem ser observadas substituições com monossacarídeos ácidos, como ácido glucurônico, ácido 4-*O*-metil-glucurônico e ácido galacturônico (CARPITA; GIBEAUT, 1993).

FIGURA 5– ESTRUTURA DAS ARABINOGALACTANAS TIPO II

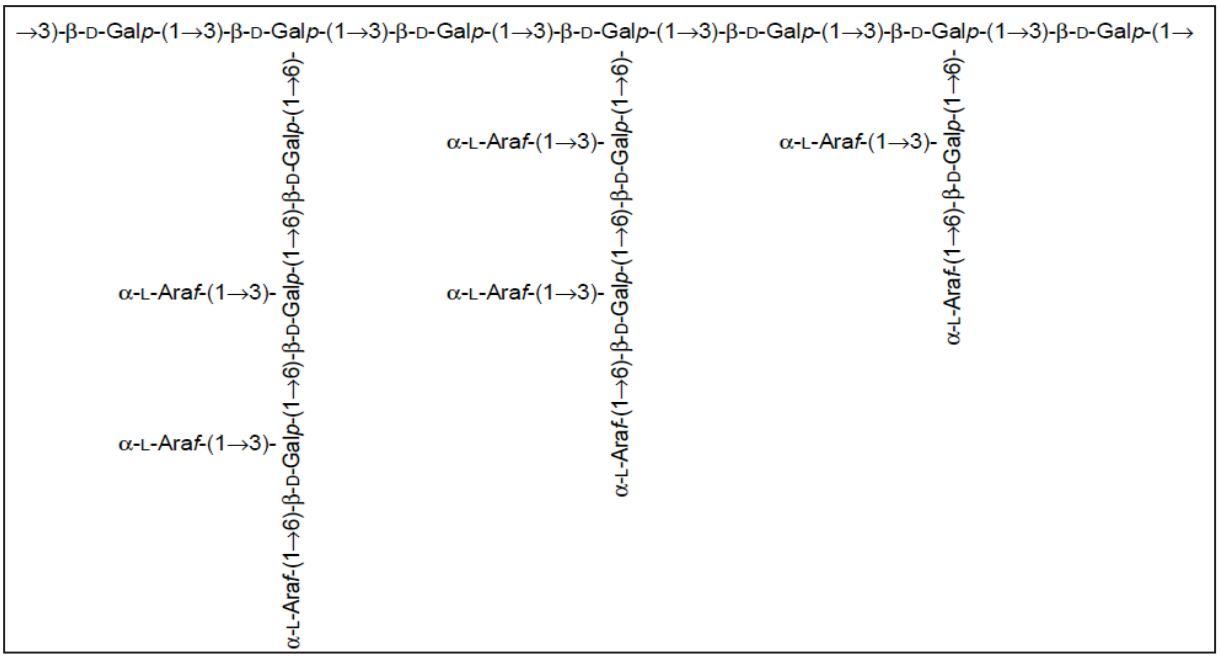

FONTE: CARPITA e GIBEAUT (1993).

2.3.3 Hemiceluloses

As hemiceluloses são polissacarídeos que ocorrem em íntima associação com a celulose, especialmente em tecidos lignificados (ASPINALL, 1973). As hemiceluloses são constituídas por unidades monossacarídicas de D-xilose, D-manose, D-galactose, D-glucose, L-arabinose, ácido 4-*O*-metilglucurônico, ácido D-galacturônico e ácido D-glucurônico, e eventualmente apresentam grupamentos *O*-acetil ligados às unidades pertencentes às cadeias principal e/ou lateral (FENGEL; WEGNER, 1989). Os principais tipos de hemiceluloses encontrados na parede celular vegetal são xilanas, mananas e xiloglucanas.

As xilanas contêm uma cadeia principal constituída por unidades de β-D-xilose (1→4)-ligadas e podem ser encontradas como arabinoxilanas (AX), glucuronoarabinoxilanas (GAX), glucuronoxilanas (GX) ou homoxilanas não substituídas. Xilanas podem ser acetiladas nas posições *O*-2 ou *O*-3 (CAFFALL; MOHNEN, 2009).

As mananas incluem as galactomananas (GMs) e as galactoglucomananas (GGMs), que são componentes estruturalmente importantes da parede celular, além de serem encontradas como polissacarídeos de reserva em alguns vegetais (CAFFALL; MOHNEN, 2009). Galactoglucomananas consistem de uma cadeia principal constituída de (1→4)-β-D-Glc*p* e (1→4)-β-D-Man*p*, e podem ser ramificadas na posição O-6 de Man*p* e/ou Glc*p* com β-D-Gal*p* (HARRIS, 2006) (FIGURA 6).

Xiloglucanas são constituídas por uma cadeia principal de unidades de β-D-glucose (1→4)-ligadas, com numerosos resíduos de α-D-xilose ligados na posição O-6 das unidades de glucose. Além disso, alguns destes resíduos de xilose podem ser substituídos com α-L-arabinose ou β-D-galactose, e algumas vezes a unidade de galactose pode estar substituída com α-L-fucose (CARPITA; GIBEAUT, 1993).

FIGURA 6 - ESTRUTURA DAS GALACTOGLUCOMANANAS

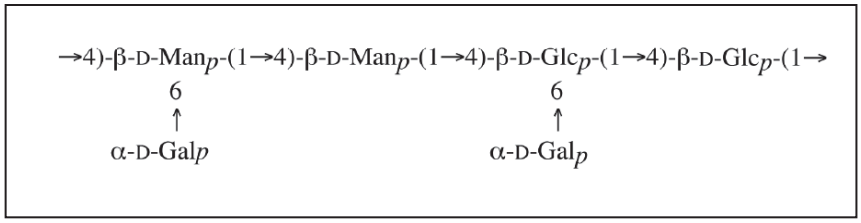

FONTE: HARRIS (2006).

2.4 METABÓLITOS SECUNDÁRIOS

Entende-se por metabolismo secundário de plantas o conjunto de processos metabólicos que originam compostos que não possuem uma distribuição universal nos vegetais (SIMÕES et al., 2007). Os metabólitos ainda não possuem suas funções fisiológicas completamente elucidadas, mas atualmente sabe-se que muitas dessas substâncias estão diretamente envolvidas nos mecanismos que permitem adequação da planta ao meio. De fato, já foram reconhecidas como funções de várias substâncias pertencentes a esta classe, por exemplo, a defesa contra herbívoros e microrganismos, a proteção contra raios UV, a atração de polinizadores ou animais dispersores de sementes, bem como sua participação em alelopatias (SIMÕES et al., 2007).

Cada família, gênero e espécie produz uma mistura característica de compostos químicos, que podem ser utilizados como caracteres taxonômicos na classificação das plantas (SIMÕES et al., 2007). Os metabólitos secundários podem

ser divididos em três grupos distintos quimicamente: terpenoides, compostos fenólicos e alcaloides (VIZZOTTO; KROLOW; WEBER, 2010).

Terpenoides são a classe estruturalmente mais variada de produtos vegetais naturais. Isopentenilpirofosfato, ou isopreno ativo, é a unidade básica de formação dos terpenos. A polimerização do isopentenilpirofosfato origina moléculas de cadeias carbonadas crescentes de cinco em cinco átomos de carbono. A molécula de isopentenil-pirofosfato ($C_5H_{12}P_2$) e seu isômero dimetilalil-pirofosfato formam trans-geranil-pirofosfato, a partir do qual formam-se os demais terpenos. Monoterpenos (C10) lactônicos são chamados de iridoides. Novas ligações cabeça-cauda entre trans-geranil-pirofosfato e isopentenil-pirofosfato resultam em sesqui (C15) e diterpenos (C20). Já a ligação cabeça-cabeça entre moléculas de farnesil-pirofosfato (C15) dará origem ao esqualeno, o precursor da maioria dos triterpenos e esteroides. Os triterpenos (C30) originam-se da ciclização do esqualeno, enquanto esteroides (C27) podem ser considerados metabólitos dos triterpenos, uma vez que se originam do cicloartenol, com a perda de três grupos metila (SIMÕES et al., 2007). As saponinas são outro importante grupo de terpenóides encontrados nas plantas. Elas são constituídas de um núcleo triterpenoidal pentacíclico, ao qual encontram-se ligados mono- e/ou oligossacarídeos, e desempenham um importante papel na defesa das plantas contra insetos e microrganismos (VIZZOTTO; KROLOW; WEBER, 2010).

Alcaloides são compostos nitrogenados farmacologicamente ativos encontrados predominantemente nas angiospermas. Uma definição para essa classe de substâncias apresenta certa dificuldades devido à ausência de uma separação precisa entre alcaloides propriamente ditos e aminas complexas de origem natural. Segundo Pelletier (1988 citado por SIMÕES et al*.,* 2007) alcaloide é uma substância orgânica de origem natural, cíclica contendo nitrogênio em um estado de oxidação negativo e cuja distribuição é limitada a organsimos vivos.

Compostos fenólicos pertencem a uma classe de moléculas que inclui uma grande diversidade de estruturas, simples e complexas, que possuem pelo menos um anel aromático no qual ao menos um hidrogênio é substituído por um grupamento hidroxila (SIMÕES et al., 2007). Em geral os compostos fenólicos costumam ser classificados nas seguintes categorias: 1) fenóis, ácidos fenólicos e ácidos fenilacéticos; 2) ácidos cinâmicos, cumarinas, isocumarinas e cromonas; 3) lignanas; 4) flavonóides; 5) ligninas; 6) taninos; 7) benzofenonas, xantonas e estilbenos; 8) quinonas; e 9) betacianinas (SIMÕES et al., 2007).

Os ácidos fenólicos caracterizam-se por terem um anel benzênico, um grupamento carboxílico e um ou mais grupamentos hidroxila e/ou metoxila na molécula. Eles podem ser divididos em duas classes: ácidos hidroxibenzoicos e hidroxicinâmicos. Os primeiros são componentes das complexas estruturas dos taninos hidrolisáveis e são menos abundantes nos vegetais consumidos pelos humanos (BRAVO, 1998). Os ácidos hidroxicinâmicos são mais abundantes na natureza, sendo que alguns exemplos desta classe de compostos são: ácido caféico, *p*-cumárico, ferúlico e sinápico. Na maioria das vezes estes ácidos hidroxicinâmicos encontram-se esterificados ao ácido quínico, ácido tartárico ou carboidratos e derivados (BASTOS et al., 2007).

Lignanas são dímeros formados através do acoplamento oxidativo de álcoois cinamílicos entre si ou destes com ácido cinâmico (SIMÕES et al., 2007). Elas estão presentes na natureza preferencialmente na forma livre em relação à forma de derivados glicosilados (D'ARCHIVIO et al., 2007).

Quinonas podem ser considerados como produtos de oxidação de fenóis, e sua principal característica é a presença de dois grupos carbonílicos formando um sitema conjugado. Em função do tipo de ciclo no qual o sistema de ligações duplas e cetonas conjugadas está inserido, têm-se os três principais grupos de quinona: benzo-, nafto- e antraquinona. As *o*- e *p*-quinonas são 1,2 e 1,4 dicetonas cíclicas conjugadas, respectivamente (SIMÕES et al., 2007).

2.4.1 Consituintes fitoquímicos de *Handroanthus heptaphyllus* e *Handroanthus albus*

Não foram encontrados na literatura estudos sobre a caracterização estrutural de carboidratos no gênero *Handroanthus.* Em relação aos metabólitos secundários, apenas foram evidenciados trabalhos envolvendo a espécie *H. heptaphyllus*. Garcez et al. (2007) avaliaram os compostos presentes no extrato etanólico de cascas do caule, enquanto Schmeda-Hirschmanna e Papastergiou (2003) utilizaram o extrato de madeira obtido com o solvente acetato de etila. Os estudos fitoquímicos relataram a identificação das seguintes classes de metabólitos secundários: quinonas, lignanas, triterpenos, esteroides, ácidos fenólicos, iridoides e o derivado fenilpropanoide acteosídeo (GARCEZ et al., 2007; SCHMEDA-HIRSCHMANNA; PAPASTERGIOU, 2003).

Em *H. heptaphyllus* foram identificadas principalmente *p*-naftoquinonas, apresentando anel furano (desidro-iso-α-lapachona, avicequinona A e estenocarpona B) e pirano (α-lapachona, rhinacantina A, desidro-α-lapachona, estenocarpoquinona A e β-lapachona) em sua estrutura, bem como lapachol, uma naftoquinona de esqueleto simples (FIGURA 7).

FIGURA 7 - NAFTOQUINONAS IDENTIFICADAS EM *H. heptaphyllus*.

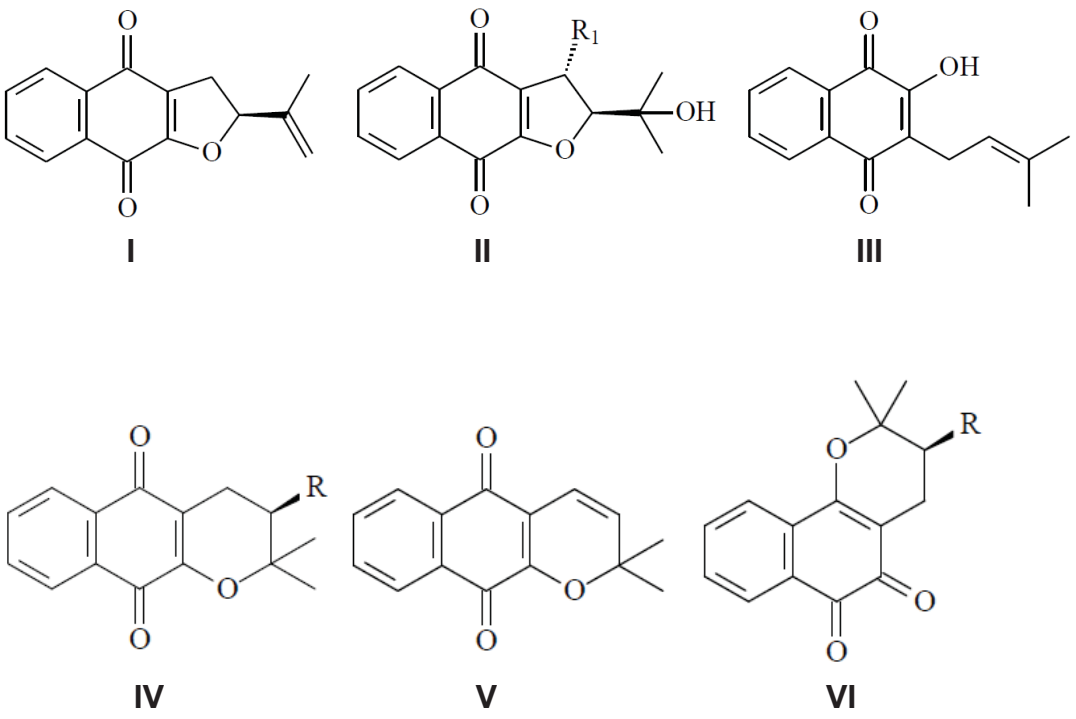

I = desidro-iso-α-lapachona
II – R1 = OH = avicequinona A
II – R1 = H = estenocarpona B
III = lapachol
IV – R = H = α-lapachona
IV – R = OH = rinacantina A
V = desidro-α-lapachona
VI – R = OH = estenocarpoquinona A
VI – R1 = H = β-lapachona

FONTE: Adaptado de MELO (2016).

As lignanas encontradas em *H. heptaphyllus* foram o secoisolariciresinol e o cicloolivil (FIGURA 8).

FIGURA 8 - LIGNANAS IDENTIFICADAS EM *H. heptaphyllus*.

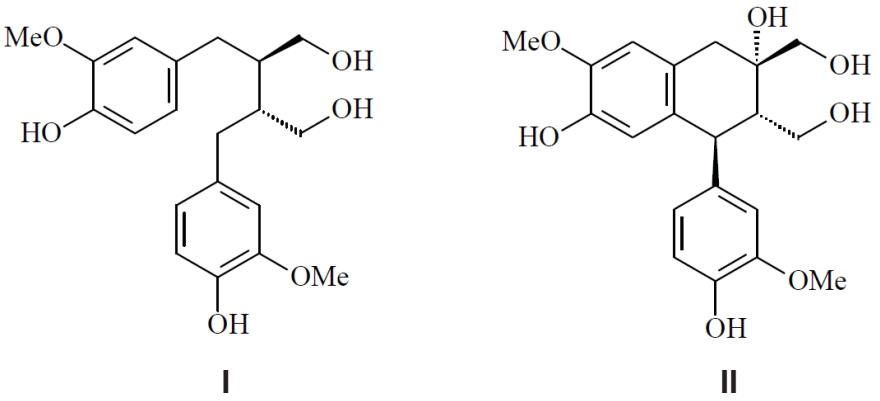

I = secoisolariciresinol

II – cicloolivil

FONTE: Adaptado de MELO (2016).

Os ácidos fenólicos identificados em *H. heptaphyllus* encontram-se descritos na FIGURA 9.

FIGURA 9 - ÁCIDOS FENÓLICOS IDENTIFICADOS EM *H. heptaphyllus*

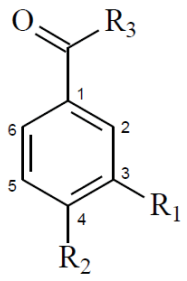

R1= H, R2 = OH, R3 = OH – ácido-4-hidroxi-benzoico

R1= H, R2 = OMe, R3 = OH - ácido-4-metoxi-benzoico

R1= OMe, R2 = OMe, R3 = OH - ácido-3,4-dimetoxi-benzoico

FONTE: Adaptado de MELO (2016).

Os iridoides e esteroides identificados em *H. heptahpyllus* estão descritos nas FIGURAS 10 e 11, respectivamente, enquanto que o triterpeno identificado nesta espécie foi o 3β,6β,21β-trihidroxiolean-12-eno.

FIGURA 10 - IRIDOIDES IDENTIFICADOS EM *H. heptaphyllus*.

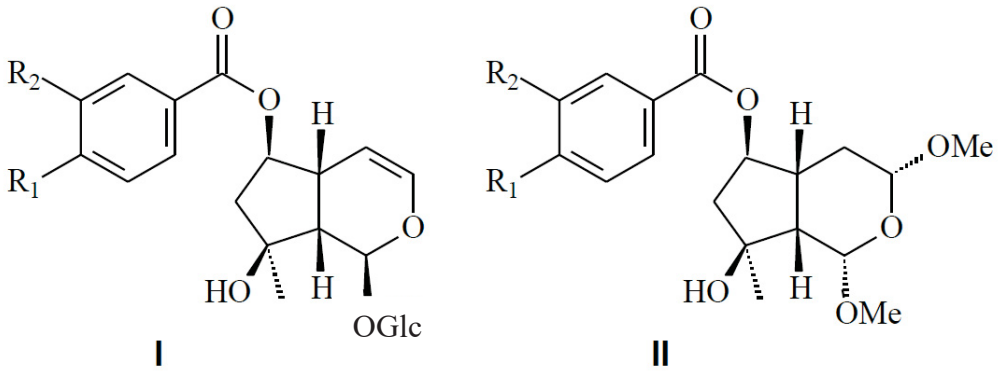

I = R1=OH e R2 = H = 6-O-(p-hidroxibenzoil-ajugol)

I = R1=OMe e R2 = H = 6-O-(p-metoxibenzoil-ajugol)

I = R1=OMe e R2 = OMe = 6-O-(3”-4”-dimetoxibenzoil)-ajugol

II = R1=OH e R2 = 8α-metil-8β-hidroxi-6β-(4’-hidroxi)-benzoiloxi-1α,3α-dimetoxi-octaidro-ciclopentan[c]-pirano

II= R1=OMe e R2 = OMe = 8α-metil-8β-hidroxi-6β-(3’,4’-dimetoxi)-benzoiloxi-1α,3α-dimetoxi-octaidro-ciclopentan[c]-pirano

FONTE: Adaptado de MELO (2016).

FIGURA 11 - ESTEROIDES IDENTIFICADOS EM *H. heptaphyllus*.

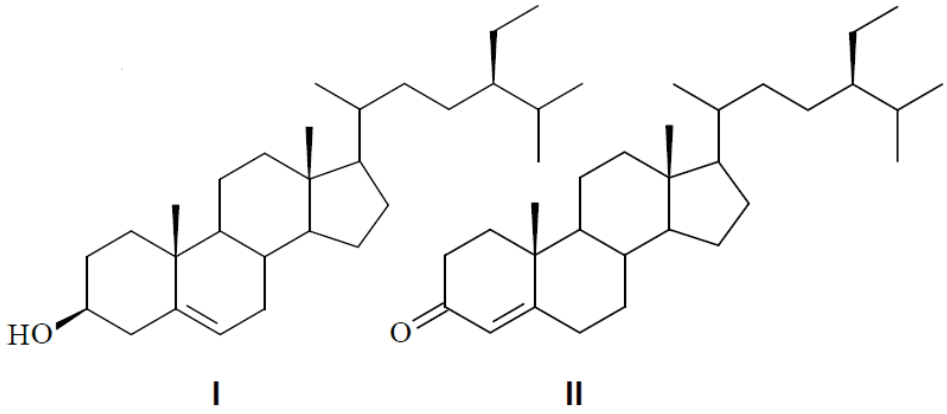

I = β-sitosterol

II = sitostenona

FONTE: Adaptado de MELO (2016).

2.5 USOS POPULARES

O ipê-roxo é muito usado na medicina popular. Da casca faz-se um chá que é usado no tratamento de gripes e depurativo do sangue. As folhas são utilizadas contra úlceras sifilíticas e blenorrágicas (MMA, 2011). A espécie também tem propriedades anticancerígenas, antirreumáticas e antianêmicas (CARVALHO, 2003).

A casca do ipê-amarelo possui propriedades terapêuticas como adstringente, usada no tratamento de garganta e estomatites. É também usada como diurético (IPEF, 2018b).

2.6 ATIVIDADES BIOLÓGICAS PROMOVIDAS POR POLISSACARÍDEOS

Os polissacarídeos isolados de fontes naturais (plantas, animais, fungos, algas) têm atraído grande interesse devido à sua variedade de atividades farmacológicas, tais como antitumoral, imunomoduladora, antioxidante, anti-inflamatória e antiúlcera gástrica (YU et al., 2018).

2.6.1 Atividade anti-inflamatória e analgésica promovida por polissacarídeos

Atividade anti-inflamatória promovida por polissacarídeos isolados de várias espécies de fungos, algas e vegetais tem sido descrita na literatura. Estudo realizado por Smiderle et al. (2008) mostrou que um polímero de (1→3), (1→6)-β-D-glucopiranose extraído com água quente do basidiomiceto *Pleurotus pulmonarius* demonstrou atividade anti-inflamatória quando administrado sistemicamente em camundongos, promovendo uma diminuição da infiltração leucocitária e redução da permeabilidade capilar peritoneal induzidas por ácido acético. Além disso, os animais previamente tratados com esta glucana mostraram uma redução de 85% nas contorções abdominais induzidas por ácido acético. Ainda, a fração inibiu significativamente o tempo de lambidas da pata nas fases inicial (dor neurogênica) e tardia (dor inflamatória) do teste da formalina. A atividade analgésica e anti-inflamatória observadas foram relacionadas à inibição de citocinas pró-inflamatórias.

Um polissacarídeo péctico com efeito anti-inflamatório no modelo de choque endotóxico foi isolado de talos de aipo (*Apium graveolens* var. Dulce). Este polímero consiste de um cadeia principal de (1→4)-α-D-galacturonana itercaladas por unidades

de [→2)-α-L-Rhap-(1→], com cadeias laterais de Ara e Gal ligadas na posição 4 dos resíduos de Rha. No modelo testado, este polissacarídeo foi responsável pelo aumento da sobrevivência de camundongos submetidos a uma dose letal de LPS (lipopolissacarídeos), sendo este efeito mediado pela diminuição na produção de interleucina-1β (IL-1β) (pró-inflamatória) e aumento de interleucina-10 (IL-10) (anti-inflamatória), e pela diminuição da migração de neutrófilos para a cavidade peritoneal após injeção de LPS (OVODOVA et al., 2009).

Ananthi et al. (2010) isolaram da alga *Turbinaria ornata* um polissacarídeo ácido que demonstrou atividade anti-inflamatória nos modelos de edema de pata induzido por carragenina em ratos e de permeabilidade vascular em camundongos. No primeiro modelo, a fração polissacarídica promoveu 60.09% de diminuição do edema após 5 h da injeção de carragenina, enquanto que, no segundo modelo, diminuiu em 65.75% a permeabilidade vascular após administração peritoneal de ácido acético.

Mzoughi et al. (2018) também demonstraram que o pré-tratamento com polissacarídeos pécticos de folhas de *Suaeda fruticosa* promoveu diminuição de 52.29% no edema de pata, 5 horas após injeção de carragenina. Estes polissacarídeos também foram submetidos à avaliação da atividade analgésica, reduzindo o número de contorçõeas abdominais induzidas por ácido acético em 63.69% e 76.59% nas doses de 50 mg/kg e 100 mg/kg, respectivamente. Sugere-se que a ação antinociceptiva pode estar relacionada à inibição de liberação de bradicinina, histamina, prostaglandinas, citocinas (fator de necrose tumoral alfa, IL-1β and interleucina-8) e substância P. Ainda, no ensaio de placa quente, a fração de polissacarídeos pécticos agiu como analgésico central e periférico, fato possivelmente correlacionado à sua capacidade de eliminação de radicais livres, uma vez que o acúmulo destes aumenta o conteúdo de Ca^{2+} nas células que desempenham um papel fundamental no processo de indução da dor.

O modelo de edema de pata induzida por carragenina também foi utilizado por Carlotto et al. (2016) para demonstrar atividade anti-edematogênica, dose-dependente e por um período de até 48 h, de polissacarídeos do extrato bruto de folhas de *Artium lappa*. Nesse mesmo estudo, a fração purificada da planta, constituída principalmente por uma ramnogalacturonana do tipo I com cadeias de arabinogalactana do tipo II, mostrou 57% de inibição 4 horas após a injeção de carragenina.

Liu e Lin (2012) avaliaram polissacarídeos isolados do suco de morango e da amora que apresentaram forte potencial anti-inflamatório via modulação do perfil de secreção de citocinas pró-/anti-inflamatórias secretadas por culturas de macrófagos estimuladas por LPS. O tratamento com os polímeros isolados diminuiu os níveis das citocinas pró-inflamatórias, incluindo IL-1β e interleucina-6 (IL-6), enquanto que aumentou o nível da citocina anti-inflamatória IL-10.

O pré- e pós-tratamento com polissacarídeos de *Ganoderma lucidum* atenuou o aumento de TNF-α (fator de necrose tumoral alfa) e IL-1β em hepatócitos primários extraídos de carpa comum (*Cyprinus carpio* L.) expostos ao agente hepatotóxico tetracloreto de carbono. O mecanismo proposto foi a redução da ativação do fator nuclear NF-κB, fator de transcrição que regula a expressão de múltiplos genes associados à resposta inflamatória e infecção (LIU, J.; WILLFÖR; XU, 2015).

2.6.2 Atividade antiúlcera gástrica

Estudo realizado por Nergard et al. (2005) mostrou que o extrato aquoso bruto das raízes de *Cochlospermum tinctorium* (composto de 59,3% de polissacarídeos e 9,3% de polifenóis) reduziu de maneira dose-dependente a formação de úlcera gástrica induzida por etanol/HCl em camundongos.

Polissacarídeos pécticos ligados a compostos fenólicos, extraídos das raízes de *Decalepis hamiltonii,* exibiram um efeito protetor contra úlceras induzidas por estresse em modelos animais. Além disso, eventos correlacionados com úlceras gástricas instaladas, como quantidade diminuída de muco gástrico e de enzimas antioxidantes, e aumento da atividade da bomba H^+/K^+ ATPase, foram suprimidos após a utilização do extrato, com retorno ao estado de homeostasia (SRIKANTA; SIDDARAJU; DHARMESH, 2007).

Estudos envolvendo polissacarídeos purificados também foram realizados para avaliação da atividade antiúlcera gástrica. Cipriani et al. (2006) demonstraram atividade antiúlcera de uma arabinogalactana tipo II, purificada a partir do chá das folhas de *Maytenus ilicifolia*, em estudo envolvendo lesão gástrica aguda induzida por etanol em ratos. Ainda, por meio do mesmo modelo de indução de úlcera, foi demonstrada a atividade antiúlcera de duas heteroxilanas ácidas, isoladas de *Maytenus ilicifolia* e *Phyllantus niruri* (CIPRIANI et al., 2008), de duas

arabinogalactanas tipo I, purificadas do farelo de soja (CIPRIANI et al., 2009) e da goma viscosa exsudada pelo cacto *Cereus peruvianus* (TANAKA et al., 2010).

Além disso, por meio do mesmo modelo de lesão gástrica aguda induzida por etanol, evidenciou-se gastroproteção promovida por: arabinanas isoladas das sementes de quinoa (*Chenopodium quinoa*) (CORDEIRO et al., 2012), arabinoxilana extraída do bagaço de cana de açúcar (MELLINGER-SILVA et al., 2011), ramnogalacturonona tipo I isolada das folhas de *Acmella oleracea* (NASCIMENTO et al., 2013), glucuronoarabinoxilana extraída de goma exsudadada de *Cocos nucifera* (SIMAS-TOSIN et al., 2014) e arabinogalactana do tipo II ligada a proteína, extraída com solução alcalina de folhas de chá verde e preto (*Camellia sinensis*) (SCOPARO et al., 2016).

Nascimento et al. (2017) evidenciaram que uma fração polissacarídica complexa contendo RGI, AGI, AGII, manana, amido e ramnana promoveu 80% de redução da lesão gástrica induzida por etanol, quando a fração polissacarídica foi administrada pela via oral, e 70% de redução, quando administrada pela via intraperitoneal. Isso indica que o efeito observado foi independente da formação de barreira citoprotetora, na qual apenas a administração oral promoveria gastroproteção. Ainda, a administração da fração polissacarídica, por ambas as vias, promoveu a inibição da depleção dos níveis de muco e GSH (glutationa reduzida) após lesão induzida por etanol, indicando que o mecanismo antiúlcera pode estar relacionado com a manutenção de mecanismos de defesa da mucosa.

2.6.3 Atividade antitumoral

Em países asiáticos os polissacarídeos extraídos de cogumelos, pertencentes principalmente à classe dos basidiomicetos, apresentam importante papel como alimento e agente medicinal no tratamento do câncer. Os principais tipos de polissacarídeos envolvidos nesta atividade são as β-glucanas e hetero-β-glucanas, extraídas de diferentes cogumelos, tais como *Agaricus blazei, Antrodia camphorate, Flammulina velutipes, Ganoderma lucidum*, *Lentinus edodes, Pleurotus ostreatus,* entre outros. O mecanismo antitumoral é mediado principalmente por meio de células T ativadas ou outras células do sistema imune (MENG; LIANG; LUO, 2016).

Ganoderma lucidum é um fungo bem conhecido pela sua atividade antitumoral, que inclui indução de parada no ciclo celular, indução de apoptose,

inibição da motilidade, da angiogênese e da mutagênese. Polissacarídeos de *G. lucidum* (1→3)-, (1→4)- and (1→6)-β-D-glucana) possuem efeitos preventivos contra o desenvolvimento de adenoma do cólon, adenocarcinoma de cólon e adenocarcinoma pulmonar em ratos (MENG; LIANG; LUO, 2016). Já do cogumelo *Lentinus edodes* foi extraído um polissacarídeo com cadeia principal de (1→3)-β-D-glucana com ação antitumoral, chamado lentinana, que é um ativador típico de células T, que melhora a atividade de macrófagos e células *natural killer* (ZHANG et al., 2011). Grifolana (polímero de (1→6)-β-D-glucana ramificado com (1→4)–β-D-glucana e polímero de (1→3)–β-D-glucana ramificado com β-D-(1→6)-glucana), que é extraído de *Grifola frondosa*, exibe atividade antitumoral em cânceres gastrointestinal, de pulmão, fígado e mama. Esse polissacarídeo é um ativador de macrófagos que aumenta a produção de citocinas sem dependência de endotoxinas. Além disso, grifolana aumentou a expressão de IL-6, IL-1 eTNF-α de macrófagos (MENG; LIANG; LUO, 2016).

Polissacarídeos com efeito antitumoral extraídos de plantas também estão descritos na literatura. Polissacarídeos do extrato alcalino das folhas de *Taxus chinensis* var. mairei, com uma cadeia principal de α-(1→3)-Ara*f*, α-(1→5)-Ara*f* and α-(1→4)-Gal*p*, bem como uma arabinogalactana do tipo II de ramos de *Morus alba* demonstraram efeito antitumoral contra células SGC-7901 (células de câncer gástrico humano) (WU et al., 2015)

Ke et al. (2011) relataram que os polissacarídeos de goji berry (*Lycium barbarum)* inibiram o crescimento e induziram apotose da linhagem celular BIU87 (carcinoma da bexiga humano). Gan et al. (2004) verificaram que uma fração polissacarídeo/proteína de goji berry inibiu significativamente o crescimento do sarcoma transplantável S180 em camundongos e aumentou a proliferação de linfócitos no baço, o nível de anticorpos produzidos por estes linfócitos, a fagocitose pelos macrófagos, a atividade do linfócito T citotóxico, o nível de expressão de mRNA de IL-2 e, ainda, reduziu a peroxidação lipídica das células do sistema imune, indicando um significativo efeito imunoestimulatório e diminuição da massa tumoral.

Ainda, extrato de jambo (*Syzygium jambos*) contendo polissacarídeos solúveis em água (HG, AG II e RG I) reduziram expressivamente o crescimento tumoral em camundongos com tumor de Erlich (TAMIELLO et al., 2018). E o polissacarídeo obtido das raízes de *Astragalus*, constituído de (1→4)-α-D-glucana substituída em O-6 por cadeia lateral de (1→6)-α-D-glucana, aumentou o número de

linfócitos no baço de ratos com câncer gástrico, além de aumentar o nível de IL-2 e a atividade de células natural killer, além de aumentar os níveis de IgA, IgG e IgM no sangue (LI et al., 2009).

2.7 ATIVIDADE ANTITUMORAL PROMOVIDA POR METABÓLITOS SECUNDÁRIOS DE IPÊS

Metabólitos secundários, principalmente aqueles descritos em cascas de *Handroanthus avellanedae,* outra espécie de ipê conhecida popularmente como ipê roxo, apresentaram efeito antitumoral em diversas linhagens celulares, principalmente devido à presença de naftoquinonas, dentre elas lapachol e lapachona, moléculas com potente atividade antiproliferativa (RAO; MCBRIDE; OLESON, 1968; SANTANA et al., 1980). Estes compostos apresentaram atividade citotóxica *in vitro* contra muitas linhagens celulares tumorais, incluindo de próstata, mama, fígado, cólon, epidermoide de boca, cérvix e pulmão, muitas delas multi-resistentes à quimioterapia (BALASSIANO et al., 2005; FIORITO et al., 2014; PINK; PLANCHON; et al., 2000; PINK; WUERZBERGER-DAVIS; et al., 2000; PLANCHON et al., 2001; WOO et al., 2006).

Zhang et al. (2015) demonstraram que uma série de furanonaftoquinonas purificadas do extrato aquoso da casca de *H. avellanedae* produziram citotoxicidade em células A549 (câncer de pulmão de não pequenas células), SiHa (linhagem tumoral de colo uterino) e MCF-7 (câncer de mama) em concentrações micromolares. Os resultados mostraram que os compostos induziram a parada do ciclo celular na fase G2/M, bem como indução da apoptose em células A549. Investigação da família da proteína ciclina por *Western blotting* mostrou que os níveis de proteína ciclina A e ciclina B foram fortemente diminuídos com o aumento do tempo de incubação com os compostos, possivelmente o principal fator que causou a parada de fase G2/M. Ainda, após a exposição das células A549 aos compostos, o nível de expressão de mRNA do supressor tumoral P53 e da proteína apoptótica BAX foi regulado positivamente. A atividade enzimática da caspase-3 também foi maior nas células A549 expostas aos compostos.

YAMASHITA et al. (2007, 2009) demonstraram atividade antitumoral estereoseletiva de naftoquinonas obtidas do extrato etanólico das cascas de *H. avellanedae* em várias linhagens celulares tumorais humanas, incluindo PC-3

(próstata), A549 (pulmão) e MCF-7 (mama), bem como atividade quimiopreventiva por inibição potente na ativação do vírus Epstein-Barr induzida por tetradecanoilforbolacetato em células Raji. Este último modelo já foi utilizado anteriormente para demonstrar atividade quimiopreventiva do extrato metanólico de *H.avellanadae,* que além disso mostrou inibição da carcinogênese induzida por 7,12,-dimetilbenz[a]antraceno em camundongos no mesmo estudo (UEDA et al., 1994).

Os metabólitos secundários lapachol, α- e β-lapachona e uma série de 25 1,4-naftoquinonas foram testados na linhagem celular de câncer esofágico (WHCO1). A maioria dos compostos exibiu citotoxicidade aumentada (IC_{50} de 1,6 a 11,7 mM) quando comparados com a droga de escolha cisplatina (IC_{50} = 16,5 mM) (SUNASSEE et al., 2013).

Sichaem et al. (2012) avaliaram 13 compostos purificados de raízes de *H. rosea* em células KB (carcinoma epidermoide de boca humano) e HeLa (carcinoma cervical humano), sendo que os mais potentes foram um ciclopenteno dialdeído, três furanonaftoquinonas, lapachol e ácido 4-metoxibenzoico.

Balassiano et al. (2005) estudaram o lapachol na redução de metástases. Células HeLa (carcinoma cervical humano) foram expostas a diferentes concentrações de lapachol, e as alterações resultantes no perfil proteico, na morfologia e na propriedade de invasividade foram estudadas. Na dose de 400 µg/mL, a viabilidade celular permaneceu inalterada, mas o lapachol induziu alterações no perfil proteico e inibiu a invasividade das células HeLa, apresentando assim grande potencial de aplicação no combate à metástase.

Além disso, β-lapachona, na forma da pró-farmaco mais solúvel em água denominado de ARQ-761, está sendo, recentemente, submetida à ensaios clínicos para avaliação no tratamento de tumores de pâncreas e de tumores sólidos avançados refratários (pulmão, colorretal, bexiga, pâncreas, mama, ducto biliar e estômago) (BEG et al., 2017; GERBER et al., 2018).

3 OBJETIVOS

3.1 OBJETIVO GERAL

Caracterizar polissacarídeos e metabólitos secundários, de folhas e cascas de *Handroanthus heptaphyllus* (ipê roxo) e *Handroanthus albus* (ipê amarelo), avaliando as propriedades gastroprotetora, anti-inflamatória e citotóxica contra células tumorais dessas biomoléculas.

3.2 OBJETIVOS ESPECÍFICOS

- Extrair, fracionar e caracterizar quimicamente polissacarídeos de folhas e cascas das espécies em estudo;
- Extrair, desenvolver métodos de fracionamento/purificação e realizar análises estruturais dos metabólitos secundários de cascas de *H. heptaphyllus*;
- Avaliar a atividade citotóxica *in vitro* das frações de metabólitos secundários de cascas de *H. heptaphyllus* nas linhagens tumorais Caco-2 (adenocarcinoma de cólon humano) e MCF-7 (adenocarcinoma mamário humano);
- Avaliar a atividade citotóxica *in vitro* das frações contendo polissacarídeos das cascas das espécies em estudo nas linhagens tumorais Caco-2 e MCF-7;
- Avaliar a atividade anti-úlcera gástrica das frações contendo polissacarídeos das folhas de *H. heptaphyllus;*
- Avaliar as atividades anti-inflamatória e analgésica das frações contendo polissacarídeos das folhas de *H. albus.*

4 ARTIGO 1: A POLYSACCHARIDE FRACTION FROM "IPÊ-ROXO" (*Handroanthus heptaphyllus*) LEAVES WITH GASTROPROTECTIVE ACTIVITY

(Carbohydrate Polymers, Volume 226, 15 December 2019)

Juliane Carlotto [a,#], Daniele Maria-Ferreira [a,b,#], Lauro Mera de Souza [c], Bruna Barbosa da Luz [b], Jorge Luiz Dallazen [b], Maria Fernanda de Paula Werner [b,*], Thales Ricardo Cipriani [a,*]

[a] *Departamento de Bioquímica e Biologia Molecular, Universidade Federal do Paraná, CEP 81.531-980, CP 19046, Curitiba, PR, Brazil*
[b] *Departamento de Farmacologia, Universidade Federal do Paraná, CEP 81.531-980, Curitiba, PR, Brazil*
[c] *Instituto de Pesquisa Pelé Pequeno Príncipe, Faculdades Pequeno Príncipe, CEP 80250-060, Curitiba, PR, Brazil*

* Corresponding authors:
Pharmacological assays: mfernanda.werner@ufpr.br (M.F. Werner)
Chemical characterization: trcipriani@ufpr.br (T.R. Cipriani)

[#] These authors contributed equally to this work.

ABSTRACT

A polysaccharide fraction from *Handroanthus heptaphyllus* leaves was obtained with a simple and quick fractionation method. Methylation analysis and NMR spectroscopy strongly suggest the presence of a complex polysaccharide fraction mainly constituted by a type II arabinogalactan. This is the first report in literature on structural elucidation of polysaccharides of species from genus *Handroanthus.* Oral and intraperitoneal administration of the polysaccharide fraction from *Handroanthus heptaphyllus* (HHSF) protected the gastric mucosa in an acute model of gastric lesion induced by ethanol, preserving gastric mucus. Furthermore, in the indomethacin model, HHSF reduced wounded area and inhibited mucus and GSH depletion. HHSF also accelerated gastric ulcer healing, accompanied by the maintenance of GSH levels. Collectively, these results showed that HHSF has an interesting antiulcerogenic activity and could constitute an interesting option for the treatment of gastric ulcer.

Keywords: *Handroanthus heptaphyllus*; polysaccharide; type II arabinogalactan; gastroprotective activity; gastric ulcer.

4.1 INTRODUCTION

Peptic ulcer disease, including both gastric and duodenal ulcers, represents a global health problem and is one of the most common disorders affecting the gastrointestinal system, with high morbidity and mortality (ROBERTS-THOMSON, 2018). Besides hindering a person's daily life activities, it can be associated with serious and life-threatening complications, such as bleeding and/or perforation, that may require surgery (SCALLY et al., 2018). The management of peptic ulcer disease and its complications aims for the inhibition of gastric acid secretion using proton pump inhibitors (PPI), like omeprazole, and H_2 receptor antagonist, such as ranitidine. However, recent studies show that these drugs have a variety of adverse effects and the search for new therapy to treat peptic ulcer disease remains of utmost importance (PRABHU; SHIVANI, 2014)

The plant *Handroanthus heptaphyllus*, commonly known as "ipê-roxo", "lapacho" or "pau d'arco", has been traditionally used for the treatment of various conditions, including inflammation, bacterial infection and digestive disorders (GOEL et al., 1987; GUIRAUD et al., 1994). In fact, some studies have showed several biological activities for *Handroanthus*, such as antitumor (UEDA et al., 1994; ZHANG et al., 2015; YAMASHITA et al., 2007; YAMASHITA et al., 2009), anti-inflammatory (BYEON et al., 2008), antioxidant (PARK et al., 2003) and antidepressive (FREITAS et al., 2013). Some of the activities presented by *Handroanthus* were attributed to the secondary metabolites lapachol and β-lapachone. However, other active compounds could be found, such as polysaccharides.

The therapeutic potential of polysaccharides has been demonstrated in literature and has been the focus of study in recent years due to beneficial pharmacological properties. Indeed, they display several functions, such as antioxidant (NASCIMENTO et al., 2017), immunomodulatory (WANG et al., 2018), anti-diabetes (HU et al., 2017), in addition to gastroprotective activity (MARIA-FERREIRA et al., 2014; CORRÊA-FERREIRA et al., 2018), and accordingly, polysaccharides could provide a valid alternative to improve ulcer healing and prevent disease recurrence. For this reason, the aim of this study was to investigate the gastric protective and healing effects of a polysaccharide fraction isolated from *Handroanthus heptaphyllus* in acute and chronic experimental models of gastric ulcer in rats.

4.2 MATERIALS AND METHODS

4.2.1. Plant material, extraction and fractionation

Leaves of *Handroanthus heptaphyllus* were collected in the Municipal Garden of Barreirinha, located in Curitiba, State of Paraná (PR), Brazil. The plant is deposited in the Herbarium of the Botany Department of Federal University of Paraná, as voucher nº. UPCB 85422.

Leaves were dried in air circulation oven at 50 ºC for 48 h and then milled leaves (200 g) were extracted with H_2O (500 mL) under conditions of reflux for 2 h (x 3). The aqueous extracts were obtained by vacuum filtration, combined, evaporated to a small volume (200 mL), and added to cold EtOH (x 3 vol.). The resulting precipitate was separated by vacuum filtration, dissolved in H_2O, dialyzed at a 12-14 kDa cut-off membrane and freeze-dried, to give the crude polysaccharide fraction (HHCP-*Handroanthus heptaphyllus* Crude Polysaccharide). This fraction was dissolved in H_2O (200 mL) at room temperature, then submitted to freeze-thawing process until no more precipitate appeared (GORIN; IACOMINI, 1984). Insoluble and soluble polysaccharide fractions were separated by centrifugation (9,000 rpm, 15 min, 10 ºC), and freeze-dried, generating HHSF (*Handroanthus heptaphyllus* Soluble Fraction) and HHIF (*Handroanthus heptaphyllus* Insoluble Fraction).

4.2.2. HPSEC analysis

Homogeneity of HHSF was determined by high-performance size-exclusion chromatography (HPSEC). Analysis of the sample was performed on a Waters chromatograph equipped with four Ultrahydrogel columns connected in series (2000, 500, 250, 120; with exclusion sizes of 7×10^6, 4×10^5, 8×10^4, and 5×10^3 Da; Milford, MA, USA), attached to a Waters 2410 refraction index (RI) detector (Milford, MA, USA). HPSEC-RI data were collected and analyzed using Wyatt Technology ASTRA software, version 4.70.07. The eluent was 0.1 M aq. $NaNO_2$ containing 200 ppm aq. NaN_3 at 0.6 mL/min. The sample, previously filtered through a membrane (0.22 µm), was injected (100 µL loop) at a concentration of 1 mg/mL, and analyzed at 25 °C. The peak elution time of each polysaccharide was compared with a calibration curve

obtained using standard dextrans (266 kDa, 124 kDa, 72.2 kDa, 40.2 kDa, 17.2 kDa and 9.4 kDa, from Sigma).

4.2.3. Monosaccharide analysis

The sample HHSF (2 mg) was hydrolyzed with 1 M TFA (1 mL) at 100 ºC for 16 h, the solution was then evaporated, and the residue dissolved in H_2O (1 mL). The hydrolyzate was treated with $NaBH_4$ (2 mg), and, after 18 h, concentrated HOAc (0.5 mL) was added, the solution evaporated to dryness and the resulting boric acid removed as trimethyl borate by co-evaporation with MeOH. Acetylation was carried out with Ac_2O-pyridine (1:1 v/v, 0.6 mL) at room temperature for 18 h, and the resulting alditol acetates were extracted with $CHCl_3$. These were analyzed by GC-MS (Varian Saturn 2000R - 3800 gas chromatograph coupled to a Varian Ion-Trap 2000R mass spectrometer), using a DB-225 column (30 m x 0.25 mm i.d.) programmed from 50 to 220 ºC at 40 ºC/min, with He as carrier gas. Components were identified by their typical retention times and electron ionization mass spectra relative to alditol acetates prepared from standard monosaccharides (Sigma-Aldrich). The monosaccharide analysis result was given as mol%, calculated according to Pettolino et al. (2012).

Uronic acid content was determined spectrofotometrically using the *m*-hydroxybiphenyl method according to Filisetti-Cozzi and Carpita (1991).

4.2.4. Methylation analysis

HHSF (5 mg) was per-*O*-methylated according to the method of Ciucanu & Kerek (1984), using DMSO-MeI and powdered NaOH. The product was hydrolyzed using two different conditions: 1) with 1 M TFA (1 mL) at 100 ºC for 16 h, followed by TFA evaporation, and dissolution of the hydrolysate in H_2O (1 mL); or 2) with 72% H_2SO_4 (w/v; 250 µL) at 0 °C for 1 h, followed by addition of H_2O (2 mL), heating at 100 °C for 16 h, neutralization with $BaCO_3$ and filtration. The mixture of *O*-methyl aldoses obtained by both hydrolysis methods was reduced with $NaBD_4$ (2 mg), and acetylated as described above to give a mixture of partially *O*-methylated alditol acetates. These were analyzed by GC-MS using the same conditions as described for alditol acetates, except the final temperature was 215 ºC. They were identified by their typical retention times and electron ionization mass spectra relative to partially *O*-methylated alditol

acetates prepared from standard monosaccharides (Sigma-Aldrich) according to Sassaki et al. (2005).

4.2.5. NMR spectroscopy

The HSQC/DEPT correlation map was obtained using a 400 MHz Bruker model DRX Avance spectrometer with a 5 mm inverse probe, at 50 °C in D_2O. Chemical shifts (δ) were expressed in ppm relative to acetone, at δ 30.2/2.22 ($^{13}C/^{1}H$). The correlation map was handled using Topspin® (Bruker) computer program and NMR signals were assigned based on literature data.

4.2.6. Phenolic compounds, total sugar and protein contents

The phenolic compounds content was determined as gallic acid equivalent (GAE, % w/w), using the spectrophotometric method of Singleton and Rossi (1965) and the protein content was determined spectrophotometrically according to Bradford (1976). The total sugar content was determined according to Dubois et al. (1956), using a calibration curve of arabinose: galactose: glucose (1:1:1), and was expressed as arabinose: galactose: glucose equivalent (AGGE, % w/w).

4.2.7. Animals

Female Wistar rats, obtained from the Federal University of Paraná colony (~ 200 g), were kept in plastic cages (maximum of 5 rats per cage) and maintained under controlled laboratory conditions (22 ± 2 ºC, and 12 hours - light/dark cycle), with free access to food (Nuvi-Lab CR-1, Quimtia S/A, Colombo, PR, Brazil) and water. All experimental protocols were approved by the Committee of Animal Experimentation of Federal University of Paraná (CEUA/BIO – UFPR; approval number 1093) and were conducted in agreement with the “Guide for the Care and Use of Laboratory Animals” (8^{th} edition, National Research Council, 2011).

4.2.8. Absolute ethanol-induced gastric lesions in rats

Hemorrhagic acute gastric lesions were induced by oral administration (p.o.) of absolute ethanol (Neon Comercial®, Suzano, SP, Brazil), as previously described by Robert and coworkers (1979) with minor modifications. Fasted female rats (18 hours) were orally (p.o.) pretreated with a single oral dose of vehicle (C: water, 1 mL/kg), omeprazole (O: 40 mg/kg), HHCP (HHCP: 0.1, 1, 10 and 30 mg/kg), HHSF (HHSF: 10 mg/kg) or intraperitoneally (i.p.) with HHSF (HHSF: 1 mg/kg) 1 h (v.o.) or 30 min (i.p.) before the oral administration of ethanol P.A. (1 mL/200 g). One hour later, the animals were euthanized by thiopental overdose (100 mg/kg, i.p.) followed by cervical dislocation. Their stomachs were excised, opened along the smaller curvature and photographed to measure the extent (mm^2) of gastric lesions using a computerized planimetry software (ImageJ® 3.0).

4.2.9. Gastric lesions induced by indomethacin in rats

Following the protocol proposed by Okada et al. (1989), fasted rats (16 hours) with free access to water were orally pretreated with vehicle (C: water, 1 mL/kg), omeprazole, prostaglandin E2 (PGE2: 20 µg/kg), (O: 40 mg/kg), or HHSF (HHSF: 10 mg/kg). One hour later, the animals received a single oral dose of indomethacin (100 mg/kg) and 6 hours later were euthanized as previously described. The same procedure described before was employed to analyze the indomethacin-induced gastric lesions. The results are shown in mm^2.

4.2.10. Induction of hypersecretion by pylorus ligation in rats

Gastric secretion was evaluated according to Shay (1945). Female rats were fasted for 16 hours in steel cages to avoid coprophagy. On the day of the experiment, under anesthesia, the stomach of the animals was exposed, the pylorus was located and ligated to maintain the gastric content in the stomach. The animals were treated by intraduodenal route with vehicle (C: water, 1 mL/kg), HHSF (HHSF: 10 mg/kg), or by oral route with omeprazole (O: 40 mg/kg), immediately after (i.d.) or 1 h before (p.o.) pylorus ligature. Four hours later, the animals were euthanized, their stomach was pinched, and gastric secretion collected and centrifuged at 1500 rpm for 20 min to measure the secreted volume, pH and acidity.

4.2.11. Chronic gastric ulcer induced by acetic acid

Chronic gastric ulcer was induced by acetic acid according to Okabe et al. (1971), with modifications. Animals were anesthetized with xylazine and ketamine (10 and 5 mg/kg, i.p., respectively) and then a laparotomy was made. The stomach was exposed and 80% acetic acid (0.5 mL) was applied to the serosal surface of the stomach for 1 min with a 6 mm diameter cylinder. The acetic acid was aspirated, and the stomach was washed with sterile saline. After the surgery, the animals were fasted for 24 hours, and 48 hours after the ulcer induction they were orally treated twice a day with vehicle (C: water, 1 mL/kg), omeprazole (O: 40 mg/kg) or HHSF (HHSF: 10 mg/kg), for 5 days. At the end of the experimental protocol, the rats were euthanized as previously described and their stomach was removed. The ulcer area (mm^2) was measured as length (mm) x width (mm).

4.2.12. Determination of gastric wall mucus

Gastric wall mucus was measured using the glandular segments of the stomach from ethanol and indomethacin induced lesions. Briefly, the tissue was weighed and complexed with a 0.1% Alcian Blue (pH 5.0) solution. After 2 hours at room temperature, excess dye was removed twice with 250 mM sucrose, first for 15 min and after that for 45 min, and then, dye complexed with gastric wall mucus was extracted with 500 mM magnesium chloride, which was stirred intermittently for 2 hours. The resultant solution was mixed with the same volume of diethyl ether (Vetec Quimica®) and centrifuged for 10 min at 3600 rpm. The absorbance was measured at 580 nm and the results were expressed in mg of Alcian Blue/g of tissue, based on a standard curve of Alcian Blue (6.25–100 mg) (Corne et al., 1974).

4.2.13. Determination of non-protein sulfhydryl groups

For the determination of GSH content, the stomach samples of ethanol, indomethacin and acetic acid experiments were homogenized with 200 mM potassium phosphate buffer (pH 6.5). GSH levels in gastric mucosa were determined by the method of Sedlak and Lindsay (1968) with minor modifications. In brief, homogenate aliquots maintained at 4 ºC were mixed with 12.5% trichloroacetic acid before being

centrifuged at 3000 rpm for 15 min. Later, the supernatant of the samples was added to a 96-well plate with 400 mM TRIS-HCl buffer (pH 8.5) and 10 mM 5,5′-dithiobis-(2-nitrobenzoic acid) (DTNB) for the colorimetric reaction. Absorbance was read at 412 nm and the results were expressed as µg of GSH/g of tissue based on a standard curve of GSH (0.375–3 µg).

4.2.17. Statistical analysis

Results were expressed as mean ± standard error of the mean (SEM) and statistical differences between experimental groups was determined using one-way analysis of variance (ANOVA) followed by Bonferroni's post-hoc test. The analyses were performed using GraphPad Prism® software, version 6.0 (GraphPad Software, San Diego, USA). ED_{50} value was determined by nonlinear regression analysis and reported as geometric mean. Differences were significant when $p<0.05$.

4.3 RESULTS AND DISCUSSION

4.3.1. Structural analysis of the polysaccharide fraction of Handroanthus heptaphyllus

A quick and convenient method for extraction and fractionation was used to generate the polysaccharide fraction of *Handroanthus heptaphyllus*. Dried and milled leaves (200 g) were extracted with boiling water and the aqueous extract was treated with excess EtOH to provide a crude precipitate of polysaccharides (4.3 %), then submitted to freeze-thawing process, resulting in a soluble (HHSF; 3.7 %) and an insoluble fraction (HHIF; 0.15 %). Considering the high yield and solubility of HHSF in relation to HHIF, only the soluble fraction was analyzed.

The elution profile of HHSF on HPSEC-RI showed a polydisperse profile, suggesting the presence of a complex polysaccharide fraction (Fig. 1). The molecular weights of the two major HHSF peaks, which have retention times of 56.8 and 60.1 min, were < 9.4 kDa. This fraction showed 35 g% of AGGE and contained, in its monosaccharide composition, glucose (41 mol%), galactose (23.2 mol%), arabinose (14.1 mol%), mannose (10.3 mol%), rhamnose (7.3 mol%), fucose (2.1 mol%) and xylose (2.1 mol%) as neutral monosaccharides, as well as uronic acids (5.9 g%). This

fraction also showed phenolic compounds content of 27.3 g% of GAE and a trace of protein.

FIG. 1. ELUTION PROFILE OF HHSF ON HPSEC (RI DETECTION).

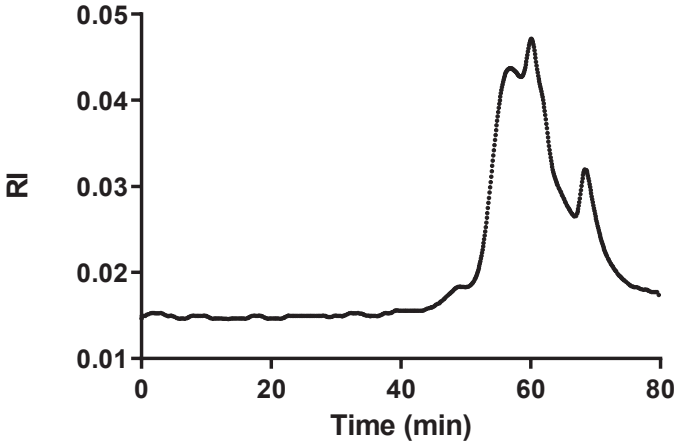

Glycosidic linkage analysis by methylation demonstrated the presence of several partially O-methylated alditol acetates derivatives (Table 1), corroborating a complex polysaccharide fraction. Moreover, it was possible to identify an excessive number of non-reducing end-units in the analysis, since the ratio of terminals to branch points was very high. The methylation analysis was repeated using another hydrolysis procedure and the result was confirmed. Specially, the presence of terminals of rhamnose, mannose and glucose in the polysaccharide fraction is ruled out by the NMR results shown below, which did not demonstrate the presence of chemical shifts of these monosaccharides. The terminals of rhamnose, mannose and glucose are probably linked to the phenolic compounds found in the fraction, which are probably slightly soluble in the NMR analysis condition and, therefore, undetectable.

The partially *O*-methylated alditol acetates derivatives demonstrated that galactose units are mainly linked at O-3, O-3,6 and O-6, as shown by the presence of alditol acetates of 2,4,6-Me_3-Gal (4.1 mol%), 2,4-Me_2-Gal (6.1 mol%) and 2,3,4-Me_3-Gal (3.9 mol%) respectively. These kinds of derivatives are found in type II arabinogalactans (AG II), which consist of (1→3)-linked β-D-Gal*p* main chain, linked at O-6 by (1→6)-linked β-D-Gal*p* side chains (Carpita & Gibeault, 1993; Pettolino et al*.,* 2012). Part of the remaining O-3 and O-6 galactosyl positions in this polymer could be linked by nonreducing end-units of Ara*f* and Gal*p* and side chains of arabinans, which consist of (1→5)-, (1→3)- and (1→2,5)-linked Ara*f* units, as demonstrated by the

presence of alditol acetates of 2,3-Me_2-Ara (1.6 mol%), 2,5-Me_2-Ara (2.7 mol%) and 3-Me_2-Ara (2.9 mol%) respectively. The probable structure of the HHSF backbone is shown in Figure S1.

TABLE 1. PROFILE OF PARTIALLY *O*-METHYLATED ALDITOL ACETATES AND MONOSACCHARIDE STRUCTURES OF HHSF OBTAINED ON METHYLATION ANALYSIS.

O-Me-alditol acetate	Structure	mol%
Arabinose		
2,3,5-Me_3-Ara	Ara*f*-(1→	9.2
2,5-Me_2-Ara	→3)-Ara*f*-(1→	2.7
2,3-Me_2-Ara	→5)-Ara*f*-(1→	1.6
3-Me-Ara	→2,5)-Ara*f*-(1→	2.9
Xylose		
2,3-Me_2-Xyl	→4)-Xyl*p*-(1→	3.0
Rhamnose		
2,3,4-Me_3-Rha	Rha*p*-(1→	5.8
3,4-Me_2-Rha	→2)-Rha*p*-(1→	1.1
Fucose		
2,3,4-Me_3-Fuc	Fuc*p*-(1→	1.6
Galactose		
2,3,4,6-Me_4-Gal	Gal*p*-(1→	7.9
2,4,6-Me_3-Gal	→3)-Gal*p*-(1→	4.1
2,3,4-Me_3-Gal	→6)-Gal*p*-(1→	3.9
2,4-Me_2-Gal	→3,6)-Gal*p*-(1→	6.1
Manose		
2,3,4,6-Me_4-Man	Man*p*-(1→	3.7
2,4,6-Me_3-Man	→3)-Man*p*-(1→	4.2
Glucose		
2,3,4,6-Me_4-Glc	Glc*p*-(1→	22.7
2,4,6-Me_3-Glc	→3)-Glc*p*-(1→	3.9
2,3,6-Me_3-Glc	→4)-Glc*p*-(1→	5.1
2,3,4-Me_3-Glc	→6)-Glc*p*-(1→	8.7
3,4-Me_2-Glc	→2,6)-Gal*p*-(1→	1.7

AG II is the main polysaccharide present in the fraction, according to methylation analysis. However, the methylation analysis results suggest the presence of other polysaccharides in minor proportions in HHSF. The presence of →4)-Xyl*p*-(1→ (3.0 mol%) could indicate a xylan (Carpita & Gibeault, 1993; Pettolino et al., 2012). The presence of →3)-Man*p*-(1→ (4.2 mol%) could indicate a mannan, although polysaccharides with this type of linkage are not very common in plants. Starch can also be present, since the alditol acetate of 2,3,6-Me_3-Glc (5.1 mol%) was observed and indicates the presence of (1→4)-linked Glc*p* units (Pettolino et al*.,* 2012).

Furthermore, (1→2)-linked α-L-Rha*p* units have been observed (3,4-Me_2-Rha; 1.1 mol%), which, together with the fact that uronic acid has been detected by colorimetric assay, strongly suggests the presence of a type I rhamnogalacturonan. This pectic polysaccharide is commonly found in primary cell walls of plants, and it is formed by sequences of alternating (1→4)-linked Gal*p*A (usually methyl-esterified) and (1→2)-linked Rha*p* units (Carpita & Gibeault, 1993; Mohnen, 2008).

NMR analysis is in accordance with methylations analysis, since the signals in the correlation map indicated that this fraction is mainly constituted by AG II with side chains of arabinans (Fig. 2). $^{1}H/^{13}C$ HSQC showed correlations at δ 103.1/4.49 of C-1/H-1 of β-D-Gal*p* units, and at δ 80.7/3.73 of C-3/H-3 of 3-*O*- and 3,6-di-*O*-linked β-D-Gal*p* units and at δ 66.9/3.88 of C-6/H-6 from β-D-Gal*p* units 6-*O*-linked and 3,6-di-*O*-linked. Typical signals of C-1/H-1 at 109.5/5.26, 107.5/5.21 and 107.5/5.08 of α-L-Ara*f* units were also observed (Carlotto et al., 2016; Nascimento et al., 2017; Scoparo et al., 2016). $^{1}H/^{13}C$ HSQC of HHSF also showed signals at δ 98.6/4.99 (C-1/H-1) and 53.3/3.81 (–CO_2-$\underline{CH}_3$) typical of (1→4)-linked 6-OMe-α-D-Gal*p*A units. The presence of C-6/H-6 of α-L-Rha*p* units was shown by resonances at δ 16.8/1.26 (Ovodova et al., 2009; Popov, et al., 2011; Carlotto et al., 2016). These signals can be present in type I rhamnogalacturonans, corroborating the methylation analysis.

Therefore, the results above suggested that HHSF contains mainly AG II. This is the first report in literature on structural elucidation of the polysaccharides that compose primary cell walls of species of genus *Handroanthus.* This type of polysaccharide has been isolated from different plants and associated with several pharmacological properties, such as anti-edematogenic (CARLOTTO et al., 2016), antiviral (OLIVEIRA et al., 2013), anti-ulcer (CIPRIANI et al., 2006; NASCIMENTO et al., 2017; SCOPARO et al., 2016) and immune-enhancing activity (YAO et al., 2018; DUAN et al., 2003). In this work, the polysaccharide fraction was obtained with a simple and rapid fractionation method, without multiple fractionation steps, increasing its potential pharmacological use.

FIG. 2. $^{1}H/^{13}C$ HSQC OF HHSF.

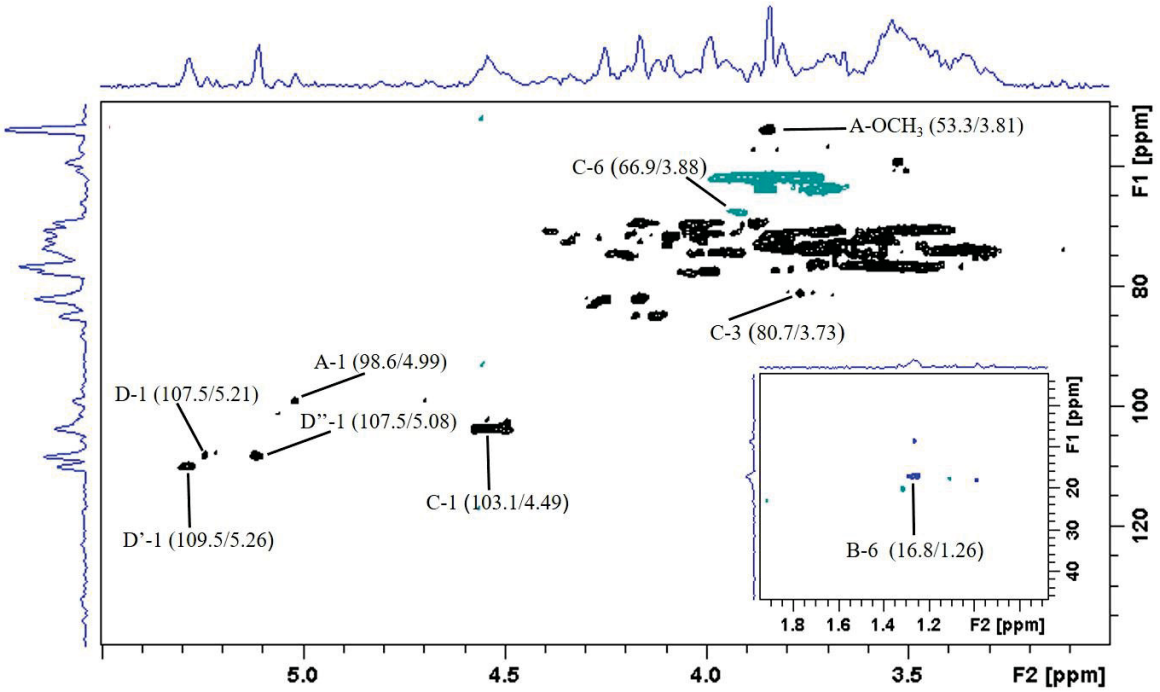

Solvent D_2O at 50 °C; numerical values are in δ ppm. A (6-OMe-α-D-Gal*p*A-), B (α-L-Rha*p*), C (β-D-Gal*p*), D, D'and D'' (α-L-Ara*f*). The letters are followed by the carbon number of the monosaccharide unit.

4.3.2. Effect of HHCP on gastric lesions induced by ethanol

Various studies have demonstrated that natural products and compounds isolated from them can effectively provide therapeutic benefit in both experimental and clinical studies, representing an interesting alternative for the treatment of gastric ulcer (BI; MAN; MAN, 2014). For instance, several researchers have shown the gastroprotective properties of plant polysaccharides by different mechanisms, including increased gastric mucus and/or scavenging radicals (MARIA-FERREIRA et al., 2014; NASCIMENTO et al., 2017), or even protective coating (KHOTIMCHENKO; KROPOTOV; KHOTIMCHENKO, 2001). Therefore, to investigate the potential gastroprotective effect of HHCP and HHSF, we performed the gastric lesions model induced by ethanol.

Ethanol is a well-known necrotizing agent that rapidly penetrates the gastric mucosa, leading to erosion and ulcer formation by reducing protective factors (non-protein sulfhydryl groups, mucus barrier, bicarbonate secretion) and increasing aggressive factors (e.g. free radicals) (LI et al., 2018). The pretreatment of the animals

with HHCP (1, 3, 10 and 30 mg/kg) significantly reduced hemorrhagic gastric lesions in 28.84, 72.90, 63.95 and 72.08%, respectively, when compared to the control group (C: 172.05 ± 18.31 mm^2). In addition, the positive control of the test, omeprazole (40 mg/kg), prevented hemorrhagic lesion formation in 93.39% (O: 6.21 ± 0.93 mm^2) (Fig. 3A). The crude polysaccharide was submitted to a fractionation step, generating a soluble polysaccharide fraction (HHSF), which maintained gastroprotective effect (Fig. 3B and S2). For the experimental protocols with HHSF, only its theoretical ED_{50} (10 mg/kg) was employed. It is noteworthy to mention that the gastroprotective ability of polysaccharides, in particular those which are characterized as AG II, has already been mentioned previously. A study showed that an AG II isolated from the leaves of *M. ilicifolia* (Celastraceae) significantly prevented ethanol-induced gastric lesions in rats at an ED_{50} of 9.3 mg/kg (Cipriani et al., 2006), and Scoparo et al. (2016) also demonstrated gastroprotective effect of this type of polysaccharide of green and black teas, corroborating our data.

Since the deleterious effects of ethanol result in depletion of defensive mechanisms, such as mucus barrier and GSH, additional experiments were carried out to measure these parameters. Accordingly, HHSF (10 mg/kg) was able to preserve the mucus layer in 20.59% when compared to the control group (C: 2211.42 ± 120.75 µg of Alcian blue/g of tissue) (Fig. 3C). On the other hand, only the positive control of the test (omeprazole) was able to prevent depletion of GSH levels in comparison to the control group (C: 1161.77 ± 118.45 µg of GSH/g of tissue) (Fig. 3D), suggesting that the gastroprotective effect of HHSF could be attributed to the maintenance of the mucus barrier or achieved by coating the gastric mucosa. To discard the latter hypothesis, animals were pretreated by intraperitoneal route with HHSF (1 mg/kg). Again, a significant decrease in the formation of ethanol-induced gastric lesions (60.59%) was observed when compared to the control group (C: 229.78 ± 38.48 mm^2) (Fig 4A). Furthermore, mucus level was preserved in 34.73% when compared to the control group (C: 1485.77 ± 90.34 µg of Alcian blue/g of tissue) (Fig. 4B), and interestingly, by this route of administration, GSH levels were preserved in 55.38% when compared to the control group (C: 1400.65 ± 132.39 µg of GSH/g of tissue) (Fig. 4C).

FIG. 3. EFFECT OF HHCP AND HHSF ON ACUTE GASTRIC LESIONS INDUCED BY ETHANOL P.A. IN RATS.

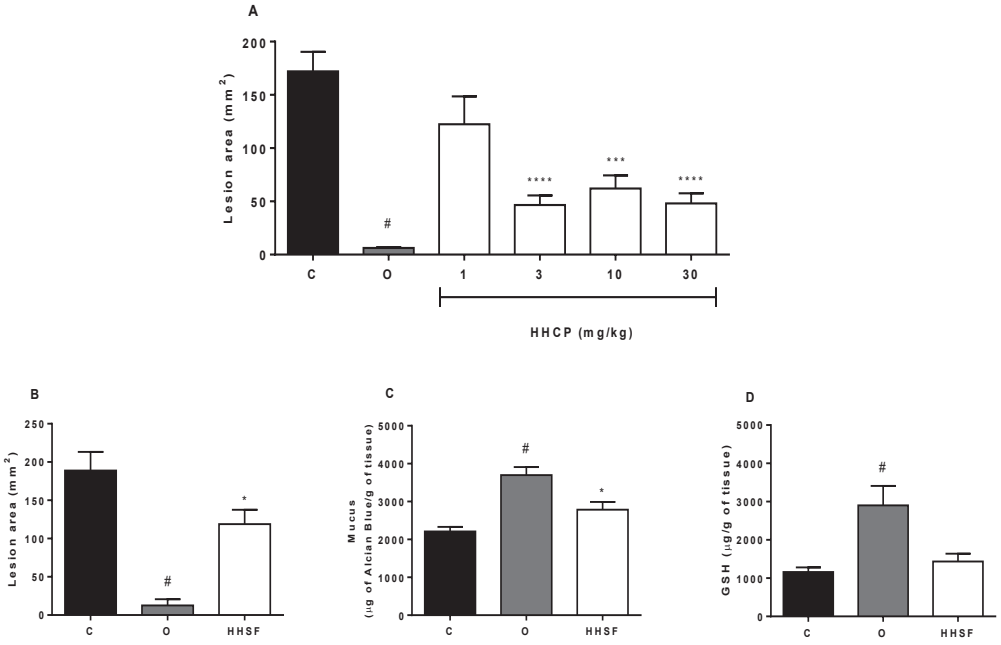

The panel A and B shows the lesion area (mm^2); C, mucus levels (µg of Alcian Blue/g of tissue) and D, glutathione levels (µg of GSH/g of tissue). The animals were orally treated with vehicle (C: water 1 mL/kg), omeprazole (O: 40 mg/kg), HHCP (1-30 mg/kg) or HHSF (ED_{50}: 10 mg/kg), 1 hour before oral ethanol (1 mL/200 g) administration. The results are expressed as mean ± S.E.M. *#P <0.05, *P <0.05, ***P < 0.001* and *****P < 0.0001* when compared to control group (C).

FIG. 4. EFFECT OF HHSF ON ACUTE GASTRIC LESIONS INDUCED BY ETHANOL P.A. IN RATS.

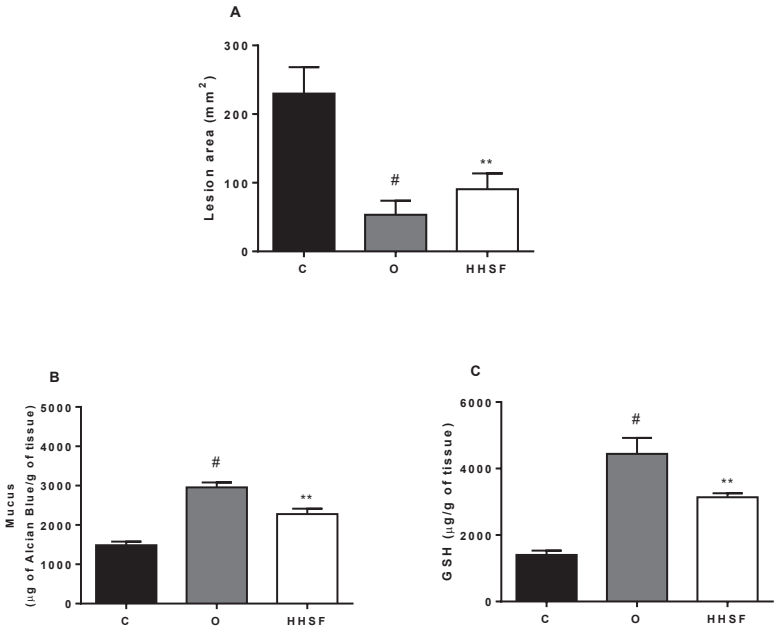

The panel A shows the lesion area (mm^2), B mucus content (µg of Alcian Blue/g of tissue) and C glutathione levels (µg of GSH/g of tissue). The animals were treated with vehicle (C: water 1 mL/kg, i.p.), omeprazole (O: 40 mg/kg, v.o.) or HHSF (ED_{50}: 1 mg/kg, i.p.), 60 (v.o.) or 30 minutes (i.p.), respectively, before oral ethanol P.A. (1 mL/200g) administration. The results are expressed as mean ± S.E.M. #P <0.05 and **P <0.01 when compared to control group (C)

4.3.3. Effect of HHSF on gastric lesions induced by indomethacin

Besides regular alcohol ingestion and smoke, higher ulcer incidence usually occurs in people who use therapeutic nonsteroidal anti-inflammatory drugs (NSAIDs), and the administration of indomethacin, for instance, provides a good experimental model to analyze the potential therapeutic effect of new compounds against this aggressor agent. Indomethacin induces gastric damage, including ulceration, bleeding and perforation by the inhibition of cyclooxygenase, and also for its prooxidant potential, changing the endogenous antioxidant defensive system (TIJANI; OLALEYE; FAROMBI, 2018). The anti-ulcer effect of HHSF was also observed in this model, reducing the lesion area in 54.40% when compared to the control group (C: 8.08 ± 1.65 mm^2). The positive control of the test, Prostaglandin E2, reduced ulcer formation in 78.95% (Fig. 5A). The observed protection seems to be related to the maintenance of protective factors, since HHSF inhibited the depletion of mucus (Fig. 5B) and GSH (Fig. 5C) levels in 70.28 and 57.62%, respectively, in comparison to the control group (Mucus, C: 2660.57 ± 69.71 µg of Alcian blue/g of tissue; GSH, C: 1007.43 ± 87.17 µg of GSH/g of tissue). Our results are partially in accordance with previous studies obtained with a polysaccharide-rich fraction of *Termitomyces eurhizus* in the indomethacin induced gastric ulceration. In this case, in particular, even though it is isolated from non-similar plants and presents a different composition, the fraction effectively prevented gastric ulceration (CHATTERJEE et al., 2013).

4.3.4. Effect of HHSF on gastric acid secretion

Antisecretory drugs, such as omeprazole, are effective antiulcer agents. Thus, we have evaluated if HHSF could affect gastric acid secretion. The results demonstrated that the polysaccharide administration in animals with gastric hypersecretion induced by pylorus ligature did not alter volume, pH and total acidity of the gastric content. In the opposite way, omeprazole significantly decreased volume, pH and total acidity of acid gastric secretion in 20.42, 70.94 and 57.16%, respectively, when compared to control (C: Volume: 13.12 ± 0.65 mL; pH: 2.13 ± 0.09; Total acidity: 0.005 ± 0.0007 mEq[H^+]/ml) (Fig. 6). It was demonstrated that another AG II, isolated from *Maytenus ilicifolia*, did not reduce gastric acid secretion of rats either (Baggio et al., 2012). This was observed with other types of polysaccharides, since Maria-Ferreira

et al. (2014) showed a rhamnogalacturonan isolated from *Acmella oleraceae* that did not reduce gastric secretion of rats either. The ability of polysaccharides to modify the parameters mentioned above is controversial and seems to be related to the structure of the polysaccharides, since Yamada (1995) showed a rhamnogalacturonan from *Bupleurum falcatum* that presents anti-secretory activity on acid and pepsin. Furthermore, this difference in pharmacological activity confers advantage to HHSF, since prolonged suppression of gastric acid secretion is associated to some unwanted effects, including risk of bone fracture, *Clostridium difficile* diarrhea, pneumonia, hypomagnesemia and vitamin B12 deficiency (NEHRA et al., 2018).

FIG. 5. EFFECT OF HHSF ON ACUTE GASTRIC LESIONS INDUCED BY INDOMETHACIN IN RATS.

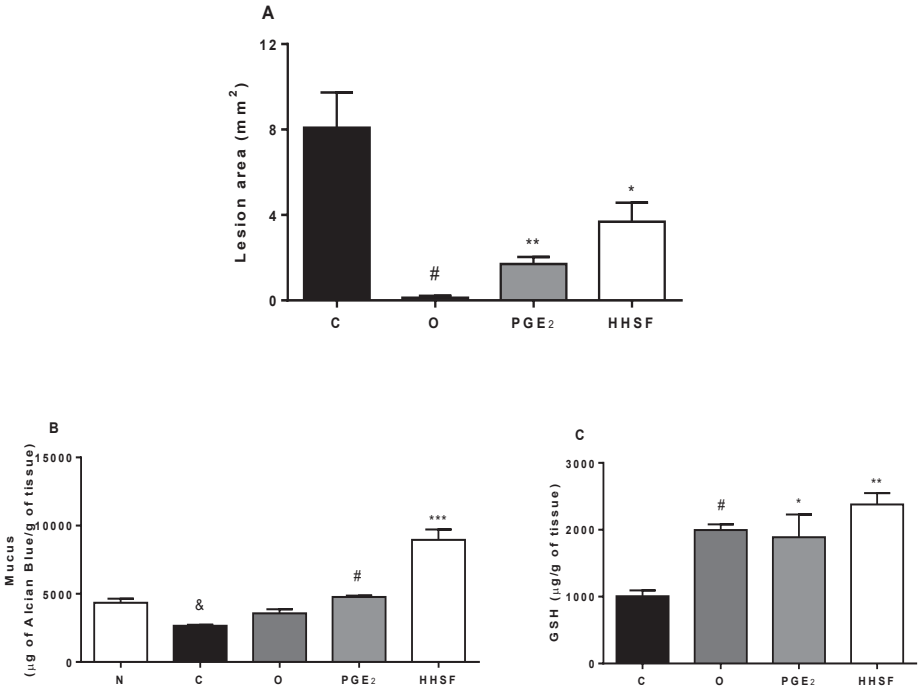

The panel A shows the gastric ulcer area (mm^2), B mucus content (µg of Alcian Blue/g of tissue) and C glutathione levels (µg of GSH/g of tissue). The animals were orally treated with vehicle (C: water 1 mL/kg), prostaglandin E_2 (PGE_2: 20 µg/kg) or HHSF (ED_{50}: 10 mg/kg), 1 hour before oral indomethacin (100 mg/kg) administration. The results are expressed as mean ± S.E.M. $^{\#}P<0.05$, $^{*}P<0.05$, $^{**}P < 0.01$ and $^{***}P < 0.001$ when compared to control group (C). $^{\&}P<0.05$ when compared to the naive (N) group.

FIG. 6. EFFECT OF INTRADUODENAL (I.D.) ADMINISTRATION OF HHSF ON VOLUME, pH AND TOTAL ACIDITY ON PYLORUS LIGATURE IN RATS.

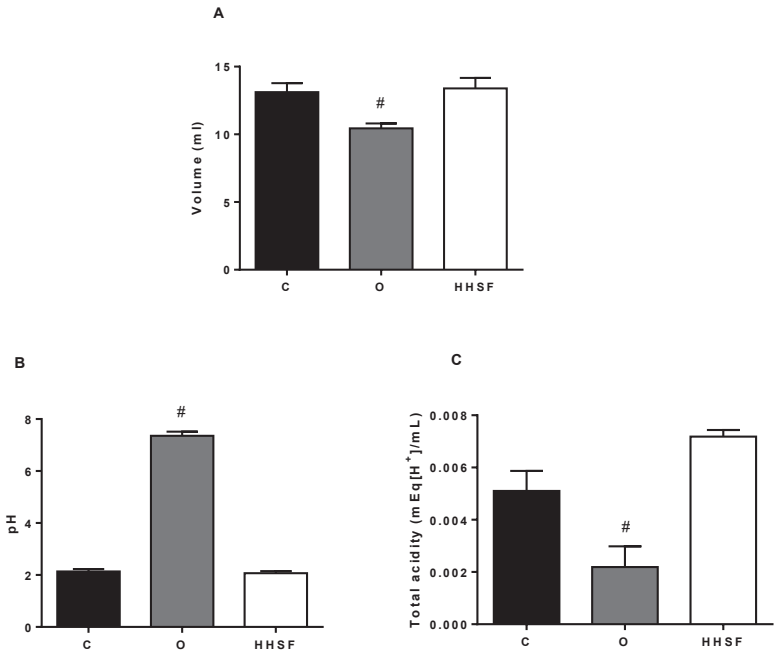

The panel A shows the volume (mL), B pH and C total acidity (mEq [H+] mL/4 h). The animals were treated with vehicle (C: water 1 mL/kg), omeprazole (O: 40 mg/kg) or HHSF (ED_{50}: 10 mg/kg) after pylorus ligation. The results are expressed as mean ± S.E.M. $^{\#}P<0.05$ when compared to control group (C).

4.3.5. Effect of HHSF on chronic ulcer model induced by acetic acid

Additionally, the acetic acid ulcer model, established by Okabe et al. in 1969, was used to evaluate the ulcer healing effect of HHSF. The animals treated with 10 mg/kg of HHSF twice a day for 5 days had a significantly reduced ulcer area (36.91%) when compared to the control group (C: 183.90 ± 15.81 mm^2). Similarly, omeprazole also accelerated gastric healing in 49.69% (Fig. 7A and S3). Furthermore, the result was accompanied by the maintenance of GSH levels (HHSF: 702.8 ± 53.73 µg of GSH/g of tissue), when compared to the control group (C: 424.63 ± 24.28 µg of GSH/g of tissue; O: 591.60 ± 47.19 µg of GSH/g of tissue) (Fig. 7B). Therefore, this data suggests that the healing of epithelial mucosa promoted by the polysaccharide may occur by increasing protective factors. Besides, in agreement with our data, it was reported that a pectic polysaccharide of swallow root (*Decalepis hamiltonii*) enhanced the healing of acetic acid ulcer in rats through the improvement of antioxidant defense, represented by the increase of glutathione levels (SRIKANTA; SATHISHA; DHARMESH, 2010).

FIG. 7. EFFECT OF HHSF ON CHRONIC GASTRIC ULCER INDUCED BY 80% ACETIC ACID IN RATS.

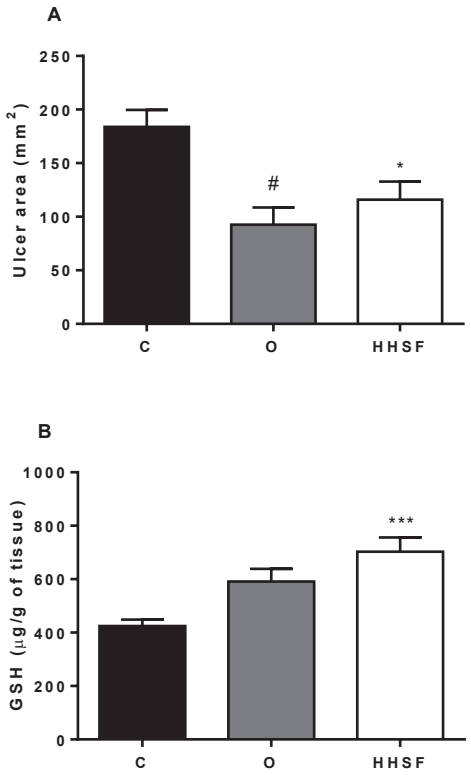

The panel A shows the ulcerated area (mm^2) and B the glutathione levels (µg of GSH/g of tissue). The animals were orally treated with vehicle (C: water, 1 mL/kg), omeprazole (O: 40 mg/kg) or HHSF (ED_{50}: 10 mg/kg) twice a day for five days after the gastric ulcer induction. The results are expressed as mean ± S.E.M. $^{\#}P<0.05$, $^{*}P<0.05$ and $^{***}P<0.001$ when compared to the ulcerated control group (C).

4.4. CONCLUSION

A polysaccharide fraction from *H. heptaphyllus* leaves, consisting mainly of AG II, was obtained with a simple and quick fractionation method. This is the first report in literature on structural elucidation of polysaccharides of species of genus *Handroanthus.* This fraction presented gastroprotective and gastric ulcer healing effects in acute and chronic *in vivo* assays, which seem to be related to the inhibition of mucus and GSH depletion. This study reinforces the findings that polysaccharides are molecules that protect the gastric mucosa and can heal ulcers. In addition, although *H. heptaphyllus* is not often indicated to prevent or treat gastric ulcers, this potential of the plant has been demonstrated here, and can be better explored.

Acknowledgements

The authors would like to thank the Brazilian agencies Conselho Nacional de Desenvolvimento Científico e Tecnológico (CNPq – Grant number 449176/2014-2) and Coordenação de Aperfeiçoamento de Pessoal de Nível Superior (CAPES) for financial support. D.M.F. received a CAPES post-doctoral fellowship (PNPD/CAPES).

Conflict of Interests

The authors declare that there is no conflict of interest.

4.5 SUPPLEMENTARY MATERIAL

FIGURE S1. BACKBONE STRUCTURE OF HHSF.

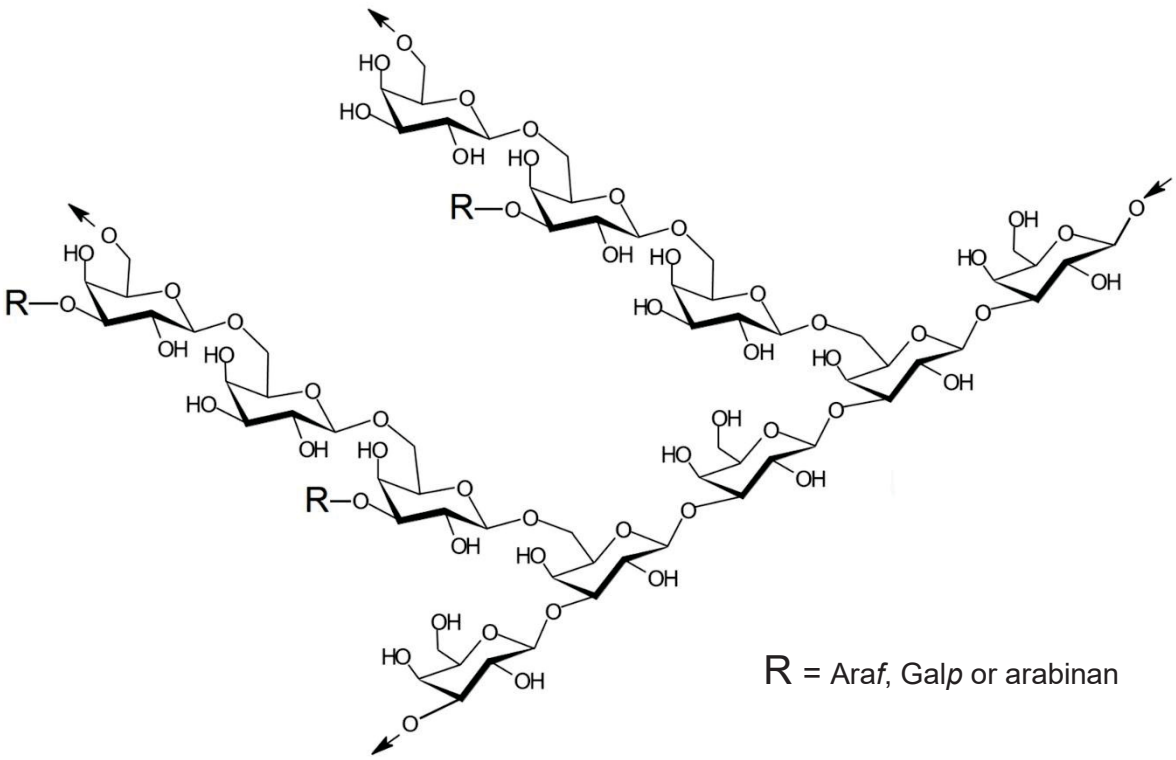

FIGURE S2. REPRESENTATIVE IMAGES OF ACUTE GASTRIC LESIONS INDUCED BY ETHANOL P.A. IN RATS.

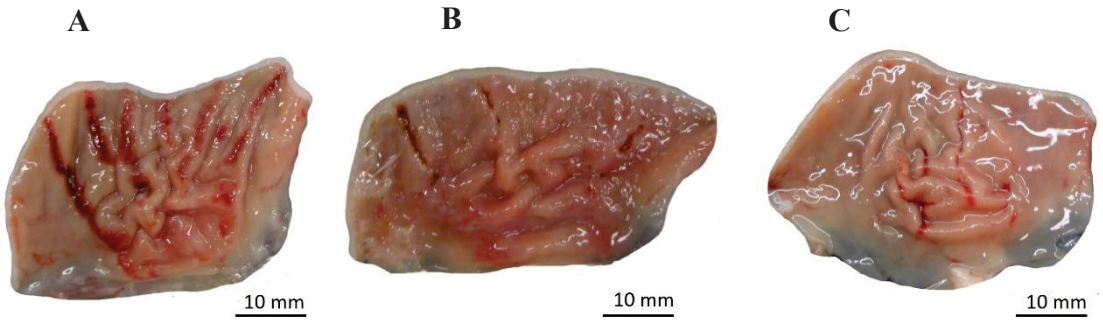

The panel A, B and C shows the stomachs of animals orally pretreated with vehicle (water 1 mL/kg), omeprazole (40 mg/kg) and HHSF (ED_{50}: 10 mg/kg), respectively.

FIGURE S3. REPRESENTATIVE IMAGES OF CHRONIC GASTRIC ULCER INDUCED BY 80% ACETIC ACID IN RATS..

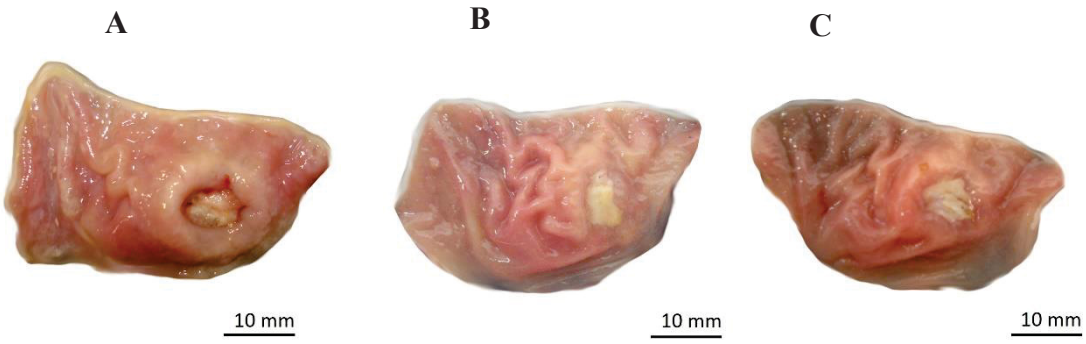

The panel A, B and C shows the stomachs of animals orally treated with vehicle (water 1mL/kg), omeprazole (40 mg/kg) and HHSF (ED_{50}: 10 mg/kg), twice a day for five days after the gastric ulcer induction

5 ARTIGO 2: A POLYSACCHARIDE FRACTION FROM *Handroanthus albus* (YELLOW IPÊ) LEAVES WITH ANTINOCICEPTIVE AND ANTI-INFLAMMATORY ACTIVITIES

Juliane Carlotto [1,#], Daniele Maria-Ferreira [1,2,3,#], Jorge Luiz Dallazen [2], Bruna Barbosa da Luz [2], Lauro Mera de Souza [3], Maria Fernanda de Paula Werner [2], Thales Ricardo Cipriani [1,*]

[1] Departamento de Bioquímica e Biologia Molecular, Universidade Federal do Paraná, Curitiba, PR, Brazil

[2] Departamento de Farmacologia, Universidade Federal do Paraná, Curitiba, PR, Brazil

[3]Instituto de Pesquisa Pelé Pequeno Príncipe, Faculdades Pequeno Príncipe, Curitiba, PR, Brazil

*Corresponding authors:

Pharmacological assays: mfernanda.werner@ufpr.br (M.F. Werner)

Chemical characterization: trcipriani@ufpr.br (T.R. Cipriani)

# These authors contributed equally to this work.

ABSTRACT

H. albus, commonly known as yellow *ipê*, is a native and widely distributed tree in Brazil. A polysaccharide fraction from its leaves (HASP) was obtained with a simple and rapid fractionation method. Monosaccharide composition, glycosidic linkage analysis by methylation and NMR spectroscopy strongly suggest that HASP is a complex polysaccharide fraction mainly constituted by type II arabinogalactan, and type I rhamnogalacturonan, mannan, starch and xylan in minor proportion. HASP was able to promote antinociception on formalin-induced (second phase) and on glutamate-induced nociception, besides reducing the number of abdominal contortions induced by acetic acid. Moreover, HASP reduced acetic acid-induced leukocyte infiltration in the peritoneal cavity and showed anti-edematogenic activity, decreasing mechanical allodynia and myeloperoxidase activity on carrageenan-induced paw edema. These results showed that the polysaccharide fraction HASP from *H. albus* leaves has interesting antinociceptive and anti-inflammatory activities.

5.1 INTRODUCTION

H. albus (Cham.) Mattos, commonly known as yellow *ipê*, is a native and widely distributed tree in Brazil, with economic importance because of its ornamental and medicinal value. The species from genus *Handroanthus* have been traditionally used for ethnopharmacological purposes, and previous studies revealed beneficial effects to treat several complications, such as cancer, inflammation, bacterial and fungal infections, and stomach disorders (PEREIRA et al., 2013; QUEIROZ et al., 2008; SICHAEM et al., 2012; WOO et al., 2006; ZHANG et al., 2015). In fact, natural products are an important source of new therapeutic bioactive molecules which may be useful for the management and prevention of diseases (DUTRA et al., 2016).

Polysaccharides are compounds that have attracted attention in the field of biochemistry and pharmacology because they exhibit multiple biological activities, including anti-inflammatory (SOUSA et al., 2018), antioxidant (THAMBIRAJ et al., 2018), antidepressive (WANG et al., 2010), among several others. The beneficial effects of genus *Handroanthus* are mainly attributed to its secondary metabolites (BORGES et al., 2019; GRAZZIOTIN et al., 1992; SUO et al., 2013; ZHANG et al., 2015; ZHANG; HASEGAWA; OHTA, 2016). However, when in traditional medicine its leaves are used to prepare teas (infusion or decoction), water soluble polysaccharide are extracted and ingested. In this regard, our group showed that a polysaccharide fraction obtained from aqueous extract of *Arctium lappa* leaves had anti-edematogenic activity on carrageenan-induced paw edema (CARLOTTO et al., 2016), suggesting that polysaccharides from plants may be promising alternatives for treating pain and inflammation.

It is well known that pain and inflammation can result in serious consequences. Inflammation is an immunological defense mechanism of the body that operates during perturbations of the homeostasis. It involves various events such as cellular migration and release of mediators that are commonly associated with tissue damage and pain, demanding pharmacological treatment (SERHAN; CHIANG; DALLI, 2017). Despite recent progress in the development of anti-inflammatory therapies, the currently available drugs used in clinical practice has had numerous failures in terms of efficacy, tolerability, and toxicity. For instance, the long-term use of non-steroidal and steroidal anti-inflammatory drugs lead to the development of multiple adverse effects including hormonal and cardiovascular side effects, gastric bleeding and nephrotoxicity

(WONGRAKPANICH et al., 2018). Therefore, the search for new effective and potent analgesic and anti-inflammatory drugs are still ongoing. Considering this, here we described the chemical structure of a polysaccharide fraction isolated from aqueous extract of *H. albus* leaves and reported the findings on its antinociceptive and anti-inflammatory effects.

5.2 MATERIALS AND METHODS

5.2.1. Plant material, extraction and fractionation of polysaccharides

H. albus leaves were collected in Paulo Frontin, State of Paraná (PR), Brazil. The plant is deposited in the Herbarium of the Botany Department of Federal University of Paraná, as voucher nº UPCB 85420.

Dried and milled leaves (200 g) were extracted with H_2O (500 mL) under conditions of reflux for 2 h (x 3). The aqueous extracts were obtained by vacuum filtration, combined, evaporated to a small volume (200 mL), and added to cold EtOH (x 3 vol.). The resulting precipitate was separated by vacuum filtration, dissolved in H_2O, dialyzed at a 12-14 kDa cut-off membrane and freeze-dried, to give the crude polysaccharide fraction (HACP). This fraction was dissolved in H_2O (200 mL) at room temperature, and then submitted to freezing and thawing process until no more precipitate appeared (GORIN; IACOMINI, 1984). Insoluble and soluble fractions were separated by centrifugation and freeze-dried, generating HAIP (*H. albus* cold water insoluble polysaccharide fraction) and HASP (*H. albus* cold water soluble polysaccharide fraction).

5.2.2. HPSEC analysis

Homogeneity of HASP was determined by high-performance size-exclusion chromatography (HPSEC). The analysis was performed on a Waters chromatograph equipped with four Ultrahydrogel columns connected in series, with exclusion limits of 7×10^6, 4×10^5, 8×10^4, and 5×10^3 Da, attached to a Waters 2410 refractive index detector (RID) (Milford, MA, USA). The eluent was 0.1 M aq. $NaNO_2$ containing 200 ppm aq. NaN_3 at 0.6 mL/min. The samples, previously filtered through a membrane (0.22 µm), was injected (100 µL loop) at a concentration of 1 mg/mL, and analyzed at

25 °C. The elution time of HASP was compared with a calibration curve obtained with standard dextrans of 266, 124, 72.2, 40.2, 17.2, 9.4, and 5 kDa (Sigma-Aldrich).

5.2.3. Monosaccharide analysis

Neutral monosaccharides composition of HASP was determined by GC-MS analysis of alditol acetates derivatives. HASP (2 mg) was submitted to hydrolysis with 1 M TFA (1 mL) at 100 ºC for 16 h. The solution was evaporated, the residue dissolved in H_2O, treated with $NaBH_4$ (2 mg) and after 18 h, neutralized with HOAc. The solution was then evaporated to dryness and the resulting boric acid removed as trimethyl borate by co-evaporation with MeOH. Acetylation was carried out with Ac_2O-pyridine (1:1 v/v, 0.6 mL) at room temperature for 18 h. Then, the resulting alditol acetates were extracted with $CHCl_3$ and analyzed by GC-MS (Varian Saturn 2000R - 3800 gas chromatograph coupled to a Varian Ion-Trap 2000R mass spectrometer), using a DB-225 column (30 m x 0.25 mm i.d.) programmed from 50 to 220 ºC at 40 ºC/min, with He as carrier gas. Alditol acetates were identified by their typical retention times and electron ionization mass spectra relative to alditol acetates prepared from standard monosaccharides (Sigma-Aldrich). The monosaccharide analysis result was given as mol%, calculated according Pettolino et al. (2012).

Uronic acid content was determined spectrophotometrically using the *m*-hydroxybiphenyl method according to Filisetti-Cozzi and Carpita (1991).

5.2.4. Methylation analysis

HASP (5 mg) was per-*O*-methylated according to the method of Ciucanu and Kerek (1984), using DMSO-MeI and powdered NaOH. The product was hydrolyzed using two different conditions: 1) with 1 M TFA (1 mL) at 100 ºC for 16 h, followed by TFA evaporation and dissolution of the hydrolysate in H_2O (1 mL); or 2) with 72% H_2SO_4 (w/v; 250 µL) at 0 °C for 1 h, followed by addition of H_2O (2 mL), heating at 100 °C for 16 h, neutralization with $BaCO_3$ and filtration. The mixtures of *O*-methyl aldoses obtained by both hydrolysis methods were reduced with $NaBD_4$ (2 mg), and acetylated as described above (section 5.2.3) to give a mixture of partially *O*-methylated alditol acetates. These were analyzed by GC-MS using the same conditions as described for alditol acetates, except the final temperature was 215 ºC. They were identified by their

typical retention times and electron ionization mass spectra relative to partially *O*-methylated alditol acetates prepared from standard monosaccharides (Sigma-Aldrich) according to Sassaki et al. (2005).

5.2.5. NMR spectroscopy

HSQC/DEPT correlation map was obtained using a 400 MHz Bruker model DRX Avance spectrometer with a 5 mm inverse probe, at 50 °C in D_2O. Chemical shifts (δ) were expressed in ppm relative to acetone, at δ 30.2/2.22 ($^{13}C/^{1}H$). The correlation map was processed and analyzed using the Topspin® software (Bruker) and the $^{13}C/^{1}H$ correlations were assigned based on literature data.

5.2.6. Phenolic compounds, total sugar and protein contents

The phenolic compounds content was determined as gallic acid equivalent (GAE, % w/w), according to the spectrophotometric method of Singleton e Rossi (SINGLETON; ROSSI; 1965), and the protein content was determined spectrophotometrically according to Bradford (1976).). The total sugar content was determined according to Dubois et al. (1956), using a calibration curve of arabinose: galactose: glucose (1:1:1), and was expressed as arabinose: galactose: glucose equivalent (AGGE, % w/w).

5.2.7. Animals

Experiments were conducted with Swiss (*Mus musculus*) adult mice (25 - 30 g) housed in a 12 h light/dark cycle, at 22 ± 2 ºC, air exhaustion, with free access to water and food (Nuvilab CR-1, Quimtia S/A, Colombo, PR, Brazil). All protocols were approved by the Institutional Animals Ethics Committee (approval number 1093) and conducted in agreement with the “Guide for the Care and Use of Laboratory Animals” (8th edition, National Research Council, 2011).

5.2.8. Formalin-induced nociception

Mice were intraperitoneally (i.p.) pretreated with vehicle (V: sterile saline, 10 mL/kg), diclofenac (DICLO: 10 mg/kg), HACP (0.1; 0.3 and 1 mg/kg) or HASP (0.125; 0.25 and 0.5 mg/kg). After 30 min, the animals received intraplantar injection of formalin (2.5%, 20 µL, i.pl.) on the right hind paw, and the nociception was evaluated by quantifying the licking time in two phases, 0-5 min (neurogenic phase or first phase) and 15-30 min (inflammatory phase or second phase) after injection of formalin (HUNSKAAR; HOLE, 1987; TJØLSEN et al., 1992).

5.2.9. Glutamate-induced nociception

Mice received vehicle (V: sterile saline, 10 mL/kg, i.p.), morphine (MOR: 1 mg/kg, subcutaneously, s.c.) or HASP (0.25 mg/kg, i.p.). After 30 min, the nociception was induced by injection of glutamate (GLU: 20 µmol/20 µL, i.p.), and the licking time was recorded for 15 min (BEIRITH et al. 2002; RODRIGUES et al. 2012).

5.2.10. Acetic acid-induced writhing and leukocyte infiltration

Mice were pretreated with vehicle (V: sterile saline, 10 mL/kg, i.p.), dexamethasone (DEXA: 1 mg/kg, i.p.) or HASP (0.25 mg/kg, i.p.), 30 min before the injection of 0.6% acetic acid (450 µL, i.p.). The number of abdominal writhing was evaluated cumulatively for 20 min. After, animals were euthanized by cervical dislocation, and their peritoneal cavity was washed with heparinized saline (1 mL, 25 UI/mL). The fluid was collected and diluted with Türk solution (1:20) to count the total leukocyte using a Neubauer chamber (RODRIGUES et al., 2012).

5.2.11. Carrageenan-induced acute mechanical allodynia and paw edema

Mice were placed and acclimated in individual boxes (18 cm × 11 cm × 20 cm) on an elevated mesh platform for 1 h, then pretreated with vehicle (V: sterile saline, 10 mL/kg, i.p.), dexamethasone (DEXA: 1 mg/kg, i.p.) or HASP (0.25 mg/kg, i.p.). After 30 min, the acute inflammatory response was induced by intraplantar injection of carrageenan (300 µg/20 µL, i.pl.). The mechanical withdrawal threshold (allodynia) was accessed with Von Frey filaments stimulation (0.004 – 4g) based on the Up-and-Down method to determinate 50% threshold (g) (CHAPLAN et al., 1994; DIXON,

1980). Concomitantly, the paw thickness (edema) was measured using a digital micrometer and expressed as “variation of millimeter (Δ mm)” between the basal value and the test value at each evaluation (ROSSATO et al., 2015). Both parameters were evaluated previously (B: basal values) and 1, 2, 3, 4, 5 and 6 h after carrageenan injection.

5.2.12. Myeloperoxidase (MPO) assay

The tissue MPO enzyme activity (an indirect marker of neutrophil infiltration) was measured on the peak of the anti-allodynic and anti-edematogenic effects (3 h) promoted by HASP (0.25 mg/kg) on carrageenan-induced acute inflammation. Then, mice were pretreated with vehicle (V: sterile saline, 10 mL/kg, i.p.), dexamethasone (DEXA: 1 mg/kg, i.p.) or HASP (0.25 mg/kg, i.p.) 30 min before carrageenan injection (300 µg/20 µL, i.pl.). After 3 h, the plantar surfaces of injected paws were excised and homogenized with 200 mM potassium phosphate buffer (pH 6.5). The homogenate was centrifuged at 9000 g for 20 min, and the pellet obtained was re-suspended in 1 mL of 80 mM potassium phosphate buffer (pH 5.4) plus hexadecyltrimethylammonium bromide (HTAB) and centrifuged at 11000 g for 20 min. The MPO levels were determined with 0.017% H_2O_2 and 3,3’,5,5’-tetramethylbenzidine (18.4 mM TMB) at 620 nm according to (BRADLEY et al., 1982; DE YOUNG et al., 1989) and expressed as optical density (O.D.)/mg of protein, which was determined according to Bradford (1976).

5.2.13. Statistical analyses

The results were expressed as mean ± S.E.M. and evaluated with one or two-way analysis of variance (ANOVA), followed by the Bonferroni multiple comparison test. The theoretical ID_{50} value (i.e. the dose of the polysaccharide fraction required to inhibit formalin-induced nociception by 50%) was determined by nonlinear regression analysis (sigmoidal dose-response) and recalculated based on the yield of HACP and HASP. Significant difference was considered when $^{*}P < 0.05$, $^{**}P < 0.01$, $^{***}P < 0.001$, and $^{****}P < 0.0001$, and all the analyzes were performed using the GraphPad Prism® version 6.0 (GraphPad Software, San Diego, USA).

5.3 RESULTS

5.3.1. Extraction and fractionation of polysaccharides

Crude polysaccharides from *H. albus* leaves (200 g) were extracted with boiling water and recovered by precipitation with excess EtOH, dialysis and freeze-drying (HACP, 1.8 %). HACP was submitted to freeze-thawing process, yielding the soluble (HASP; 0.98 %) and insoluble (HAIP; 0.61 %) polysaccharide fractions. Considering the higher water solubility of HASP in relation to HAIP, only the first one fraction was analyzed.

5.3.2. HPSEC and monosaccharide analysis

HASP showed a polydisperse elution profile on HPSEC, with a major peak at 55.8 min (Fig. 1), corresponding to a molecular weight of 7.94 kDa, and showed total sugar content of 38 g% of AGGE. This fraction was mainly composed of galactose (30.7 mol%), glucose (24.3 mol%), arabinose (18.0 mol%), mannose (16.5 mol%), rhamnose (5.2 mol%), xylose (2.9 mol%) and fucose (2.4 mol%), as well as uronic acids (5.3 g%). This fraction also showed total phenolic content of 19.3 g% of GAE and did not show protein.

FIG. 1. ELUTION PROFILE OF HASP ON HPSEC

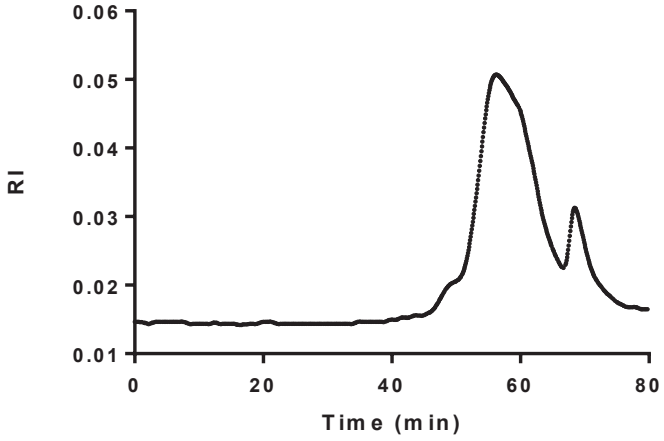

5.3.3. Methylation analysis

Glycosidic linkage analysis by methylation (Table 1) showed an excessive number of non-reducing terminals of Glc*p* (19.8 mol%) and a very high non-reducing terminals to branch points ratio in HASP. The methylation analysis was repeated using another hydrolysis procedure and the result was confirmed. This suggests that the non-reducing terminals of Glc*p* are not part of the polysaccharide structures and are possibly related to the phenolic compounds present in HASP.

Methylation analysis of HASP strongly suggests that type II arabinogalactan is the major polysaccharide in the fraction, since alditol acetates of 2,4,6-Me_3-Gal (7.0 mol%), 2,4-Me_2-Gal (13.7 mol%), 2,3,4-Me_3-Gal (3.5 mol%) were found. These methylated derivatives are from (1→3), (1→3,6) and (1→6)-linked Gal*p* units, which are present in type II arabinogalactan. This class of polysaccharides have a (1→3)-linked β-D-Gal*p* main chain, linked at O-6 by (1→6)-linked β-D-Gal*p* side chains. Part of the remaining O-3 and O-6 galactosyl positions in this polymer could be linked by non-reducing terminals of arabinose, galactose and rhamnose, as demonstrated by the presence of alditol acetates of Ara*f* (3.0 mol%), Gal*p* (6.1 mol%) and Rha*p* (2.7 mol%). In addition, alditol acetates of 2,5-Me_2-Ara (1.8 mol%), 2,3-Me_2-Ara (0.8 mol%) and 3-Me_2-Ara (2.9 mol%) were also found, which are from (1→3)-, (1→5)- and (1→2,5)-linked Ara*f* units, respectively, probably of arabinans side chains in type II arabinogalactan (CARPITA; GIBEAUT, 1993; PETTOLINO et al., 2012).

Moreover, the methylation analysis also indicated the presence of other polysaccharides in minor proportions in HASP. Mannan, starch and xylan could be present, since alditol acetates of 2,4,6-Me_3-Man (5.3 mol%), 2,3,6-Me_3-Glc (7.4 mol%), 2,3-Me_2-Xyl (2.2 mol%) were found (Pettolino et al., 2012). In addition, the presence of alditol acetates of 3,4-Me_2-Rha (1.2 mol%), which, together with the fact that uronic acid has been detected by colorimetric assay, strongly suggests the presence of type I rhamnogalacturonan, which it is formed by sequences of alternating (1→4)-linked Gal*p*A (usually methyl-esterified) and (1→4)-linked Rha*p* units (CARPITA; GIBEAUT, 1993; MOHNEN, 2008).

TABLE 1 - PROFILE OF PARTIALLY *O*-METHYLATED ALDITOL ACETATES AND MONOSACCHARIDE STRUCTURES OF HASP OBTAINED ON METHYLATION ANALYSIS.

O-Me-alditol acetate	Structure	mol%
Arabinose		
2,3,5-Me_3-Ara	Ara*f*-(1→	3.0
2,5-Me_2-Ara	→3)-Ara*f*-(1→	1.8
2,3-Me_2-Ara	→5)-Ara*f*-(1→	0.8
3-Me-Ara	→2,5)-Ara*f*-(1→	2.9
Xylose		
2,3-Me_2-Xyl	→4)-Xyl*p*-(1→	2.2
Rhamnose		
2,3,4-Me_3-Rha	Rha*p*-(1→	2.7
3,4-Me_2-Rha	→2)-Rha*p*-(1→	1.2
Fucose		
2,3,4-Me3-Fuc	Fuc*p*-(1→	1.2
Galactose		
2,3,4,6-Me_4-Gal	Gal*p*-(1→	6.1
2,4,6-Me_3-Gal	→3)-Gal*p*-(1→	7.0
2,3,4-Me_3-Gal	→6)-Gal*p*-(1→	3.5
2,4-Me_2-Gal	→3,6)-Gal*p*-(1→	13.7
3,6-Me_2-Gal	→2,4)-Gal*p*-(1→	1.9
Manose		
2,3,4,6-Me_4-Man	Man*p*-(1→	2.8
2,4,6-Me_3-Man	→3)-Man*p*-(1→	5.3
Glucose		
2,3,4,6-Me_4-Glc	Glc*p*-(1→	19.8
2,4,6-Me_3-Glc	→3)-Glc*p*-(1→	7.0
2,3,6-Me_3-Glc	→4)-Glc*p*-(1→	7.4
2,3,4-Me_3-Glc	→6)-Glc*p*-(1→	7.6
3,4-Me_2-Glc	→2,6)-Gal*p*-(1→	2.1

5.3.4. NMR analysis

The $^{1}H/^{13}C$ HSQC of HASP (Fig. 2) showed correlations at δ 103.4/4.50 of C-1/H-1 of β-D-Gal*p* units, at δ 80.6/3.74 of C-3/H-3 of 3-*O*- and 3,6-di-*O*-linked β-D-Gal*p*. Correlations of C-1/H-1 of non-reducing terminals, 5-*O*- and 3,5-di-*O*-linked α-L-Ara*f* units were observed at δ 109.6/5.25, 107.7/5.21 and 107.5/5.08, respectively. Moreover, inverted C5/H5 signals appeared at δ 66.9/3.92 for 5-O- and 3,5-O-linked α-L-Ara*f* units (CANTU-JUNGLES et al., 2017; CARLOTTO et al., 2016; KLOSTERHOFF et al., 2018; NASCIMENTO et al., 2017; SCOPARO et al., 2016). These results corroborate the methylation data, demonstrating that type II arabinogalactan is the major polysaccharide in HASP.

$^{1}H/^{13}C$ correlations were also observed at δ 99.9/4.91 (C-1/H-1), 71.1/5.12 (C-5/H-5), and 53.3/3.81 (–CO_2-$\underline{CH_3}$) typical of (1→4)-linked 6-*O*Me-α-D-Gal*p*A units, and at δ 99.2/5.13 (C-1/H-1) of α-D-Gal*p*A units. The presence of C-6/H-6 of α-L-Rha*p* units was shown by resonance at δ 17.1/1.27 (CARLOTTO et al., 2016; OVODOVA et al., 2009; POPOV et al., 2011). These signals can be present in type I rhamnogalacturonans, corroborated by methylation analysis. $^{1}H/^{13}C$ correlations of other polysaccharides or phenolic compounds present in HASP were not observed because they are in small amount in the fraction or because they are insoluble in the NMR analysis condition.

FIG. 2. $^{1}H/^{13}C$ HSQC OF HASP.

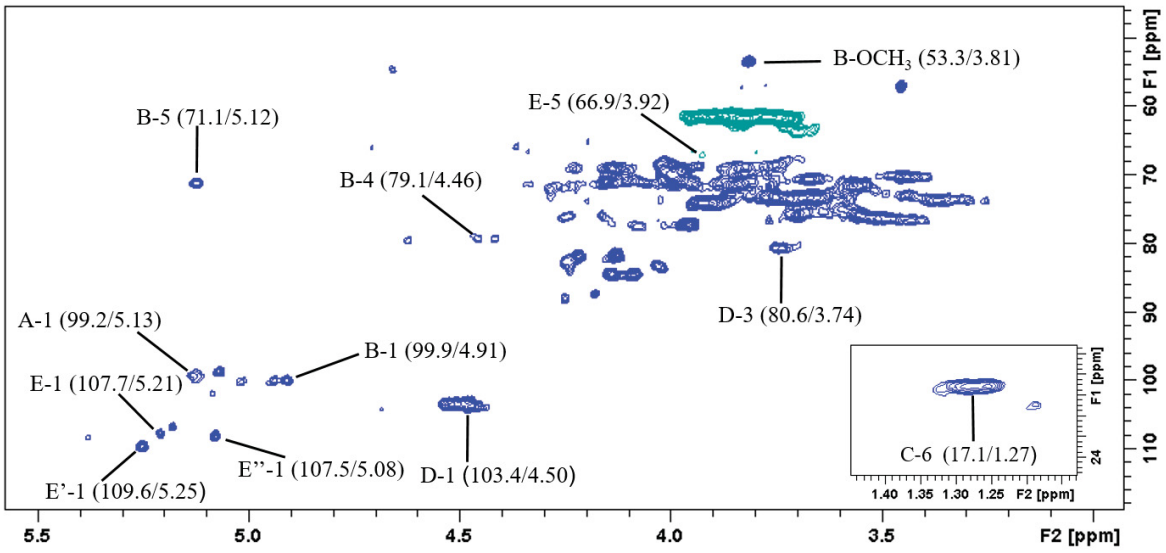

Solvent D_2O at 50 °C; numerical values are in δ ppm. A (α-D-Gal*p*A), B (6-OMe-α-D-Gal*p*A), C (α-L-Rha*p*), D (β-D-Gal*p*), E, E' and E'' (α-L-Ara*f*). The letters are followed by the carbon number of the monosaccharide unit.

5.3.5. HACP and HASP attenuated formalin-induced nociception

Intraperitoneal pretreatment with HACP and diclofenac did not attenuate the nociception induced by intraplantar injection of formalin in the first phase of the test (V: 75.5 ± 4.8 s) (Fig. 3A). However, in the second phase the licking behavior was reduced by 37.5% and 80.7 % at 0.3 and 1 mg/kg of HACP (Fig. 3B), respectively, when compared to the vehicle group (V: 177.7 ± 20.7 s). The positive control (10 mg/kg diclofenac) reduced the formalin-induced nociception in the second phase in 54.0%.

Based on a nonlinear regression analysis of the inhibitory action of HACP on formalin test and on its yield (61.5%), the theoretical 50% inhibitory dose (ID_{50}) of HASP was determined at 0.25 mg/kg. Thus, the formalin test was repeated with HASP at 0.25 mg/kg and also with 0.125 and 0.5 mg/kg (i.p.). Intraperitoneal administration of HASP at 0.125, 0.25 and 0.5 mg/kg and diclofenac at 10 mg/kg reduced the formalin-induced licking behavior only in the second phase of the test, by 35.0%, 54.3%, 59.7% and 40.8%, respectively (Fig. 3D), when compared to the vehicle group (V: 122.0 ± 13.9 s).

FIG. 3. EFFECT OF HACP AND HASP ON FORMALIN-INDUCED NOCICEPTION

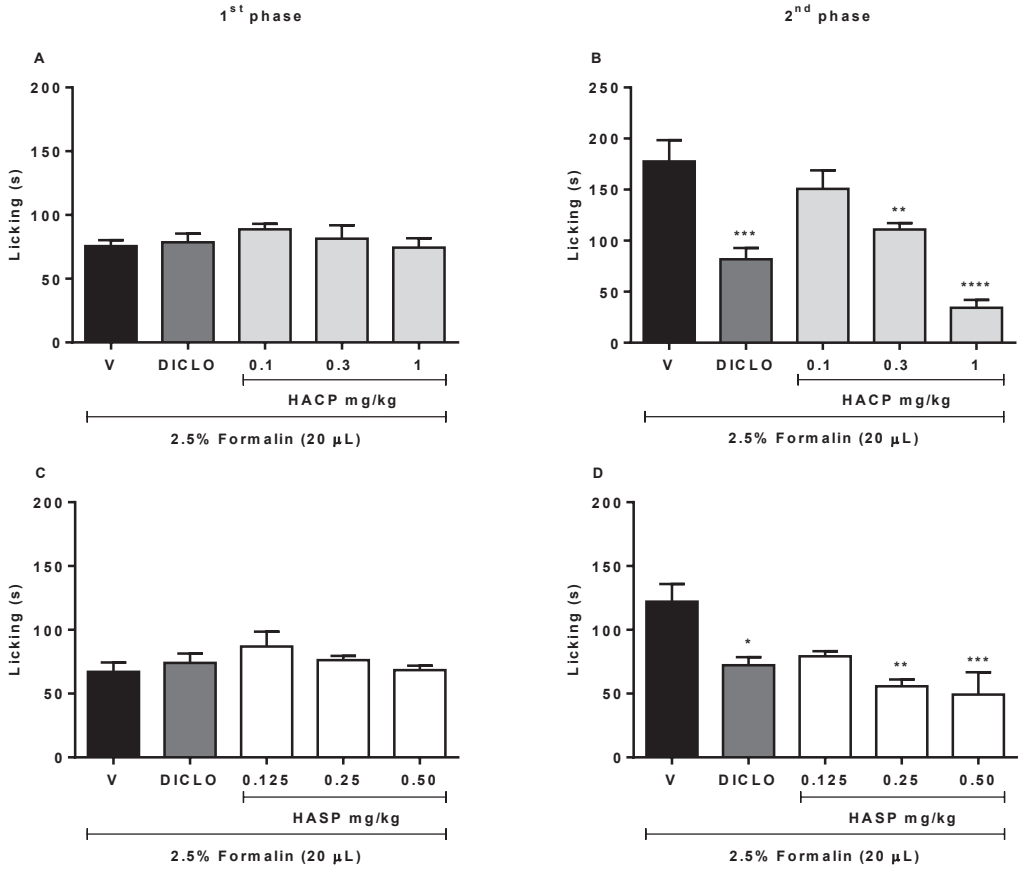

Mice were pretreated with vehicle (V: sterile saline, 10 mL/kg), diclofenac (DICLO: 10 mg/kg, i.p.), HACP (0.1, 0.3 and 1 mg/kg, i.p.) and HASP (0.125, 0.25 and 0.5 mg/kg, i.p.) 30 min before the formalin-induced nociception (2.5% FORM: 20 µL/i.pl.). The licking behavior was evaluated in first (Panel A and B: 0 - 5 min) and second (Panel B and D: 15 - 30 min) phases. Data were expressed as mean ± SEM (n= 5 - 8). *$P < 0.05$; **$P < 0.01$; ***$P < 0.001$; ****$P < 0.0001$ when compared to the vehicle (V) group (ANOVA followed by Bonferroni test).

5.3.6. HASP attenuated glutamate-induced nociception

Pretreatment with HASP (0.25 mg/kg, i.p.) and morphine (MOR: 1 mg/kg, s.c.) attenuated the glutamate-induced licking behavior by 48.3% and 74.0%, respectively (Fig. 4), when compared to the vehicle group (V: 177.2 ± 5.5 s).

FIG. 4. EFFECT OF HASP ON GLUTAMATE-INDUCED NOCICEPTION.

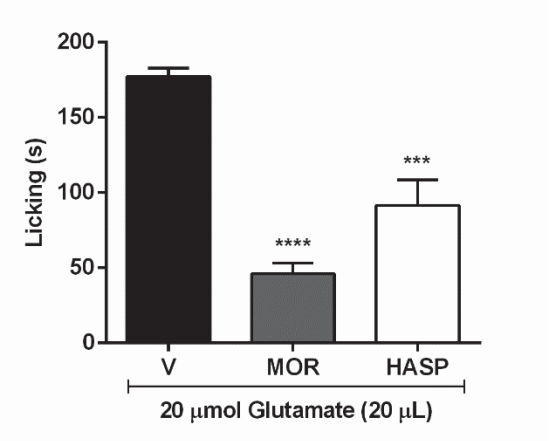

Mice were pretreated with vehicle (V: sterile saline, 10 mL/kg), morphine (MOR: 1 mg/kg, s.c.), HASP (0.25 mg/kg, i.p.) 30 min before the glutamate-induced nociception (20 µmol/20 µL, i.pl.). The licking behavior was evaluated for 15 min. Data were expressed as mean ± SEM (n= 5 - 6). *** *P*< 0.001; ****P < 0.0001 when compared to the vehicle (V) group (ANOVA followed by Bonferroni test).

5.3.7. HASP attenuated acetic acid-induced writhing and leukocyte infiltration

Pretreatments with HASP (0.25 mg/kg, i.p.) and dexamethasone (DEXA: 1 mg/kg, i.p.) reduced the number of abdominal contortions induced by 0.6% acetic acid (i.p.) by 30.0% and 57.5% (Fig. 5A), respectively, when compared to the vehicle group (V: 48.0 ± 2.4). Total leukocyte in the peritoneal cavity decreased by 49.5% and 45.7% in mice pretreated with HASP and DEXA (Fig. 5B), respectively, when compared to the vehicle group (V: 151.4 ± 19.4 x 10^6).

FIG. 5. EFFECT OF HASP ON ACETIC ACID-INDUCED WRITHING AND LEUKOCYTE INFILTRATION.

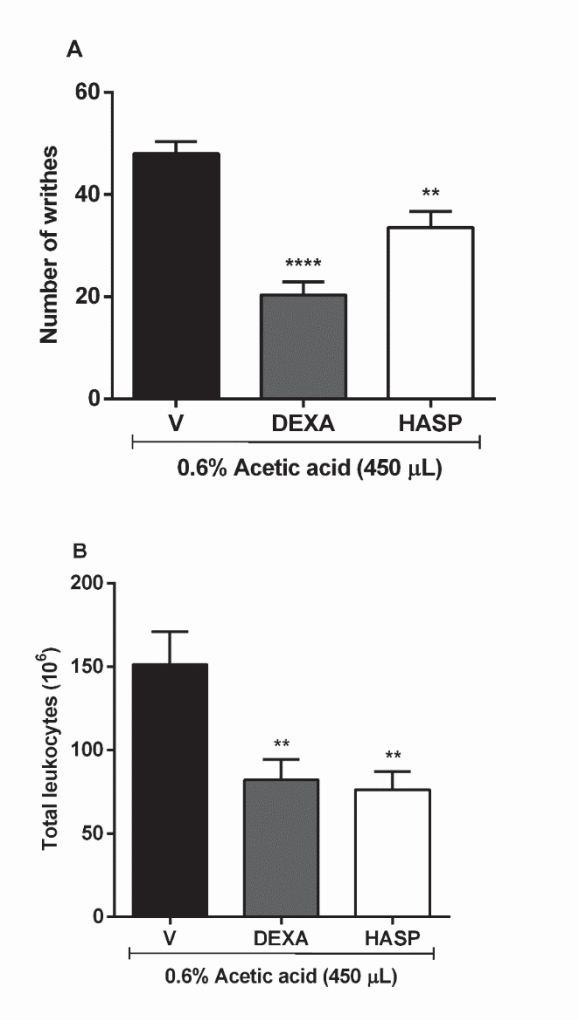

Mice were pretreated with vehicle (V: sterile saline, 10 mL/kg, i.p.), dexamethasone (DEXA: 1 mg/kg, i.p.) and HASP (0.25 mg/kg, i.p.) before the intraperitoneal injection of 0.6% acetic acid. The abdominal constrictions were evaluated cumulatively for 20 min (Panel A) and the total leukocyte count (10^6) in Neubauer chamber (Panel B). Data were expressed as mean ± SEM (n= 5 - 8). ***P* < 0.01; *****P* < 0.0001 when compared to the vehicle (V) group (ANOVA followed by Bonferroni test).

5.3.8. HASP attenuated carrageenan-induced mechanical allodynia and paw edema

Intraplantar injection of carrageenan induced an intense mechanical allodynia in mice pretreated with vehicle, decreasing from 1.7 ± 0.2 g (basal value) to 0.3 ± 0.1 g at 1 h, to 0.06 ± 0.1 g at 3 h, and to 0.04 ± 0.0 g at 6 h (Fig. 6A). Pretreatment with HASP (0.25 mg/kg, i.p.) significantly prevented the mechanical allodynia by 89.5%, 73.9%, 65.9%, 46.5% and 45.4%, 1, 2, 3, 4 and 5 h after carrageenan injection, respectively (Fig. 6A), when compared to the basal value (B: 1.6 ± 0.3 g). Similarly, the pretreatment with dexamethasone (DEXA: 1 mg/kg) also prevented the mechanical

allodynia by 86.5%, 62.9%, 69.8%, 65.2% and 60.8%, 1, 2, 3, 4 and 5 h after carrageenan injection, respectively (Fig. 6A), when compared to the basal value (B: 1.7 ± 0.2 g).

Intraplantar injection of carrageenan increased the mice paw thickness by 1.2 ± 0.1 mm at 1 h, by 1.6 ± 0.2 mm at 3 h, and by 1.8 ± 0.1 mm at 6 h (vehicle group, Fig. 6B). On the other hand, intraperitoneal pretreatment with HASP and DEXA significantly reduced the carrageenan-induced edema from 1 h up to 6 h after carrageenan injection when compared to the vehicle group (Fig. 6B).

3.9. HASP decreased myeloperoxidase (MPO) activity in paw tissue

Pretreatment with HASP (0.25 mg/kg, i.p.) and dexamethasone (DEXA: 1 mg/kg, i.p.) decreased the MPO activity induced by carrageenan by 54.4% and 47.8%, respectively (Fig. 6C), when compared to the vehicle group (V: 10.5 ± 1.0 O.D./mg of protein).

FIG. 6. EFFECT OF HASP ON CARRAGEENAN-INDUCED MECHANICAL ALLODYNIA, PAW EDEMA AND MPO ACTIVITY.

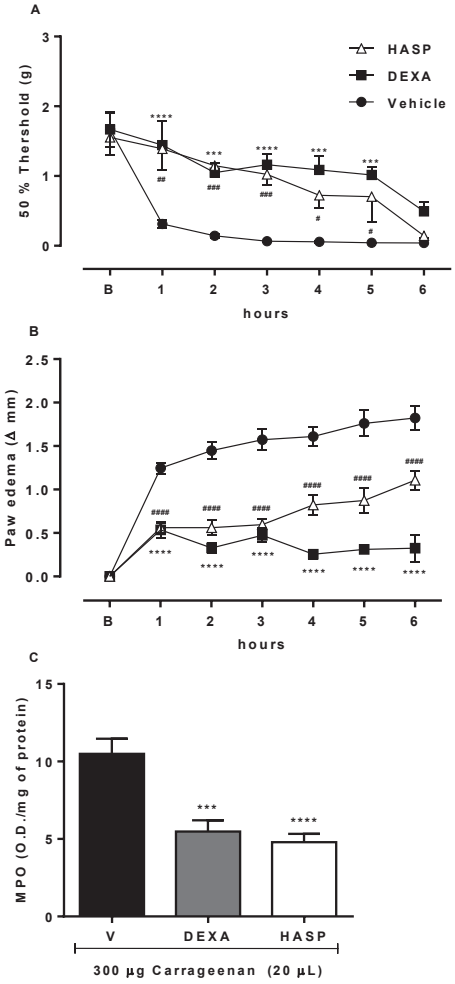

Mice were pretreated with vehicle (V: sterile saline, 10 mL/kg), dexamethasone (DEXA: 1 mg/kg, i.p.) and HASP (0.25 mg/kg, i.p.) 30 min before the intraplantar injection of carrageenan (300 µg/20 µL, i.pl.). Mechanical allodynia (Panel A) and paw edema (Panel B) were measured at basal (B), and 1, 2, 3, 4, 5 and 6 h after carrageenan injection. Data were expressed as mean ± SEM (n= 7 – 8, two-way ANOVA followed by Bonferroni test). MPO activity (Panel C) was measured in paw tissue after 3 h of carrageenan injection. Data were expressed as mean ± SEM (n= 8, one-way ANOVA followed by Bonferroni test). *$P < 0.05$; **$P < 0.01$; ***$P < 0.001$; ****$P < 0.0001$ when compared to the vehicle (V) group.

5.4. DISCUSSION

H. albus polysaccharides had never been studied before. Now, a simple and rapid method for extraction and fractionation was used to get an aqueous soluble polysaccharide fraction from *H. albus* leaves (HASP). Without multiple fractionation steps, the potential application of this polysaccharide fraction is increased.

On HPSEC analysis, HASP showed a polydisperse elution profile, containing a major peak, suggesting a heterogeneous fraction. Monosaccharide composition, methylation and NMR analyses strongly suggest that HASP is a complex polysaccharide fraction, mainly composed of type II arabinogalactan, with arabinans side chains, in addition to type I rhamnogalacturonan, mannan, starch and xylan in minor proportion.

Pectic polysaccharides from primary cell wall of dicotyledons are structurally very complex (HARRIS, 2006). In cell wall, type II arabinogalactan can be found associated to type I rhamnogalacturonans, linked at C-4 of rhamnosyl units (CARPITA; GIBEAUT, 1993). Type II arabinogalactans associated with type I rhamnogalacturonans have been isolated from leaves of other plants, such as *Arctium lappa*, *Maytenus ilicifolia*, *Nerium indicum*, *Diospyros kaki*, *Croton cajucara* and *Stevia rebaudiana* (CARLOTTO et al., 2016; CIPRIANI et al., 2006; DE OLIVEIRA et al., 2013; DONG; FANG, 2001; DUAN et al., 2003; NASCIMENTO et al., 2017). However, they have specific structural differences, such as monosaccharide composition, length of the side chains, presence of acetyl groups, proportion of 6-*O*Me-α-D-Gal*p*A, etc.

As previously mentioned, the genus *Handroanthus* is widely studied and presents metabolites with important pharmacological effects. However, there is no report in the scientific literature about *H. albus* polysaccharides and their possible pharmacological effects. Thus, in the present study, we investigated the antinociceptive and anti-inflammatory activities of a polysaccharide fraction isolated from *H. albus* leaves, to better know about this specie and validate its use in traditional medicine.

Formalin test is commonly used to evaluate nociception since it induces a distinct biphasic response. The first one (neurogenic pain) is associated with direct activation of nociceptors, and the second one (inflammatory pain) is described as an inflammatory response of damaged tissue and subsequent release of some mediators, such as histamine, prostaglandin, and serotonin. While classical nonsteroidal anti-inflammatory drugs inhibit the late phase, opioids inhibit both phases (HUNSKAAR; HOLE, 1987; TJØLSEN et al., 1992). As presented in Figure 3, HACP promoted antinociception in the late phase of formalin test. After, this crude polysaccharide fraction was fractionated to give HASP, and its theoretical ID_{50} was calculated. Similarly, HASP also reduced the nociceptive response during the second phase, indicating that both fractions presented potential anti-inflammatory effect. Based on the

formalin test, all subsequent experiments with HASP were performed using only the dose corresponding to its ID_{50}, to reduce the use of animals.

Glutamate is a major excitatory neurotransmitter of the central and peripheral nervous system. It is involved in the transmission of nociceptive signals and maintenance of pain response. Moreover, the activation of nociceptive neurons by glutamate can lead to the release of proinflammatory mediators like nitric oxide (NO) and NO-related substances, substance P and proinflammatory cytokines that could be involved in nociceptive transmission (WOZNIAK et al., 2012). Despite we did not observe reduction of nociceptive response in the first phase of formalin test, HASP effectively reduced the nociception induced by direct activation of nociceptors through intraplantar injection of glutamate, suggesting its involvement in the glutamatergic system.

Besides the nociception models described above, the abdominal contortion test induced by acetic acid is another very sensitive, convenient and classic method to study antinociceptive compounds. Acetic acid is an irritant agent that induces behavioral responses when administered intraperitoneally. These responses depend on the activation of peritoneal macrophages and mast cells, which release substances that sensitize visceral afferent nociceptive neurons (MULEY; KRUSTEV; MCDOUGALL, 2016). Our data demonstrated that intraperitoneal treatment with HASP inhibited the total number of abdominal contortions induced by acetic acid. Nascimento et al. (2015) also observed that the intraperitoneal administration of a type I arabinogalactan significantly reduced the number of abdominal contortions induced by acetic acid, but on the other hand, different from our results, the arabinogalactan did not reduce the nociception induced by intraplantar injection of formalin in mice. Therefore, the *in vivo* responses depend on specific characteristics of each polysaccharide such as molar mass, monosaccharide composition, length of the side chains, presence of specific groups and their distribution on the polymer, and types of glycosidic linkages, since these characteristics may play a critical role in the physicochemical and bioactive properties of the molecule (LIU, J.; WILLFÖR; XU, 2015). Moreover, as a complementary response, HASP also remarkably reduced leukocyte infiltration into the peritoneal cavity, confirming the involvement of inflammatory mediators in HASP antinociception. Considering the results above, we suggested that HASP has a potent anti-inflammatory activity.

To confirm this effect, we performed the carrageenan-induced acute inflammatory response. The intraplantar injection of carrageenan induce an intense immune cell migration, which is responsible for the production and release of pro-inflammatory mediators, such as lipid derivatives (prostaglandin E_2), histamine, and cytokines (interleukins). These mediators induce vascular permeability and plasma extravasation, resulting in edema, and also peripheral activation and/or sensitization of primary sensory neurons (nociceptors), contributing to the induction of mechanical allodynia (pain induced by normally innocuous mechanical stimuli) near to the injured tissue (DALLAZEN et al., 2019).

Some studies have shown the anti-inflammatory effect of polysaccharides through this experimental model. For instance, polysaccharides fractions characterized as pectins from peel and pulp of *Opuntia microdasys var. rufida* cladodes were able to reduce the carrageenan-induced paw edema (JOUINI et al., 2018). Carlotto et al. (CARLOTTO et al., 2016) showed the anti-edematogenic effect of three complex polysaccharide fractions, constituted mainly by arabinogalactans and type I rhamnogalacturonan, on carrageenan-induced paw edema. Here, we also noticed a significant reduction of carrageenan-induced paw edema with maintenance of the response until the sixth hour after carrageenan injection. In addition, we observed a decrease in carrageenan-induced mechanical allodynia and importantly, a significant decrease in MPO activity, which means a reduction of neutrophil migration to the inflamed site.

Thus, together with the reduced leukocyte infiltration observed after intraperitoneal injection of acetic acid, these results indicate that the polysaccharide fraction HASP has anti-inflammatory therapeutic potential.

5.5 CONCLUSIONS

A polysaccharide fraction from *H. albus* leaves, consisting mainly of type II arabinogalactan, showed antinociceptive and anti-inflammatory effects. The polysaccharide fraction was able to promote antinociception in the late phase of formalin-induced nociception, after direct activation of nociceptors through intraplantar injection of glutamate, and reducing the number of abdominal contortions induced by acetic acid. Moreover, HASP reduced leukocyte infiltration after intraperitoneal injection of acetic acid, and on carrageenan-induced paw edema model, showed anti-

edematogenic effect, decreased mechanical allodynia and myeloperoxidase activity. In addition to the remarkable antinociceptive and anti-inflammatory effects of HASP, its potential application is increased by the fact that it can be obtained through a simple extraction and fractionation protocol.

Acknowledgements

The authors would like to thank the Brazilian agencies *Conselho Nacional de Desenvolvimento Científico e Tecnológico* (CNPq – Grant number 449176/2014-2) and *Coordenação de Aperfeiçoamento de Pessoal de Nível Superior* (CAPES) for financial support. D.M.F. received a CAPES post-doctoral fellowship (PNPD/CAPES).

Conflict of Interests

The authors declare that there is no conflict of interest.

6 ARTIGO 3: POLYSACCHARIDE FRACTIONS FROM *Handroanthus heptaphyllus* and *Handroanthus albus* BARKS: STRUCTURAL CHARACTERIZATION AND CYTOTOXIC ACTIVITY

Juliane Carlotto [a], Lauro Mera de Souza [b], Thales Ricardo Cipriani [a,*]

[a] *Departamento de Bioquímica e Biologia Molecular, Universidade Federal do Paraná, CEP 81.531-980, CP 19046, Curitiba, PR, Brazil*

[b] *Instituto de Pesquisa Pelé Pequeno Príncipe, Faculdades Pequeno Príncipe, CEP 80250-060, Curitiba, PR, Brazil*

* Corresponding author:
trcipriani@ufpr.br (T.R. Cipriani)

ABSTRACT

Polysaccharide fractions named HHBSF and HABSF were obtained from aqueous extract of *Handroanthus heptaphyllus* and *Handroanthus albus* barks, respectively. Comparative analysis by methylation and NMR strongly suggest that HHBSF and HABSF are constituted by type II arabinogalactan (AG II), galactoglucomannan, type I rhamnogalacturonan (RGI), and arabinan. AG II in HABSF showed a higher percentage of 6-*O*- than 3-*O*-linked Gal*p* units. RG I in HABSF was constituted by non-methyl-esterified and non-acetylated 4-*O*-linked Gal*p*A units, while HHBSF presented methyl and non-methyl-esterified 4-*O*-linked Gal*p*A, *O*-acetylated at *O*-2 or *O*-3. These fractions were evaluated for their cytotoxicity against tumor cells potential. Using MTT cell viability assay, only HABSF significantly inhibited growth of MCF-7 (CC_{50} = 327 µg/mL) and Caco-2 (CC_{50} = 2258 µg/mL) cells in a concentration-dependent manner. HABSF showed simultaneously cell viability above 95% on Vero cells at dose of 327 µg/mL. Differences in fine structure of the polysaccharide could explain the different cytotoxic effects of HHBSF and HABSF. The potential antitumor effects of polysaccharides from *Handroanthus albus* barks has been demonstrated here and can be better explored in further studies.

6.1 INTRODUCTION

The global cancer burden is estimated to have risen to 18.1 million new cases and 9.6 million deaths in 2018 (The International Agency for Research on Cancer (IARC) Report, 2018). One in 5 men and one in 6 women worldwide develop cancer during their lifetime, and one in 8 men and one in 11 women die from the disease. Female breast and colorectal cancers are among top 3 cancers in terms of incidence and within the top 5 in terms of mortality (The International Agency for Research on Cancer (IARC) Report, 2018). Chemotherapy is one of the most common treatments for cancer. However, it has many limitations, since cancerous cells can develop drug resistance mechanisms and chemotherapies promote several side effects (DE MELO et al., 2011).

Natural products have played an important role in the development of new antitumor medicines. Barks of trees of the genus *Handroanthus* are well known by potent antiproliferative property, mainly due to their naphthoquinones, particularly lapachol and lapachone (UEDA et al., 1990; WOO et al. 2006). These molecules have been assayed against a range of tumor cell lines, including breast, esophageal, human cervix adenocarcinoma, leukemia and prostate lines, along with several multidrug-resistant cell lines (BALASSIANO et al., 2005; FIORITO et al., 2014; PINK; PLANCHON; et al., 2000; PINK; WUERZBERGER-DAVIS et al., 2000; PLANCHON et al., 2001; QUEIROZ et al., 2008; SUNASSEE et al., 2013). However, besides naphthoquinones, other active compounds could be found in barks of *Handroanthus* spp., such as polysaccharides.

Studies have demonstrated that polysaccharides from different sources exhibit antitumor activity either by immunopotentiation and restoration of tumor-suppressed host immune system, or inhibiting proliferation of various tumor cell lines by inducing cell apoptosis (MENG; LIANG; LUO, 2016; WANG et al., 2016; WU et al., 2015; YANG et al., 2019; ZHU et al., 2016).

Considering the potent antiproliferative property related to barks of species of the genus *Handroanthus* and the importance of polysaccharides as antitumor compounds, the aim of this study was to extract polysaccharides from *H. heptaphyllus* and *H. albus* barks, to characterize them structurally and to evaluate their cytotoxic effects on human colon cancer Caco-2 and human breast cancer MCF-7 cells.

6.2 MATERIALS AND METHODS

6.2.1. Plant material, extraction and fractionation

Barks of *H. heptaphyllus* were collected in the Municipal Garden of Barreirinha, located in Curitiba, PR, Brazil. Barks of *H. albus* were collected in Paulo Frontin, PR, Brazil. The plants are deposited in the Herbarium of the Botany Department of Federal University of Paraná, as vouchers nº. UPCB 85422 and 85420, respectively.

Dried and milled barks (100 g) were defatted and depigmented with $CHCl_3$:MeOH (500 mL, 2:1, v/v) under conditions of reflux for 2 h (x 3), then were extracted with H_2O (500 mL) under conditions of reflux for 2 h (x 3). The aqueous extracts were obtained by vacuum filtration, combined, evaporated to a small volume (200 mL), and added to cold EtOH (x 3 vol.). The resulting precipitate was separated by vacuum filtration, dissolved in H_2O, dialyzed at a 12-14 kDa cut-off membrane and freeze-dried, to give the crude polysaccharide fractions HHBCP (*H. heptaphyllus* barks - crude polysaccharide) and HABCP (*H. albus* barks - crude polysaccharide). These fractions were dissolved in H_2O (200 mL) at room temperature, then submitted to freeze-thawing process (GORIN; IACOMINI, 1984), resulting in cold water soluble and insoluble fractions, which were separated by centrifugation (9,000 rpm, 15 min, 10 ºC) and freeze-dried. The following fractions were thus obtained: HHBSF (*H. heptaphyllus* barks - soluble fraction), and HABSF (*H. albus* barks - soluble fraction), HHBIF (*H. heptaphyllus* barks - insoluble fraction), and HABIF (*H. albus* barks - insoluble fraction).

6.2.2. HPSEC analysis

High-performance size-exclusion chromatography (HPSEC) was performed on a Waters chromatograph equipped with four Ultrahydrogel columns connected in series (2000, 500, 250, 120; with exclusion sizes of 7×10^6, 4×10^5, 8×10^4, and 5×10^3 Da; Milford, MA, USA), attached to a Waters 2410 refraction index (RI) detector (Milford, MA, USA). HPSEC-RI data were collected and analyzed using the Wyatt Technology ASTRA software, version 4.70.07. The eluent was 0.1 M aq. $NaNO_2$ containing 200 ppm aq. NaN_3, at 0.6 mL/min. The sample, previously filtered through a membrane (0.22 µm), was injected (100 µL loop) at a concentration of 1 mg/mL, and analyzed at 25 °C. The peak elution times were compared with a calibration curve

obtained using standard dextrans (266 kDa, 124 kDa, 72.2 kDa, 40.2 kDa, 17.2 kDa, 9.4 and 5 kDa (from Sigma).

6.2.3. Monosaccharide analysis

The samples HHBSF and HABSF (2 mg) were hydrolyzed with 1 M TFA (1 mL) at 100 ºC for 16 h, the solutions were then evaporated, and the residues dissolved in H_2O (1 mL). The hydrolysates were treated with $NaBH_4$ (2 mg), and, after 18 h, concentrated HOAc (0.5 mL) was added, the solutions evaporated to dryness and the resulting boric acid removed as trimethyl borate by co-evaporation with MeOH. Acetylation was carried out with Ac_2O-pyridine (1:1 v/v, 0.6 mL) at room temperature for 18 h, and the resulting alditol acetates were extracted with $CHCl_3$. These were analyzed by GC-MS (Varian Saturn 2000R - 3800 gas chromatograph coupled to a Varian Ion-Trap 2000R mass spectrometer), using a DB-225 column (30 m x 0.25 mm i.d.) programmed from 50 to 220 ºC at 40 ºC/min, with He as carrier gas. Components were identified by their typical retention times and electron ionization mass spectra relative to alditol acetates prepared from standard monosaccharides (Sigma-Aldrich). The monosaccharide analysis result was given as mol%, calculated according to Pettolino et al. (2012).

Uronic acid content was determined spectrophotometrically using the *m*-hydroxybiphenyl method, according to Filisetti-Cozzi and Carpita (1991).

6.2.4. Carboxyl-reduction and methylation analysis

HHBSF and HABSF (5 mg) were per-*O*-methylated according to the method of Ciucanu and Kerek (1984), using DMSO-MeI and powdered NaOH. The products were hydrolyzed using two different conditions: 1) with 1 M TFA (1 mL) at 100 ºC for 16 h, followed by TFA evaporation, and dissolution of the hydrolysate in H_2O (1 mL); or 2) with 72% H_2SO_4 (w/v; 250 µL) at 0 °C for 1 h, followed by addition of H_2O (2 mL), heating at 100 °C for 16 h, neutralization with $BaCO_3$ and filtration. The mixture of *O*-methyl aldoses obtained by both hydrolysis methods was reduced with $NaBD_4$ (2 mg), and acetylated as described above (section 2.3) to give a mixture of partially *O*-methylated alditol acetates. These were analyzed by GC-MS using the same conditions as described for alditol acetates, except the final temperature was 215 ºC.

They were identified by their typical retention times and electron ionization mass spectra relative to partially *O*-methylated alditol acetates prepared from standard monosaccharides (Sigma-Aldrich), according to Sassaki et al. (2005).

HHBSF and HABSF (20 mg) were carboxyl-reduced by the carbodiimide method, using $NaBH_4$ as the reducing agent (Taylor and Conrad, 1972). After dialysis at a 6–8 kDa cut-off membrane, the material was freeze-dried and submitted to another cycle of carboxyl-reduction. The carboxyl-reduced polysaccharides were then submitted to the methylation protocol and derivatization to partially *O*-methylated alditol acetates.

6.2.5. NMR spectroscopy

HSQC/DEPT correlation map was obtained using a 400 MHz Bruker model DRX Avance spectrometer with a 5 mm inverse probe, at 50 °C in D_2O. Chemical shifts (δ) were expressed in ppm relative to acetone at δ 30.2/2.22 ($^{13}C/^{1}H$). The correlation map was handled using the Topspin® software from Bruker and the $^{13}C/^{1}H$ correlations were assigned based on literature data.

6. 2.6. Phenolic compounds and protein contents

The phenolic compounds content was determined as gallic acid equivalent (GAE, % w/w), according to the spectrophotometric method of Singleton e Rossi (SINGLETON; ROSSI; 1965), and the protein content was determined spectrophotometrically according to Bradford (1976).). The total sugar content was determined according to Dubois et al. (1956), using a calibration curve of arabinose: galactose: glucose (1:1:1), and was expressed as arabinose: galactose: glucose equivalent (AGGE, % w/w).

6. 2.7. Cell lines

MCF-7 cells (human breast adenocarcinoma cell line), purchased from the Cell Bank of Rio de Janeiro, Brazil (BCRJ code 162), and Vero cells (African green monkey kidney cell line), purchased from the Cell Bank of Rio de Janeiro, Brazil (BCRJ code 245), were cultivated in DMEM/F-12 medium (Dulbecco's Modified Eagle

Medium/Nutrient Mixture F-12), supplemented with 10% fetal bovine serum (FBS), and 1% of antibiotic (penicillin/streptomycin). Caco-2 cells (human colon carcinoma cell line), purchased from the Cell Bank of Rio de Janeiro, Brazil (BCRJ code 0059), were cultivated in DMEM/F-12 medium, supplemented with 20% FBS, and 1% of antibiotic (penicillin/streptomycin). Cultures were maintained in an incubator with controlled humidified atmosphere (95% air and 5% CO_2) at 37 °C.

6.2.8. Cell viability assay

Cells were cultured at a density of 5 x 10^4 cells/well diluted in FBS free medium in a 96-well plate and incubated overnight in an incubator with controlled humidified atmosphere (95% air and 5% CO_2) at 37 °C. Later, the culture medium was removed, and the cells were treated with vehicle (water 1 %), HABSF (10-2000 µg/mL), HHBSF (20-2000 µg/mL), cisplatin (2.5-100 µg/mL) or 5-fluorouracil (2-200 µg/mL), all them diluted in medium supplemented with FBS. After 48 h of incubation, the medium was removed and MTT (3-(4,5-dimethylthiazol-2-yl)-2,5-diphenyltetrazolium bromide) solution (100 µL, 0.5 mg/mL) was added to each well and incubated for 3 h at 37 °C. MTT solution was then aspired and 100 µL of dimethyl sulfoxide (Me_2SO) were added to solubilize formazan crystals. The absorbance was read at 575 nm. The treatment with vehicle alone represented the control, and cell survival was expressed as a percentage of control. The experiments were performed in quadruplicate.

6.2.9. Statistical analyses

The results were presented as mean ± S.E.M. and evaluated with one-way analysis of variance (ANOVA), followed by the Dunnett multiple comparison test. The CC_{50} value (i.e. concentration of HABSF and HBBSF (µg/mL) required for the reduction of cell viability by 50%) was determined by nonlinear regression analysis (sigmoidal dose-response). Significant difference was considered when $^*P < 0.05$; $^{**}P < 0.01$; $^{***}P < 0.001$; $^{****}P < 0.0001$, and all the analyzes were performed using the GraphPad Prism® version 7.0 (GraphPad Software, San Diego, USA).

6.3 RESULTS AND DISCUSSION

6.3.1. Extraction and structural analysis of the polysaccharide fractions

Barks of *H. heptaphyllus* and *H. albus,* two native trees species from Brazil, were used to extract polysaccharides. Barks from each tree (100 g) were defatted and depigmented and then extracted with boiling water. The aqueous extract was treated with excess EtOH to provide a crude precipitate of polysaccharides of *H. heptaphyllus* (HHBCP, 1.43 %) and *H. albus* (HABCP, 1.19 %). These crude extracts were then submitted to freeze-thawing process until no more precipitate appeared, resulting in cold water soluble (HHBSF, 0.76 % and HABSF, 0.42 %) and insoluble (HHBIF, 0.55 % and HABIF, 0.77 %) fractions. Considering the high solubility of HHBSF and HABSF in relation to HHBIF and HABIF, only the first ones were studied here.

HHBSF showed a single peak on HPSEC-RI and the retention time (R_t) was 57.7 min, which were out of the calibration curve range, corresponding to molecular weight (Mw) < 5 kDa (Fig. 1). HABSF showed a heterogeneous elution profile, suggesting the presence of a complex polysaccharide fraction. The first peak of HABSF had a molecular weight of 16.6 kDa (R_t 53.7 min) and the second peak 6.3 kDa (R_t 56.5 min) (Fig. 1).

FIG. 1. ELUTION PROFILE OF HABSF AND HHBSF ON HPSEC.

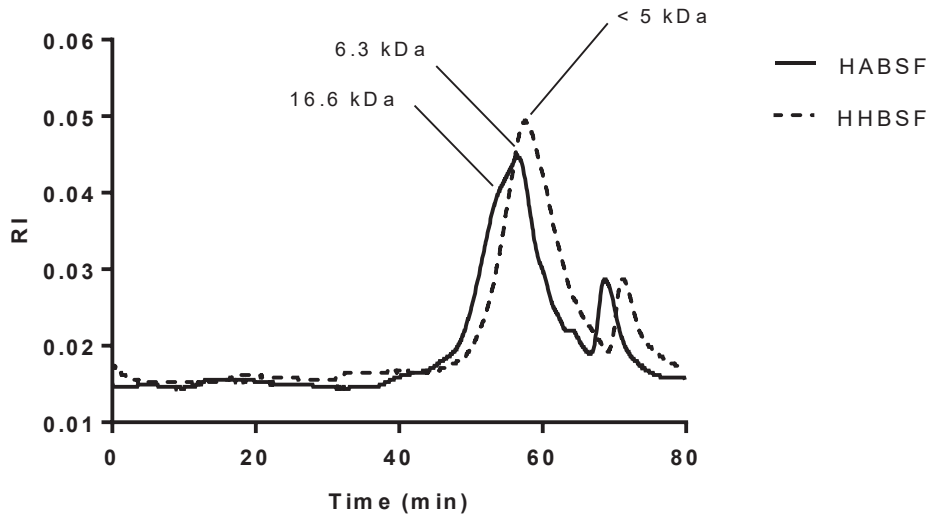

HHBSF and HABSF showed total sugar content of 47 g% and 45 g% of AGGE. Monosaccharide composition analysis of both fractions showed the presence of several monosaccharides, including mainly arabinose, galactose, glucose and mannose (Table 1). Moreover, HHBSF and HABSF showed phenolic compounds content of 17 g% and 15.3 g% of GAE, respectively, and did not show protein.

TABLE 1. MONOSACCHARIDE COMPOSITION OF HABSF AND HHBSF.

Fractions	Monosaccharides							
	mol%							g%
	Rha	Fuc	Ara	Xyl	Man	Gal	Glc	UA
HABSF	3.6	-	12.1	5.8	17.4	38.4	22.7	15.4
HHBSF	9.5	0.7	18.8	3.5	13.4	21.9	32.2	7.2

Rha (rhamnose), Fuc (fucose), Ara (arabinose), Xyl (xylose), Man (mannose), Gal (galactose), Glc (glucose), UA (uronic acid).

Glycosidic linkage analysis by methylation demonstrated the presence of several partially *O*-methylated alditol acetates derivatives (Table 2), which is characteristic of complex polysaccharide fractions. An excessive number of non-reducing end-units was detected, since the ratio of terminals to branch points was very high, mainly terminals of glucose and rhamnose. The methylation analysis was repeated using another hydrolysis procedure and the result was confirmed, indicating that these terminals could be linked to the phenolic compounds found in the fractions.

Methylation analysis strongly suggests that type II arabinogalactan (AG II) and galactoglucomannan were the major polysaccharides presents in HABSF. The partially *O*-methylated alditol acetates derivatives demonstrated that glucose and mannose units are mainly linked at O-4, as shown by presence of the derivatives 2,3,6-Me_3-Glc (12.9%) and 2,3,6-Me_3-Man (14.6%), indicating (1→4)-linked Glc*p* and (1→4)-linked Man*p*. Moreover, it was observed 2,3-Me_2-Man (3.9%) and non-reducing end-units of galactose (9.4%), suggesting galactose branches linked at O-6 of Man. A galactoglucomannan consist of a main chain of (1→4)-linked β-D-Glc*p* and (1→4)-linked β-D-Man*p*, and could be branched at O-6 position of Man*p* and/or Glc*p* units with β-D-Gal*p* units (PETTOLINO et al., 2012).

TABLE 2. PROFILE OF PARTIALLY O-METHYLATED ALDITOL ACETATES AND MONOSACCHARIDE STRUCTURES OF HABSF AND HHBSF OBTAINED ON METHYLATION ANALYSIS.

***O*-Me-alditol acetate**	**Structure**	**HABSF**	**HHBSF**
		mol%	
Arabinose			
2,3,5-Me_3-Ara	Ara*f*-(1→	1.1	3.8
2,5-Me_2-Ara	→3)-Ara*f*-(1→	1.1	1.6
2,3-Me_2-Ara	→5)-Ara*f*-(1→	0.6	3.3
2-Me-Ara	→3,5)-Ara*f*-(1→	1.4	1.9
3-Me-Ara	→2,5)-Ara*f*-(1→	2.3	1.0
Xylose			
2,3-Me_2-Xyl	→4)-Xyl*p*-(1→	4.7	6.2
Rhamnose			
2,3,4-Me_3-Rha	Rha*p*-(1→	1.9	13.2
3,4-Me_2-Rha	→2)-Rha*p*-(1→	0.5	-
3-Me-Rha	→2,4)-Rha*p*-(1→	1.7	1.2
Galactose			
2,3,4,6-Me_4-Gal	Gal*p*-(1→	9.4	4.1
2,4,6-Me_3-Gal	→3)-Gal*p*-(1→	3.6	3.3
2,3,4-Me_3-Gal	→6)-Gal*p*-(1→	11.7	3.2
2,4-Me_2-Gal	→3,6)-Gal*p*-(1→	2.5	1.7
Manose			
3,4,6-Me_3-Man	→2)-Man*p*-(1→	3.7	3.6
2,3,6-Me_3-Man	→4)-Man*p*-(1→	14.6	5.1
2,3,4-Me_3-Man	→6)-Man*p*-(1→	5.5	6.4
3,6-Me_2-Man	→2,4)-Man*p*-(1→	2.3	0.6
2,3-Me_2-Man	→4,6)-Man*p*-(1→	3.9	0.6
3,4-Me_2-Man	→2,6)-Man*p*-(1→	1.4	-
Glucose			
2,3,4,6-Me_4-Glc	Glc*p*-(1→	12.3	13.6
2,3,6-Me_3-Glc	→4)-Glc*p*-(1→	12.9	18.8
2,6-Me_2-Glc	→3,4)-Glc*p*-(1→	-	2.4
2,3-Me_2-Glc	→4,6)-Glc*p*-(1→	-	1.1
3,4-Me_2-Glc	→2,6)-Glc*p*-(1→	0.9	3.3

Methylation analysis of HABSF suggests the presence of partially *O*-methylated alditol acetates of 2,4,6-Me_3-Gal (3.6%), 2,4-Me_2-Gal (2.5%) and 2,3,4-Me_3-Gal (11.7%), demonstrating that galactose units are mainly linked at O-3, O-3,6 and O-6, respectively. These derivatives are presents in AG II, which consist of (1→3)-linked β-D-Gal*p* and (1→6)-linked β-D-Gal*p* chains connected to each other by (1→3,6)-linked branch point. Most of the remaining O-3 or O-6 galactosyl positions could be linked by non-reducing end-units of Ara*f* (CARPITA; GIBEAUT, 1993).

The presence of 2,3-Me_2-Ara (0.6%), 2-Me_2-Ara (1.4%) and 3-Me_2-Ara (2.3%) could indicate a arabinan, since it demonstrates (1→5)-, (1→3,5)- and (1→2,5)-linked Ara*f* units, respectively. Arabinans are mostly constituted by 5-linked arabinofuranosyl units forming short helical chains, and arabinosyl units could be connected to each other at O-2 and O-3, forming a diverse group of branched arabinans (CARPITA; GIBEAUT, 1993). The derivative 2,5-Me_2-Ara (1.1%) indicated (1→3)-linked Araf units, probably present as side chains.

Most of the arabinan and some of the arabinogalactan of primary cell walls is present as covalently linked side chains of type I rhamnogalacturonan (RG I), attached to the O-4 of rhamnosyl residues (CARPITA; GIBEAUT, 1993). Indeed, (1→2)-linked α-L-Rha*p* units have been observed (3,4-Me_2-Rha, 0.5%), which together with the fact that uronic acid has been detected by colorimetric assay, suggests the presence of RG I, which contains a backbone of the repeating disaccharide →2)-α-D-Gal*p*A-(1→4)-α-L-Rha*p*-(1→. Galacturonic acid residues also could be present in homogalacturonan (HG), a linear homopolymer of (1→4)-linked α-D-Gal*p*A units, which can be interspersed between RG I (MOHNEN, 2008).

Partially *O*-methylated alditol acetates derivatives of acid monosaccharides are less volatile and resistant to analysis by GC-MS. Moreover, glycosidic linkages including anomeric carbon of uronic acids units are more resistant to acid hydrolysis, and then rhamnose residues could be underestimated on methylation analysis (Taylor and Conrad, 1972) Thus, HABSF was submitted to carboxyl-reduction prior to methylation analysis to transform acid monosaccharides to their corresponding neutral monosaccharides. HABSF did not show 2,3,6-Me_3-Gal and showed 0.5% of 3,4-Me_2-Rha in methylation analysis, while carboxyl-reduced HABSF showed 13.9% of 2,3,6-Me_3-Gal and increase 3,4-Me_2-Rha to 3.7%, although the content of 3-Me-Rha was similar (1.2%). This result indicated that (1→4)-linked Gal*p*A, and (1→2)- and (1→2,4)-linked Rha*p* residues are present in HABSF, confirming the presence of RG I. The ratio between partially *O*-methylated alditol acetates of 3,4-Me_2-Rha (3.7%) and 3-Me-Rha (1.2%) indicates that approximately 1/4 of Rha*p* units are branched in the RG I. Moreover, the results showed that there is more (1→4)-linked Gal*p*A present than (1→2)- and (1→2,4)-linked Rha*p*, which indicates the presence of homogalacturonan besides RG I.

Methylation analysis results also indicated the presence of other polysaccharides in minor proportions in HABSF. The presence of →4)-Xyl*p*-(1→ (4.7%) could indicate a xylan (CARPITA; GIBEAUT, 1993; PETTOLINO et al., 2012), and the presence of →2)-Man*p*-(1→ (3.7%) and →6)-Man*p*-(1→ (5.5%) could indicate a mannan, although this type of backbone is not common in plants.

Methylation analysis of HHBSF was also compatible with the presence of AG II and galactoglucomannan as major polysaccharides. HHBSF showed only 5.1% of 2,3,6-Me_3-Man, despite showing 18.8% of 2,3,6-Me_3-Glc. Glucomannans have a main chain of (1→4)-linked β-D-Glc*p* and β-D-Man*p* units, thus the large amount of 2,3,6-Me_3-Glc in the fraction could indicate starch. RG I was also observed in minor proportion, once the carboxyl-reduced HHBSF showed 5% of 2,3,6-Me_3-Gal, 1.8 % of 3,4-Me_2-Rha and 1.3% of 3-Me-Rha. Small structural differences in AG II have also been observed in comparison with HABSF, since HHBSF had lower percentage of (1→6)-linked β-D-Gal*p* (3.2%) and the arabinan side chains have a major proportion of →5)-Ara*f*-(1→ (3.3%).

In accordance with the methylation data, NMR analysis was compatible with the presence of AG II in HABSF (Fig. 2A). The $^{13}C/^{1}H$ HSQC/DEPT correlation map showed signal at δ 103.2/4.47, which was assigned to C-1/H-1 of (1→6)- and (1→3,6)-linked β-D-Gal*p* units, and at δ 103.6/4.69 and δ 104.2/4.63 to internal (1→3)-linked β-D-Gal*p* units and terminals of β-D-Gal*p* units, respectively (DO NASCIMENTO, G. E.; IACOMINI; CORDEIRO, 2017). Correlation at δ 80.0/3.73 was assigned to C-3/H-3 of (1→3,6)-linked β-D-Gal*p* units, and at δ 69.4/4.05 to C-6/H-6 of (1→6)- and (1→3,6)-linked β-D-Gal*p* units (DO NASCIMENTO; IACOMINI; CORDEIRO, 2017). Anomeric signals of terminal, (1→5)- and (1→3,5)-linked α-L-Araf units could be observed at δ 109.1/5.25, δ 107.4/5.08 and δ 107.2/5.21, respectively (CANTU-JUNGLES et al., 2017).

$^{13}C/^{1}H$ HSQC of HABSF also showed anomeric correlations at δ 99.7/5.36 and 98.8/5.14, which were assigned to α-L-Rha*p* units and α-D-Gal*p*A units, respectively. Correlations at δ 77.8/4.46 and δ 71.6/4.74 were attributed to C-4/H-4 and C-5-H-5 of (1→4)-linked α-D-Gal*p*A units, respectively, and the presence of C-6/H-6 of α-L-Rha*p* units was shown by resonances at δ 16.7/1.29 and 16.6/1.29. These correlations are characteristic of RG I (CARLOTTO et al., 2016; OVODOVA et al., 2009; POPOV et al., 2011). Moreover, anomeric signals at δ 102.9/4.52 and δ 100.6/4.78 were assigned to

C-1/H-1 of (1→4)-linked β-D-Glc*p* and β-D-Man*p* units, respectively (BARBIERI et al., 2017; CANTU-JUNGLES et al., 2017; GUO, Q. et al., 2012). These correlations, in addition to that at δ 76.5/3.79, which can be attributed to C-4/H-4 of (1→4)-linked β-D-Glc*p* and (1→4)-linked β-D-Man*p* units, could be from galactoglucomannan (BARBIERI et al., 2017; CANTU-JUNGLES et al., 2017; GUO, Q. et al., 2012). These results confirms the methylation analysis data.

FIG. 2. $^{13}C/^{1}H$ HSQC/DEPT OF HABSF (A) AND HHBSF (B).

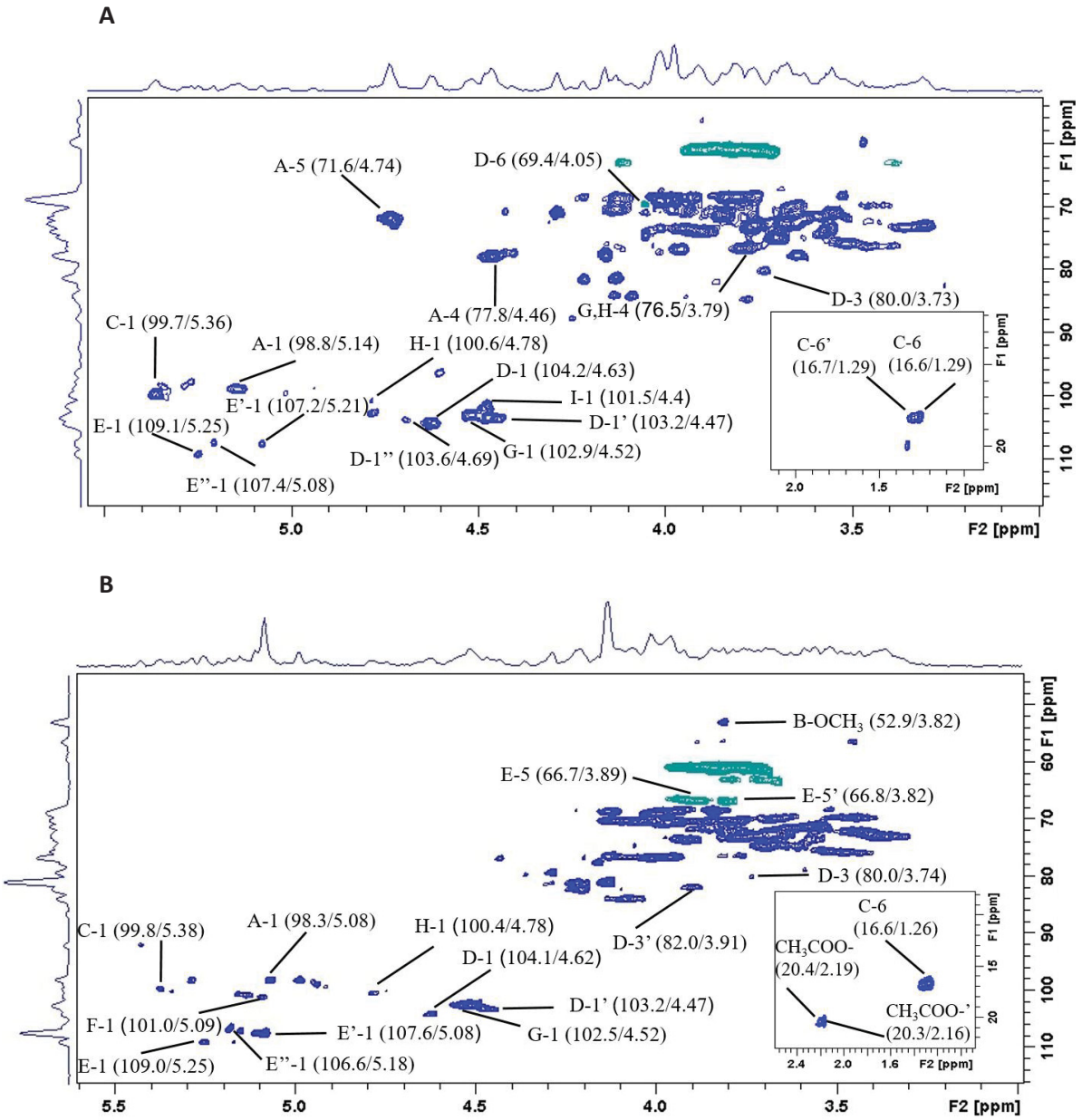

Solvent D_2O at 50 °C; numerical values are in δ ppm. A (α-D-Gal*p*A), B (6-*O*Me-α-D-Gal*p*A), C (α-L-Rha*p*), D, D' and D'' (β-D-Gal*p*), E, E' and E'' (α-L-Ara*f*), F (α-D-Glc*p*), G (β-D-Glc*p*), H (β-D-Man*p*) and I (β-D-Xyl*p*). The letters are followed by the carbon number of the monosaccharide unit.

HHBSF showed a similar $^{13}C/^{1}H$ HSQC/DEPT correlation map (Fig. 2B). The correlations at δ 103.2/4.47 and δ 104.1/4.62 were assigned to (1→6)- and (1→3,6)-linked β-D-Gal*p* units and to terminals of β-D-Gal*p* units, respectively. The correlation at δ 82.0/3.91 was attributed to C-3/H-3 of (1→3)-linked β-D-Gal*p* units (do Nascimento et al., 2017). Anomeric correlations of terminal, (1→5)- and (1→3,5)-linked α-L-Araf units can be observed at δ 109.0/5.25, δ 107.6/5.08 and δ 106.6/5.18, respectively (CANTU-JUNGLES et al., 2017). Inverted substituted C-5/H-5 of (1→5)- and (1→3,5)-linked α-L-Araf units appeared at δ 66.7/3.89 and 66.8/3.82.

HHBSF demonstrated RG I in minor proportion compared with HABSF. Anomeric correlations at δ 99.8/5.38 and δ 98.3/5.08 were assigned to α-L-Rha*p* units and α-D-Gal*p*A units, respectively. The correlation at δ16.1/1.26 was attributed to C-6/H-6 of α-L-Rha*p* units, and that at 52.9/3.82 (–CO_2-$\underline{CH_3}$) is typical of 6-*O*Me-α-D-Gal*p*A units, indicating the existence of methyl- and non-methyl-esterified (1→4)-linked α-D-Gal*p*A units in HHBSF. Moreover, typical correlations of acetyl groups were observed at δ 20.4/2.19 and 20.3/2.16 (NASCIMENTO et al., 2013; OVODOVA et al., 2009). They can be present in rhamnogalacturonans, frequently substituting Gal*p*A units at O-2 or O-3 (CARLOTTO et al., 2016; MOHNEN, 2008). Correlation at δ 102.5/4.52 was assigned to C-1/H-1 of (1→4)-linked β-D-Glc*p* units, and that at δ 100.4/4.78 to C-1/H-1 of (1→4)-linked β-D-Man*p* units (CANTU-JUNGLES et al., 2017; GUO et al., 2012), indicating the presence of glucomannan in the fraction.

In our previous work, polysaccahrides from *H. heptaphyllus* leaves were described (CARLOTTO et al., 2019). The main polymer found in leaves was AG II. RG I was identified in minor proportion and galactoglucomannan was not observed. AGII anchored in RGI have been already reported in many plants (CANTU-JUNGLES et al., 2017; CARLOTTO et al., 2016; DO NASCIMENTO; IACOMINI; CORDEIRO, 2017; NASCIMENTO et al., 2013, 2017), but they may differ in their structural details, such as relative proportion of (1→3)-, (1→6)- and (1→3,6)-linked β-D-Gal*p* units, type of non-reducing end-units, number and size of side chains, presence and distribution of acetyl groups, proportion of 6-*O*Me-D-Gal*p*A and molecular weight.

In type I cell walls, galactoglucomannans could interlock cellulose microfibrils (CARPITA; GIBEAUT, 1993). Galactoglucomannans, besides being common in seeds, have already been previously reported, for example, in *açaí* berries (*Euterpe oleraceae*) (CANTU-JUNGLES et al., 2017), gabiroba fruits (*Campomanesia*

xanthocarpa) (BARBIERI et al., 2017), apple (*Malus domestica*) (NARA et al., 2004), wood of Norway spruce (*Picea abies*) (YVONNE et al., 2017) and stems of *Dendrobium huoshanense* (PAN et al., 2012).

6.3.2. Cytotoxicity of the polysaccharide fractions

HABSF and HHBSF were tested for their effects on the proliferation of human colon carcinoma cell line (Caco-2), human breast adenocarcinoma cell line (MCF-7) and healthy cells of African green monkey kidney cell line (Vero) using the MTT cell viability assay (Fig. 3). The results showed that only HABSF significantly inhibited the growth of Caco-2 and MCF-7 cells in a concentration-dependent manner. The CC_{50} values for MCF-7 and Caco-2 cells were 327 µg/mL and 2258 µg/mL, respectively, indicating a potency almost 7 times higher on MCF-7 cells. HABSF showed simultaneously cell viability above 95% on Vero cells at the dose of 327 µg/mL, suggesting that the fraction is not toxic to normal cells. The cytotoxic activity of polysaccharides from *H. albus* barks has been demonstrated here and may be better explored in the future.

Previous studies have demonstrated that polysaccharides from different fonts exhibit antitumor activity either by activating the immune response of the host organism, or by inhibiting the proliferation of tumor cell lines by inducing cell apoptosis (MENG; LIANG; LUO, 2016; WANG et al., 2016; WU et al., 2015; YANG et al., 2019; ZHU et al., 2016).

Both HABSF and HHBSF polysaccharide fractions are constituted by AG II, galactoglucomannan and RG I, but only HABSF demonstrated cytotoxicity on Caco-2 and MCF-7 cells. AG II in HHBSF has a higher proportion of side chains of (1→5)-linked α-L-arabinans, while HABSF has a higher percentage of (1→6)-linked Gal*p* units. RG I in HABSF is constituted only by non-methyl-esterified α-D-Gal*p*A, while HHBSF presents both methyl and non-methyl-esterified (1→4)-linked α-D-Gal*p*A units, which can be *O*-acetylated at O-2 or O-3. Therefore, these structural differences of HABSF and HHBSF may appear to affect their activities.

FIG. 3. EFFECT OF HABSF AND HHBSF ON CELL VIABILITY OF MCF-7 (A AND B), CACO-2 (C AND D) AND VERO (E).

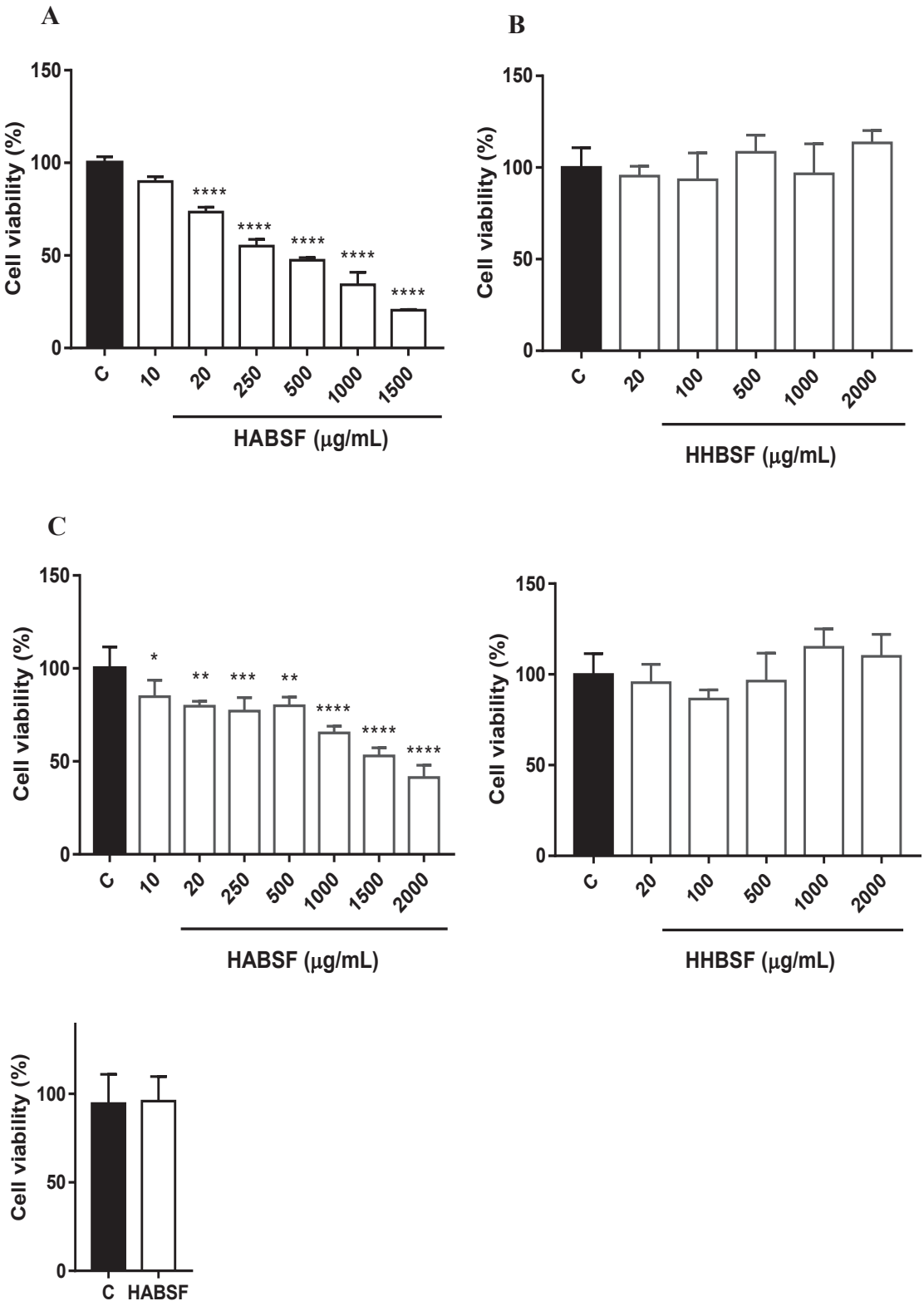

MCF-7 and Caco-2 cells were treated with control (C: water 1%), HABSF (10-2000 µg/mL) or HHBSF (20-2000 µg/mL). Vero cells were treated with vehicle (C: water 1%), and HABSF 327 µg/mL. The treatment was carried out 48 h before MTT assay. The results are expressed as mean ± S.E.M. **P <0.05, ** P <0.005, ***P < 0.001* and *****P < 0.0001* when compared to vehicle group (C).

6.4 CONCLUSION

Polysaccharide fractions obtained from *H. heptaphyllus* and *H. albus* barks were structurally characterized and their cytotoxicity effect on cancer and healthy cell lines were evaluated. Only the fraction derived from *H. albus* (HABSF) significantly inhibited the growth of MCF-7 (CC_{50} 327 µg/mL) and Caco-2 (CC_{50} 2258 µg/mL) cells in a concentration-dependent manner. The fractions from both plants are mainly constituted by AG II, galactoglucomannan and RG I. Thus, differences in the chemical structure of the polysaccharides could explain the different effects observed on tumor cells.

Acknowledgements

The authors would like to thank the Brazilian agencies *Conselho Nacional de Desenvolvimento Científico e Tecnológico* (CNPq – Grant number 449176/2014-2) and *Coordenação de Aperfeiçoamento de Pessoal de Nível Superior* (CAPES) for financial support.

Conflict of Interests

The authors declare that there is no conflict of interest.

7 ARTIGO 4: BIOGUIDED FRACTIONATION OF THE EXTRACTS FROM BARKS OF *Handroanthus heptaphyllus*: UHPLC-ESI-MS CHARACTERIZATION AND CYTOTOXIC EFFECT AGAINST TUMOR CELLS

Juliane Carlotto[1], Alan de Almeida Veiga[2,3], Mariana Millan Fachi[4], Roberto Pontarolo[4], Thales Ricardo Cipriani[1], Lauro Mera de Souza[2,3]*

[1]Departmento de Bioquímica e Biologia Molecular, Universidade Federal do Paraná; Curitiba, PR, Brazil,
[2]Instituto de Pesquisa Pelé Pequeno Príncipe, Curitiba, PR, Brazil,
[3]Faculdades Pequeno Príncipe, Curitiba, PR, Brazil,
[4]Departamento de Farmácia, Universidade Federal do Paraná; Curitiba, PR, Brazil,

*Correspondence should be addressed to:
Lauro Mera de Souza
Instituto de Pesquisa Pelé Pequeno Príncipe,
Av. Silva Jardim, 1632, Curitiba, PR, Brazil
email: lauro.bioq@gmail.com; lauro.souza@pelepequenoprincipe.org.br
phone: +55 41 3310.1035

ABSTRACT

Barks of trees of the genus *Handroanthus* are well known by the potent antiproliferative property, mainly due to their naphthoquinones. In this work, we identified several phenylpropanoid glycosides in aqueous (HHA), ethanolic (HHE) and chloroform/methanolic (HHC) extracts from barks of *H. heptaphyllus*, using ultra-high-performance liquid chromatography-mass spectrometry. Organic extracts significantly inhibited the growth of Caco-2 (CC_{50} 350 µg/mL, HHC; CC_{50} 288 µg/mL, HHE) and MCF-7 (CC_{50} 233 µg/mL, HHC; CC_{50} 198.5 µg/mL, HHE) cells in a concentration-dependent manner. In order to identify the compounds responsible by activity, HHE was submitted to liquid/liquid fractionation with further purification of compounds by semi-preparative chromatography. Chloroform fraction (HHE-C) showed the better cytotoxic effect on Caco-2 cells (CC_{50} 43 µg/mL) and on MCF-7 (CC_{50} 29 µg/mL) cells. The potency of this fraction against tumor cells was similar to the cisplatin (MCF-7) and 3.3 folds higher than 5-fluorouracil (Caco 2). Moreover, HHE-C demonstrated less toxicity to normal cells, with a viability rate above 70% on Vero cells. The main compounds identified in this fraction were triterpenoids, long-chain hydroxy fatty acids (C22 to C30), 4-methoxy-benzoic acid, 3,4-dimethoxy-benzoic acid, and lignans. These long-chain hydroxy fatty acids, as well as the triterpenoids and the lignans fragransin A2 and B2, have not been already reported in genus *Handroanthus* spp. HHE-C was submitted to semi-preparative reversed-phase liquid chromatography and 22 subfractions were generated. Their cytotoxicity was assayed and only subfraction 5 demonstrated activity. The active compound was identified as 4-methoxy-benzoic acid, using NMR and UHPLC-ESI-MS analysis.

7.1 INTRODUCTION

Cancer is a multifactorial disease leading to abnormal and uncontrolled cell division and growth. The tumor environment promotes the ability of these cells to spread and invade tissues and organs, yielding a metastasis that can affect the surrounding tissue up to distant sites. Cancers that occur in the lungs, female breast, and colorectal region account for one-third of cancer incidence and mortality worldwide (The International Agency for Research on Cancer (IARC) Report, 2018). There are many limitations for the treatments of the different types of cancer, since the cancerous cells can develop drug resistance mechanisms and the chemotherapies promote several toxic reactions and side effects. Whereas many antineoplastic drugs are not specific to cancer cells, they can also damage healthy cells, especially those with rapid turnover, such as gastrointestinal and immune cells (DE MELO et al., 2011). For these reasons the search for new therapy to treat cancer remains of utmost importance. Considering that more than 60% of the anticancer agents are derived, directly or indirectly, from natural sources (IQBAL et al., 2017), the phytochemical diversity becomes an important source of molecules for prospecting novel anticancer drugs.

Handroanthus heptaphyllus, commonly known as “ipê-roxo”, “lapacho” or “pau d’arco”, is a native tree widely distributed in Brazil, with economic importance because of its ornamental and medicinal values. Species of the genus *Handroanthus* (Bignoniaceae) have a wide application history in South and North America, for the treatment of several diseases, including syphilis, malaria, cutaneous infections, stomach disorders, fever and cancer (IWAMOTO et al., 2016; NEWMAN, 2017). A variety of chemical compounds from the secondary metabolism of *Handroanthus* spp. have been isolated and could be related to its biological activities, such as furanonaphthoquinones, naphthoquinones, quinones, benzoic acid, lignans, cyclopentane dialdehyde, flavonoids, iridoids and phenolic glycosides (WARASHINA et al. 2004; WARASHINA et al. 2005; DE ABREU et al. 2014; IWAMOTO et al. 2016; BORGES et al. 2019; MALANGE et al. 2019; PANDA et al. 2019).

Different studies have been developing the antitumor assays with *Handroanthus* spp. from extracts to isolated compounds, particularly lapachol and lapachone (UEDA et al., 1990; WOO et al. 2006; QUEIROZ et al. 2008; ZHANG et al. 2015). A significant antitumor activity of lapachol molecule was previously demonstrated in mouse models (RAO; MCBRIDE; OLESON, 1968). Further, advanced

evaluations using lapachol, β-lapachone and analogues, against a range of tumor cell lines, including breast, esophageal, human cervix adenocarcinoma, lung and prostate lines, along with several multidrug-resistant cell lines, were carried out (BALASSIANO et al., 2005; FIORITO et al., 2014; PINK; PLANCHON; et al., 2000; PINK; WUERZBERGER-DAVIS et al., 2000; PLANCHON et al., 2001; SUNASSEE et al., 2013). Moreover, clinical trials were also carried out with β-lapachone in pancreatic cancer, non-small cell lung cancer and in patients with refractory advanced solid tumors (lung, colorectal, bladder, pancreas, breast, bile duct and stomach) (BEG et al., 2017; GERBER et al., 2018).

Considering the potent antiproliferative property of the compounds obtained from species of genus *Handroanthus*, the goal of the present investigation was to evaluate the *in vitro* cytotoxic activity of the components from bark of *Handroanthus heptaphyllu*s on breast and colorectal cancer cell lines, with a bioguided fractionation and purification of the antitumor agent.

7.2 MATERIALS AND METHODS

7.2.1. Plant material

Barks of *Handroanthus heptaphyllus* were collected in the Municipal Garden of Barreirinha, located in Curitiba, State of Paraná (PR), Brazil. The plant is deposited in the Herbarium of the Botany Department of Federal University of Paraná, as voucher nº UPCB 85422.

7.2.2. *Extraction*

The dried bark was cleaned to remove any epiphyte contaminant and 100 g were milled and submitted to sequential extractions with chloroform/methanol (500 mL, 2:1, v / v), then absolute ethanol (500 mL) and purified water (500 ml). Each extraction was performed under reflux for 2 h (x 3) and, after each step, the extract was filtered at vacuum. The chloroform/methanol and ethanol extracts were evaporated to dryness to give the crude extracts HHC and HHE, respectively. The aqueous extract (HHA) was evaporated to a small volume (200 mL), and the high molecular weight components were precipitated by addition to cold ethanol (600 mL), and separated by

centrifugation (8.000 rpm at 4 ºC, 15 min). Ethanol-soluble fraction (HHA-ES) was concentrated under reduced pressure, then freeze-dried and stored at -20 ºC.

7.2.3. *Liquid/liquid fractionation*

HHE (2 g) was suspended in distilled water (100 mL) and submitted to liquid/liquid extraction, successively, with chloroform (5 x 100 mL), ethylacetate (5 x 100 mL) and *n*-butanol (5 x 100 mL). Fractions were combined and evaporated to dryness, yielding chloroform (HHE-C), ethylacetate (HHE-EA), *n*-butanol (HHE-B) and aqueous (HHE-A) fractions, which were stored at -20 ºC. All these fractions were used for *in vitro* experiments and phytochemical investigation.

7.2.4. Liquid chromatography (LC)

Analytical chromatographic separation was carried out in an Acquity-UPLC^{TM} system (Waters), incorporating a binary pump, sample manager and column oven. A BEH-C18 column (Waters), with 100 mm x 2.1 mm and 1.7 µm particle size was used. The mobile phase consisted of H_2O and acetonitrile, containing 0.1% formic acid (v/v), with two gradient methods, employed according to the polarity of the samples. Method 1: linear gradient with a flow rate of 0.4 mL.min^{-1}, increasing acetonitrile from 5 to 30% in 7 min, then to 95% in 15 min, held to 16 min, returning to the initial condition in 18 min, with 2 min else for column re-equilibration. Method 2: linear gradient with a flow rate of 0.4 mL.min $^{-1}$, increasing acetonitrile from 5 to 50% in 7 min, to 95% at 10 min, held to 16 min, returning to the initial condition in 18 min, with 2 min else for column re-equilibration. The samples (1 mg.mL^{-1}) were prepared in MeOH, held at room temperature (22 ºC), and 5 µL was injected in each analysis. Detection was provided by high-resolution mass spectrometry (HR-MS).

Purification of HHE compounds was performed on semi-preparative high performance liquid chromatography (HPLC) model Waters 600. The column was a Symmetry-C18 (Waters) with 50 mm x 7.8 mm and 5 mm of particle size. The chromatography was developed using H_2O and acetonitrile, both containing 0.1% formic acid (v/v). A linear gradient acetonitrile with a flow rate of 2 mL.min^{-1} was developed increasing acetonitrile, from 0 to 50% in 30 min, then to 95% at 40 min, held up to 45 min. The solvent system returns to initial condition in 50 min and 5 min was

used for re-equilibrating. Detection was provided by a photodiode array detector (PDA, 200–400nm).

7.2.5. High resolution mass spectrometry (HR-MS)

The HR-MS was developed on a hybrid quadrupole time-of-flight mass spectrometer (Xevo G2-S, Waters Co., Milford, USA), with an electrospray ionization interface. High purity nitrogen used as cone gas and desolvation was produced by a nitrogen generator from Peak Scientific Instruments (Chicago, USA). The collision gas used was argon with purity > 99.998% from White Martins Praxair Inc. (Curitiba, Brazil). The source temperature was 150 ºC, capillary at 3 kV, collision energy ramp of 30 – 50 eV, desolvation temperature of 350°C. All data was acquired from 100 to 1500 m/z in centroid mode, using MassLynx™ NT4.1 software (Waters Co., Milford, USA). The correction of the exact mass was performed through the leucine encephalin.

7.2.6. Nuclear magnetic resonance (NMR)

The NMR analysis was performed on an Avance HD (14.1 T, 600 MHz for ^{1}H nucleus) using a 5 mm inversed probe. Analysis was developed at 30 ºC using choroform-D1 as solvent and internal reference for chemical shifts (δ ^{13}C = 77 and ^{1}H = 7.26, calibrated from tetramethylsilane δ $^{13}C/^{1}H$ =0). 1D experiments (^{1}H) and 2D (HSQC and HMBC) were carried out. The correlation spectra were handled using the software Topspin® (Bruker) and the chemical shifts were assigned based on literature data.

7.2.7. Cell lines

MCF-7 cells (human breast adenocarcinoma cell line) were purchased from the Cell Bank of Rio de Janeiro, Brazil (BCRJ code 162) and Vero cells (African green monkey kidney cell line) were purchased from the Cell Bank of Rio de Janeiro, Brazil (BCRJ code 245). These cells were cultivated in DMEM/F-12 (Dulbecco's Modified Eagle Medium/Nutrient Mixture F-12) supplemented with 10% fetal bovine serum (FBS) and 1% of antibiotic (penicillin/streptomycin). Caco-2 cells (Human colon carcinoma cell line), purchased from the Cell Bank of Rio de Janeiro, Brazil (BCRJ

code 0059), were cultivated in DMEM/F-12 supplemented with 20% FBS, and 1% of antibiotic (penicillin/streptomycin). Cultures were incubated under controlled conditions (95% air and 5% CO_2) at 37 °C.

7.2.8. Cell viability assay

Cytotoxic effect of extracts and purified compounds on cell lines was evaluated by MTT assay (MOSMANN, 1983).Cells were cultured at a density of 5 x 10^4 cells/well diluted in FBS free medium in a 96-well plate and incubated overnight with controlled humidity (95% air and 5% CO_2) at 37 °C. Later, the culture medium was removed, and the cells were treated with extracts, pure compounds, cisplatin, 5-fluorouracil or vehicle (DMSO 1%), diluted in DMEM/F-12 supplemented with FBS. After 48 h of incubation, the solution was removed and MTT (3-(4,5-dimethylthiazol-2-yl)-2,5-diphenyltetrazolium bromide) solution (100 µL, 0.5 $mg.mL^{-1}$) was added to each well and incubated for 3 h at 37 °C. MTT solution was aspired and 100 µL of dimethyl sulfoxide (Me_2SO) were added to solubilize formazan crystals.The experiments were performed in quadruplicate.

7.2.9. Statistical analyses

The results were presented as mean ± S.E.M. and evaluated with one-way analysis of variance (ANOVA), followed by the Dunnett multiple comparison test. CC_{50} value (i.e. concentration of HHE and HHC required for the reduction of cell viability by 50%) was determined by nonlinear regression analysis (sigmoidal dose-response) and recalculated based on the yield of each derived fraction of HHE (HHE-A, HHE-B, HHE-C and HHE-EA). Statistical significance was considered as: $*P < 0.05$; $**P < 0.01$; $***P < 0.001$; $****P < 0.0001$. All the analyzes were performed using the GraphPad Prism® version 7.0 (GraphPad Software, San Diego, USA).

7.3 RESULTS AND DISCUSSION

7.3.1. Overall phytochemical investigation

Some species of *Handroanthus*, commonly known as “ipês”, are associated with many anticancer properties (Santana et al., 1980; Pink et al. 2000b, a; Planchon et al. 2001; Balassiano et al. 2005; Sunassee et al. 2013; Fiorito et al. 2014). Considering the high potential of these plants, dried and milled barks of *H. heptaphyllus* (100 g) were extracted sequentially to give the chloroform/methanol (HHC; 9.65 g), ethanol (HHE; 2.47 g) and aqueous (HHA; 6.4 g) crude extracts. The compounds present in these crude extracts were analyzed by reversed-phase UHPLC-ESI-MS and the chromatograms were qualitatively similar. The components of these crude extracts were investigated in the negative and positive ionization modes, as shown in Figure 1, which represents the total ion chromatogram (TIC) of HHE provided by analysis in both ionization modes.

The major compounds of HHE were phenylpropanoid glycosides (Table 1). In negative mode (Figure 1A), peaks **10-14** could be attributed to acteoside isomers. Acteosides are, in general, glycosides of α-L-rhamnosyl-(1→3)-β-D-glucoside hydroxytyrosol, esterified by trans-caffeic acid. Nevertheless, these phenylpropanoid glycosides also could contain allose instead of glucose, as glycan core. The acteosides commonly found in plants are the isoacteoside, with β-D-glucopyranose core, and magnolosides A, M and D, with β-D-allopyranose core (GE et al., 2017; GUO, K. et al., 2019; XUE et al., 2019; XUE; LI; YANG, 2016). Considering that compounds **10-14** are isomers, they cannot be differentiated only by the mass. The acteoside isomers gave deprotonated ions at *m/z* 623.197 $[M-H]^-$ with the fragment-ion at *m/z* 461.165 $[M-H-162.032]^-$ indicating the neutral loss of a caffeoyl residue. Another main fragment-ion at *m/z* 161.024 was consistent with a dehydrated product of caffeic acid (GUO, K. et al., 2019).

Analysis in the positive ion mode (Fig. 1B) provided additional information, confirming the proposed structures. The acteoside isomers (peaks **9**, **10** and **11**) appeared mainly as protonated ions $[M+H]^+$, at *m/z* 625.213. The fragment at *m/z* 479.158 was formed by the loss of a rhamnosyl residue $[M+H-146.055]^+$ and the ion at *m/z* 471.150, produced by the loss of hydroxytyrosol $[M+H-154.063]^+$. The ion at *m/z* 325.093 was consistent with a caffeoyl-glucosyl/allosyl residue. The higher abundant ion appeared at *m/z* 163.039, consistent with de protonated caffeoyl residue, confirming the proposed structures, being in agreement with previous report (JIA et al., 2017), as well.

FIGURE 1. UHPLC-MS CHROMATOGRAMS OF HHE IN NEGATIVE (A) AND POSITIVE (B) IONIZATION MODES

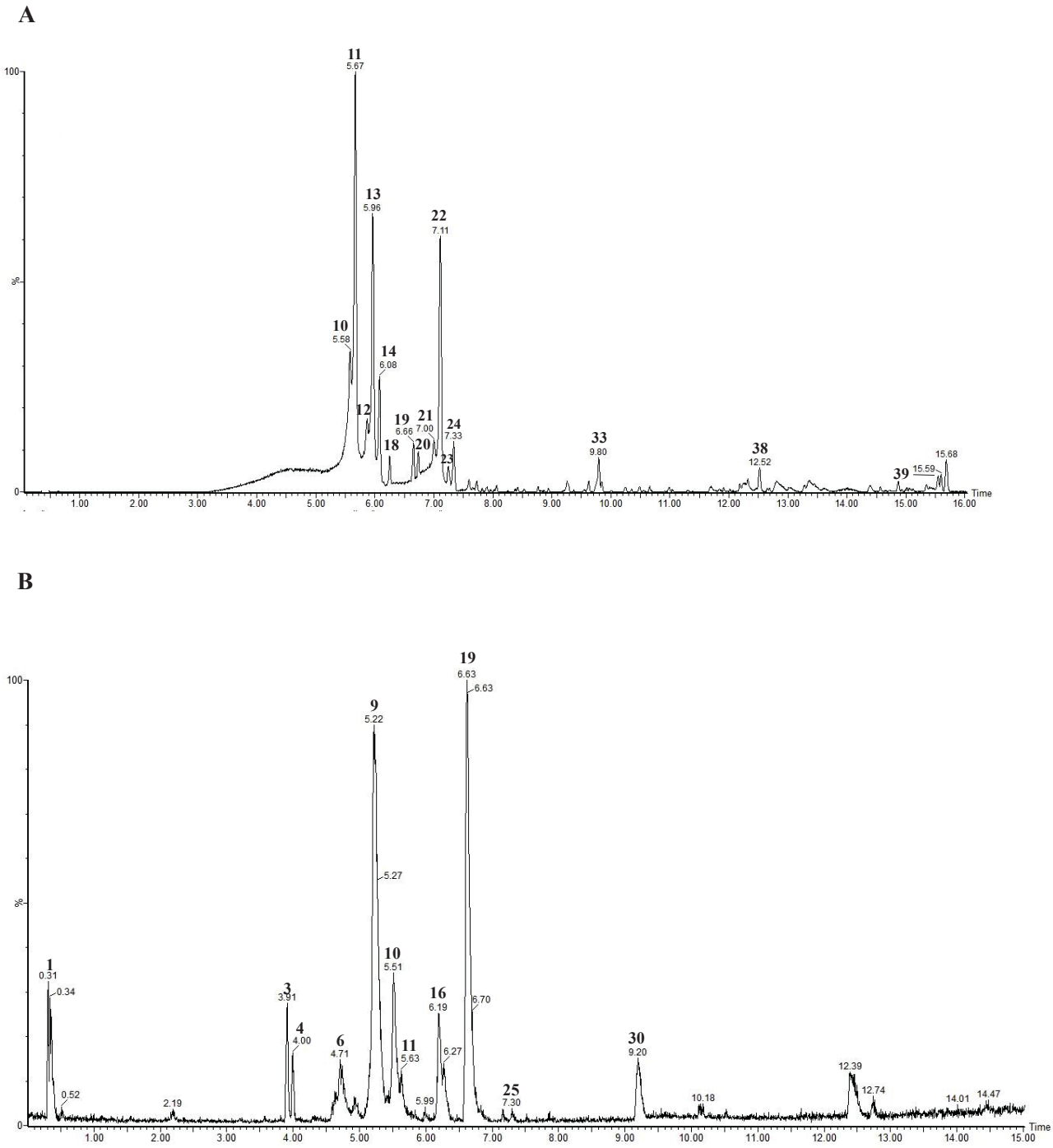

Compounds **18**-**21** were identified as acetyl acteoside isomers and showed the deprotonated ions $[M-H]^-$ at *m/z* 665.207. Fragment-ions were observed at *m/z* 623.197 (loss of acetyl group) and 503.175 (loss of caffeoyl group). Other fragments appeared at *m/z* 461.165 and 161.024, were formed from the deacetylated molecule,

as described above, being consistent with the proposed structure of acetyl acteoside (LI et al., 2008).

Liquid fractionation of the HHE yielded chloroform (HHE-C; 14.9%), ethyl acetate (HHE-EA; 19.8%), n-butanol (HHE-B; 32.2%) and aqueous (HHE-A; 33.2%) fractions. The LC-MS analysis in negative and positive mode of the fractions revealed that the HHE-A, HHE-B and HHE-EA have concentrated acteoside and acetyl-acteoside isomers (Fig. 2 and Fig. 3). The most nonpolar fraction, HHE-C, have concentrated triterpenoids, long-chain saturated hydroxyl fatty acids, phenolic acids and lignans, the most of these compounds have not been well observed in the chromatogram of crude extract (Fig. 4).

FIGURE 2. UHPLC-MS CHROMATOGRAMS OF HHE-A (A), HHE-B (B) AND HHE-A (EA) IN POSITIVE IONIZATION MODE.

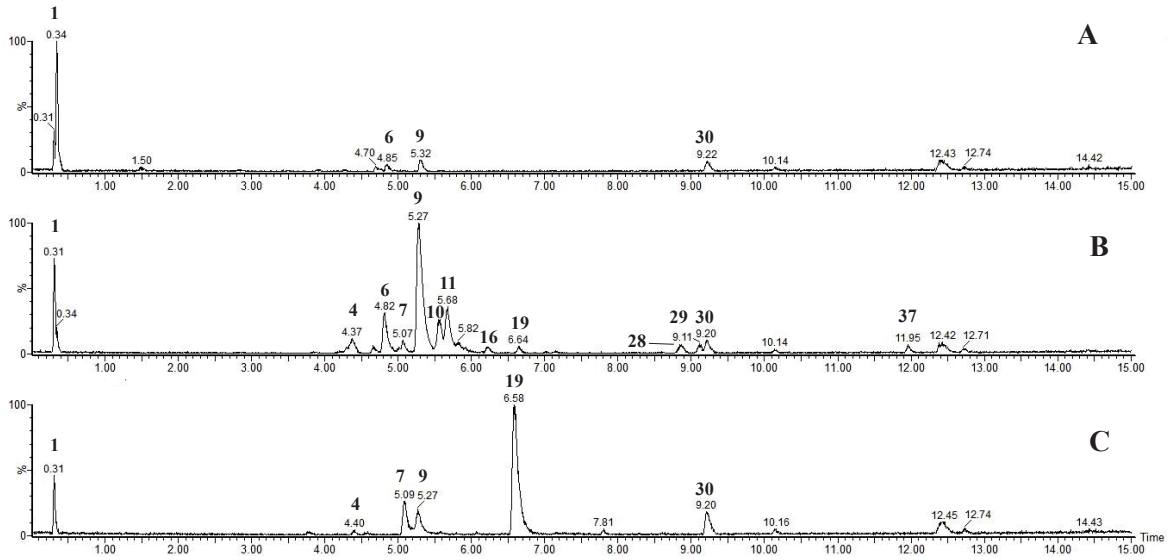

FIGURE 3. UHPLC-MS CHROMATOGRAMS OF HHE-A (A), HHE-B (B) AND HHE-EA (C) IN NEGATIVE IONIZATION MODE.

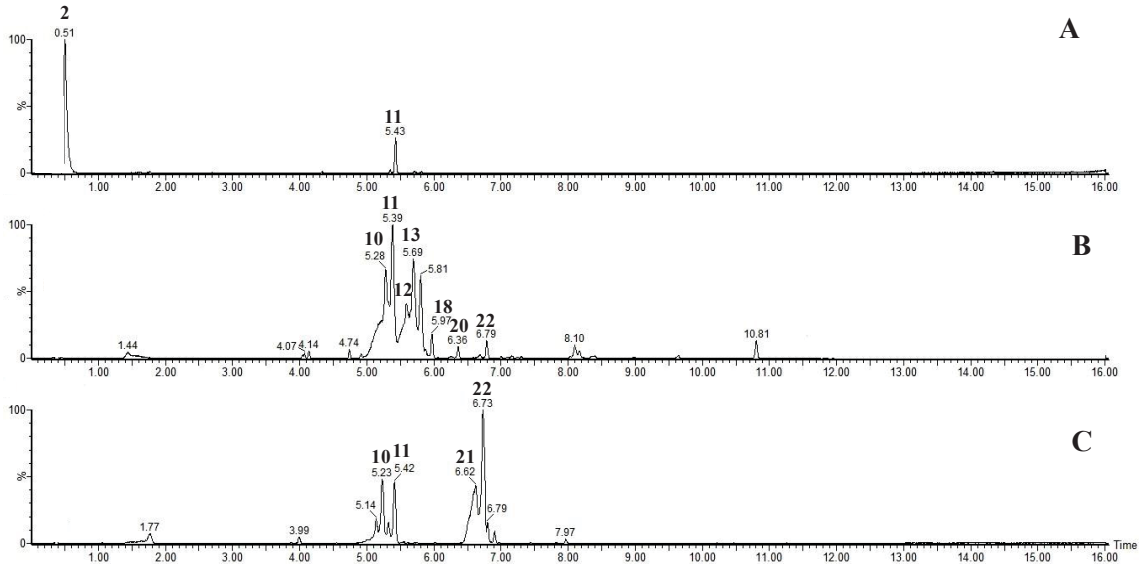

7.3.2 Cytotoxic activity and bioguided fractionation

The crude extracts of *H. heptaphyllus* were assayed for their effects on the proliferation of human colon cancer Caco-2, human breast cancer MCF-7 and healthy cells of an African green monkey (Vero cells) using the MTT assay. The results showed that only organic extracts (HHC and HHE) significantly promoted cytotoxicity on Caco-2 and MCF-7 cells in a concentration-dependent manner (Fig. 5). The CC_{50} values of HHC and HHE for Caco-2 cells was 350 µg/mL and 288 µg/mL, respectively, whereas for MCF-7 cells it was 233 µg/mL and 198.5 µg/mL, respectively.

FIGURE 4. UHPLC-MS CHROMATOGRAMS OF HHE-C IN POSITIVE (A) AND NEGATIVE (B) IONIZATION MODES.

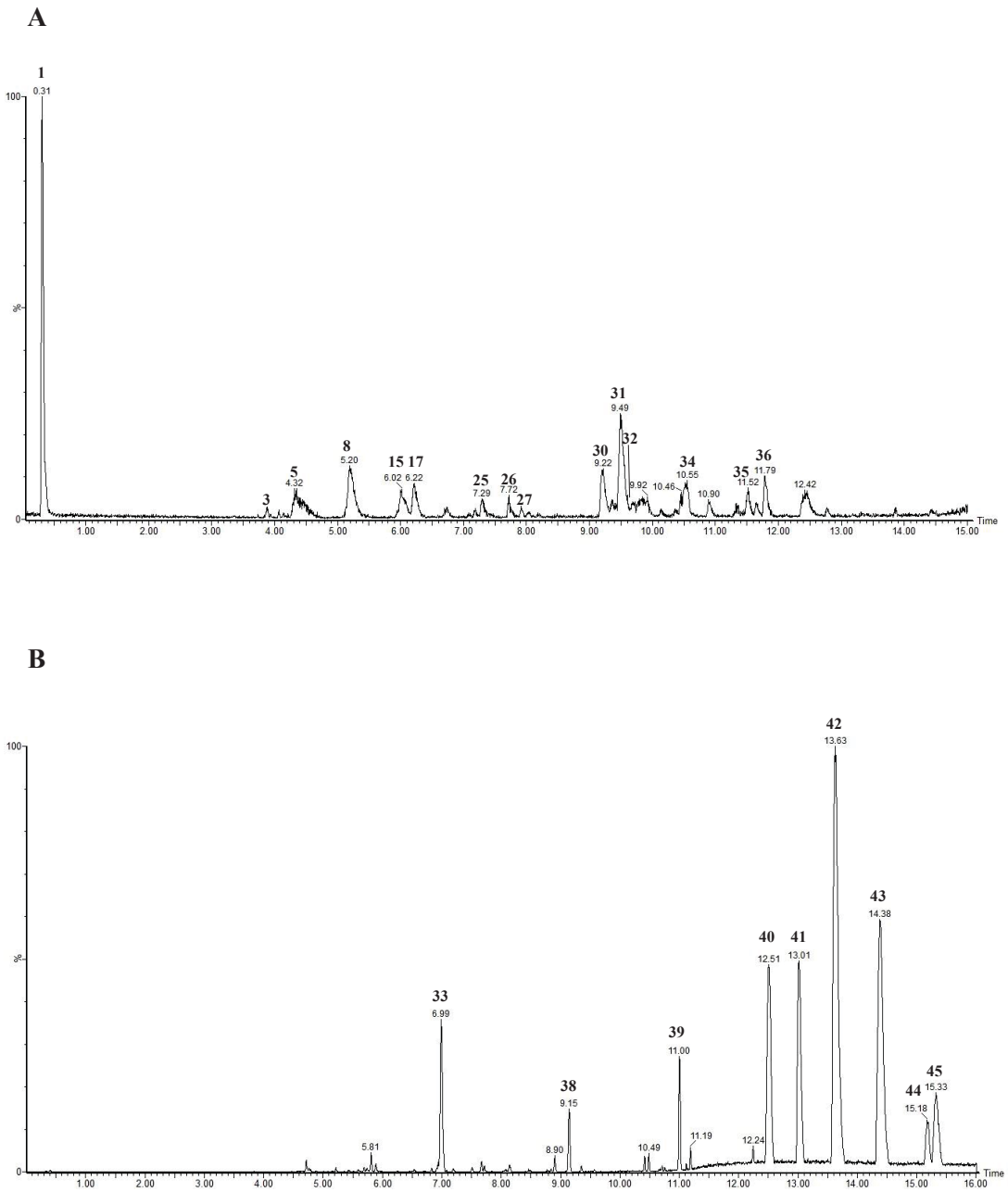

FIGURE 5. EFFECT OF HHE AND HHC ON CELL VIABILITY OF CACO-2 (A AND B), MCF-7 (C AND D) AND VERO (E AND F).

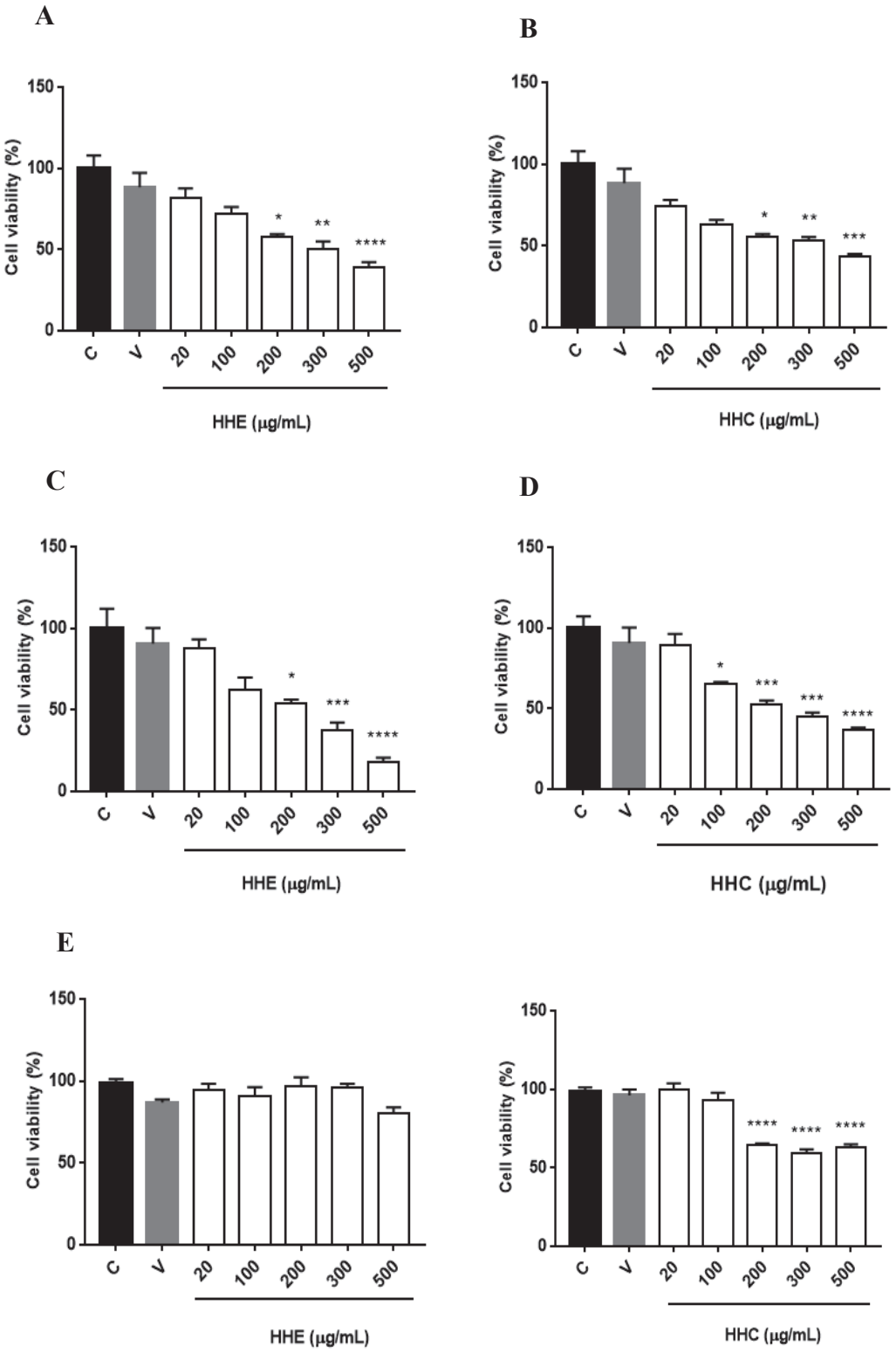

The cells were treated with medium (C: Dulbecco´s Modified Eagle Medium), vehicle (V: dimethyl sulfoxide 1%), HHE (20-500 µg/mL) or HHC (20-500 µg/mL) for 48 h before MTT assay. The results are expressed as mean ± S.E.M. *P <0.05, ** P <0.005, ***P < 0.001 and ****P < 0.0001 when compared to vehicle group (V).

As shown in Figure 5E, HHE did not show significant cytotoxic effect on Vero cells, whereas the HHC showed significant effect at doses above 200 µg/mL. In order to evaluate the active compounds, the HHE was chosen for a liquid/liquid fractionation, since this extract exhibited high toxicity to the cancer cells, with lesser harmful effects to the normal cells. The toxicity of fractions was evaluated by MTT assay, with concentrations calculated based on the CC_{50} of the original extract (HHE), considering the yield of each fraction from the HHE. Thus, each fraction was tested on Caco-2 cells at concentrations of 93 µg/mL (HHE-B), 43 µg/mL (HEE-C), 57 µg/mL (HHE-EA) and 96 µg/mL (HHE-A). The toxicity of fractions on MCF-7 cells was assayed with concentrations of 64 µg/mL (HHE-B), 29 µg/mL (HEE-C), 39 µg/mL (HHE-EA) and 66 µg/mL (HHE-A). The results demonstrated that HHE-C promoted the greatest decrease in viability on both cell lines, suggesting that active compounds was concentrated on this fraction (Fig. 6A, B).

FIGURE 6. EFFECT OF HHE FRACTIONS ON CELL VIABILITY OF CACO-2 (A) AND MCF-7 (B).

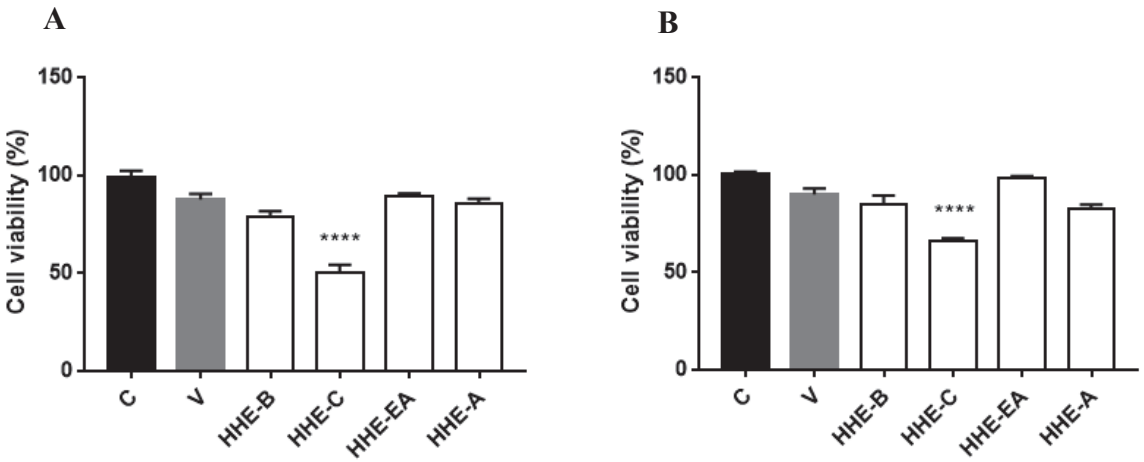

The cells were treated with medium (C: Dulbecco´s Modified Eagle Medium), vehicle (V: dimethyl sulfoxide 1%) or theoretical CC50 of HHE fractions (HHE-B, HHE-C, HHE-EA and HHE-A) for 48 h before MTT assay. The results are expressed as mean ± S.E.M. ****P < 0.0001 when compared to vehicle group (V).

We also calculated the CC_{50} for a well-known antineoplastic cisplatin and 5-fluorouracil, used for treatment of breast and colorectal cancer, respectively. The CC_{50} values were 28.9 µg/mL and 143.5 µg/mL, respectively (Fig. S1). The potency of HHE-C was similar to cisplatin on MCF-7 cells and 3.3 folds higher than 5-fluoruracil on Caco-2 cells, indicating high toxicity to the cancer cells. The toxicity to Vero cells was also investigated. Cells treated with HHE-C, 5-FU and cisplatin showed viability of

70.3%, 84.1% and 30%, respectively. These results indicated that the HHE-C is a good candidate for future experiments and identification of active compounds.

7.3.3. Chemical characterization of HHE-C

Acteoside and acetyl acteosides were not observed in the chromatogram of HHE-C in positive and negative ionization modes. In the (+) ESI-MS spectrum (Fig. 4A), peaks **3** and **5** were identified as 4-methoxy-benzoic acid and 3,4-dimethoxy-benzoic acid, respectively. These phenolic acids showed fragments that were consistent with dehydratation $[M+H-H_2O]^+$ and descarboxylation $[M+H-CO_2]^+$. Peak **25** at *m/z* 357.136 was identified as a neolignan balanophonin, since showed fragment-ions according fragmentation scheme described by Boldizsár et al. (2012). Peaks **27** and **31** were identified as lignans fragransin B2 isomers and peak **32** as fragransin A2, at m/z 425.192 and 345.173, respectively. MS/MS spectra of fragransin A2 and B2 showed fragment-ions formed by the losses of $[M+H-H_2O]^+$ and [M+H-hydroxy-methoxyphenyl]$^+$. The cleavage of 3,4 dimethyl tetrahydrofuran ring generated fragment-ions at *m/z* 165.089 and *m/z* 137.060, as major fragments for fragransin A2, and ion at *m/z* 167.072 as major fragment for fragransin B2 (RÉDEI et al., 2018), as observed herein.

Triterpenoids were also observed in positive mode (peaks **34**, **35** and **36**). Peak **34** at m/z 489.362 was identified as arjunolic acid/asiatic acid, an isomeric pair of known hydroxylated oleanane- and ursane-type triterpenes, respectively (NAKANISHI et al., 2007). In MS/MS spectrum, it was observed fragment-ion at *m/z* 471.348 and at *m/z* 453.337, which could be due to $[M+H–H_2O]^+$ and $[M+H–2H_2O]^+$, respectively. The loss of water molecules from $[M+H]^+$ ions is commonly associated with the hydroxyl group in these triterpenoids. Peak **35** showed $[M+H]^+$ at *m/z* 473.364, and fragment-ions at *m/z* 455.3521 and *m/z* 409.3379, characteristic of maslinic acid/corosolic acid, another isomeric pair of oleanane- and ursane-type triterpenes, respectively (ZOU et al., 2015). Peak **36** showed $[H+H]^+$ at *m/z* 487.343, characteristic for quillaic/gypsogenic acid. The MS/MS spectrum yielded fragments at *m/z* 423.377 $[M+H-H_2O-HCO_2H]^+$, *m/z* 407.304 $[M+H-2H_2O-CO_2]^+$ and *m/z* 395.215 $[M+H-H_2O-CO_2-CHO_2]^+$. The fragmentation of the ions $[M+H]^+$ displayed important molecular characteristics, including both forms of decarboxylation (losses of CO_2 and HCO_2H), which is typical of quillaic acid (GEVRENOVA et al., 2018, 2019).

Pentacyclic triterpenic (peaks **34**, **35** and **36**) acids usually undergo a retro-Diels–Alder reaction and generate characteristics fragments of cleavage of the C ring, which consist of ABC-rings and CDE-rings where C-ring is partial. In the MS/MS spectra of compounds above described were possible to observe fragment ions at *m/z* 207.16 $[C_{14}H_{23}O]^+$, 203.17 $[C_{15}H_{23}]^+$, 191.18 $[C_{14}H_{23}]^+$, 189.16 $[C_{14}H_{21}]^+$, which are assigned to fragments containing A, B rings or D, E rings with partial C ring, supporting the pentacyclic triterpenic backbone (TORTORA et al., 2016).

In the (-)ESI-MS analysis (Fig 2B), peak **38** showed $[M-H]^-$ at *m/z* 485.3271, characteristic for quillaic/gypsogenic acid. The most prominent fragments in MS/MS spectrum were formed by the losses of (CO_2) (*m/z* 485.327→441.337) and (H_2O + CO_2) (*m/z* 485.327→423.321). This pattern of descarboxylation (CO_2 instead of HCO_2H) was observed from gypsogenic acid (GEVRENOVA et al., 2018, 2019). Peaks **39**-**45** were tentatively identified as a homologous series of long-chain satured hydroxy fatty acids, which ranged in chain length from 22 to 30 carbon atoms (Table 1).

Long-chain saturated hydroxy fatty acids and triterpenoids were not previously reported in genus *Handroanthus*. This is also the first report of the identification of lignans fragransin A2 and B2 in *Handroanthus* spp. Balanophonin, another lignan observed herein, was previously identified by Warashina et al. (2005) in bark of *Handroanthus avelanedae*. Lignans are secondary metabolites frequently found in genus *Handroanthus*, like cycloolivil and pawlownin in *Handroanthus incana* (BRAGA DE OLIVEIRA et al., 1993), sesamolinol-type lignan in *Handroanthus argentea* (DE ABREU et al., 2014), 4-O-methylcerusin, secoisolariciresinol-glucopyranoside, lyoniresinolglucopyranoside, dihydrodehydrodiconiferylalcohol-glucopyranoside, dihydro-dehydrodiconiferylalcohol-glucopyranoside and dihydrodehydrodiconiferyl alcohol-glucopyranoside in *Handroanthus avellanedae* (IWAMOTO et al., 2016; WARASHINA; NAGATANI; NORO, 2004, 2005).

Naphthoquinones belong to another class of secondary metabolites widely found in *Handronathus* genus (ZANI et al. 1991; BRAGA DE OLIVEIRA et al. 1993; SICHAEM et al. 2012; ZHANG et al. 2015; BORGES et al. 2019; PANDA et al. 2019). This class is generally associated to antitumor activity of “ipes” (PANDA et al., 2019; SICHAEM et al., 2012; ZHANG, L. et al., 2015). In this work, we did not find naphthoquinones, nevertheless HHE-C showed significant antitumor activity, indicating that other compounds also may be related to *Handroanthus* antineoplastic activity.

7.3.4. Purification and identification of cytotoxic compound

In order to purify the compound responsible by antitumor activity, HHE-C was submitted to semi-preparative reversed-phase liquid chromatography. This method generated 22 subfractions. The cytotoxicity of these subfractions was assayed and only subfraction 5 significantly promoted cytotoxic effect on Caco-2 and MCF-7 cells (Fig. 7).

FIGURE 7. EFFECT OF SUBFRACTION 5 ON CELL VIABILITY OF CACO-2 (A) AND MCF-7 (B).

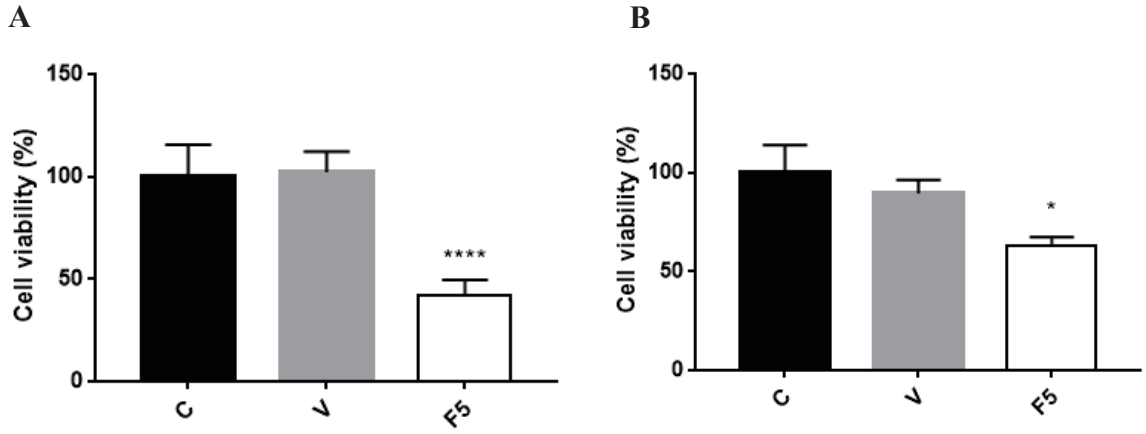

The cells were treated with medium (C: Dulbecco´s Modified Eagle Medium), vehicle (V: dimethyl sulfoxide 1%), F5 43 µg/mL (Caco-2) or F5 29 µg/mL (MCF-7) for 48 h before MTT assay. The results are expressed as mean ± S.E.M. *P <0.05, ** P <0.005, ***P < 0.001 and ****P < 0.0001 when compared to control group (C).

Subfraction 5 was analyzed by UHPLC-ESI-MS and showed an ion at *m/z* 153.1839 $[M+H]^+$, indicating a methoxy-benzoic acid (peak 3 from HHE-C chromatogram). The compound was then analyzed by NMR experiments (^{1}H, HSQC and HMBC). ^{1}H NMR (DMSO) spectrum showed a chemical shifts typical of methoxyl group, at δ 3.88 (–OCH3), and signals at δ 6.95 (2H, ArH, ^3J = 8.79 Hz) and 8.047 (2H, ArH, ^3J = 8.85 Hz). The coupling constant was typical of $^3J_{ortho,}$ indicating a *para* substitution on the aromatic ring. The ^{1}H/^{13}C HSQC (Figure 8A) showed correlations at δ 8.05/131.9 and 6.95/113.3 of C/H of aromatic ring, and 3.88/55.0 of -OCH_3. In the ^{1}H/^{13}C HMBC experiment (Figure 8B) a signal consistent to the long-range coupling of the carbonyl group at 168.9 ppm with the H2 at 8.047 ppm from aromatic ring confirmed a carboxylic group linked at C1. Other intra-ring HMBC correlations were observed (Fig 5B) and confirmed a structure of *p*-methoxy-benzoic acid, since the -OCH_3 at 3.88 ppm coupling with C4 at 163.5 ppm and H2 at 8.047 and H3 at 6.95 showed long range

coupling with C6 at 132.1 and C5 at 113.6, respectively (Ghalehshahi and Madsen 2017; Periyasamy et al., 2018).

These results indicate that the *p*-methoxy-benzoic acid is the main responsible compound for the antitumor effect of *Handroanthus heptaphyllus* barks, observed here. Benzoic acids have already been identified by Kreher et al. (1988) and Sichaem et al. (2012) in bark of *Handroanthus avelanedae* and in roots of *Handroanthus rosea,* respectively. Sichaem et al. (2012) demonstrated antitumor activity of *p*-methoxy-benzoic acid in HeLa (human cervical carcinoma) and KB (human epidermoid carcinoma) with IC_{50} of 16 and 13.61 µg/mL, respectively.

FIGURE 5. NMR ANALYSIS OF PURIFIED PEAK 2. (A) HSQC CORRELATIONS SUPPORTED BY (B) HMBC AND ^{1}H NMR.

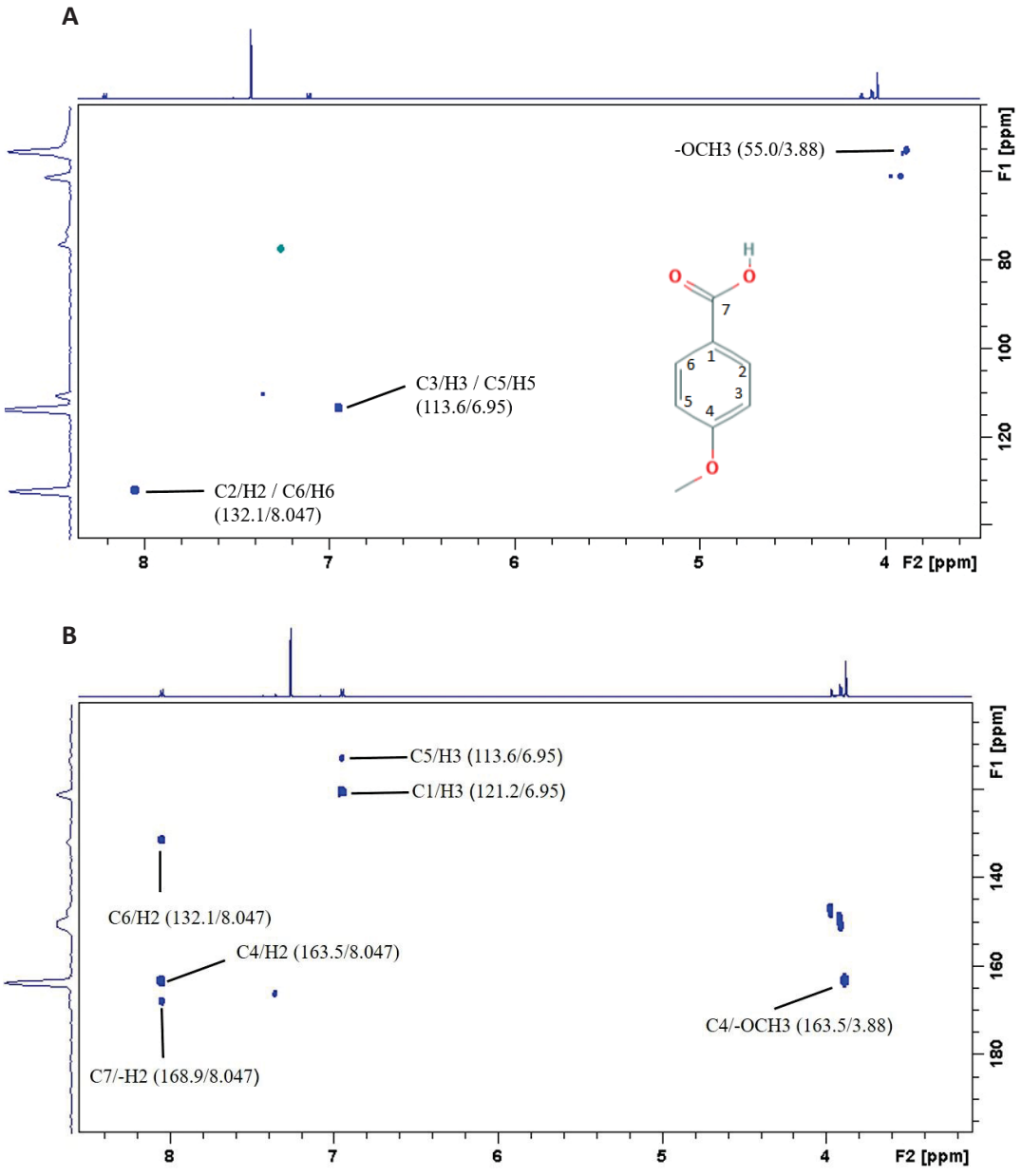

7.4 CONCLUSIONS

Based on chemical analysis, a range of phenylpropanoid glycosides could be identified in aqueous, ethanolic and chloroform/methanolic extracts of barks of *H. heptaphyllus.* Organic extracts promoted significantly cytotoxic effect on Caco-2 and MCF-7 cells in a concentration-dependent manner. For a such complex extract, a bioguided fractionation with further purification was developed. HHE-C promoted the greatest decrease in viability on both cell lines. The major compounds identified were triterpenoids, long-chain saturated hydroxy fatty acids, phenolic acids and lignans. The active compound could be achieved and identified as *p*-methoxy-benzoic acid, using NMR and UHPLC-ESI-MS analysis. This potential of the plant has been demonstrated here, and can be further better explored.

TABLE 1. UHPLC–MS (NEGATIVE MODE) OF THE COMPOUNDS FROM ETHANOLIC EXTRACT AND FRACTIONS PARTITIONED OF THE BARKS OF *Handroanthus heptaphyllus*.

Peak	MS^1 [M-H]	MS^2 negative mode (main)	MS^1 [M+H]	MS^2 positive mode (main)	Identification	Reference
1			255.9443	214.9177; 125.9872	Unknown	
2	124.9905				Unknown	
3			153.0538	135.0438; 109.0629	4-methoxy-benzoic acid	MassBank of North America
4			449.1082	413.0406; 359.0424; 329.0253; 313.0431; 299.0140; 287.0202	Orientin	Chen et al. (2016)
5			183.0662	165.0306; 153.0555; 139.0771	3,4-dimethoxy-benzoic acid	The Human Metabolome Database
6			219.1022	201.0914; 189.0924; 174.0692; 158.0057; 141.0710	Unknown	
7			479.1597	325.0941; 317.1107; 181.0542; 163.0414	Calceolarioside A	Friščić et al. (2016)
8			219.1025	201.0933; 189.0920; 174.0694; 158.0047; 141.0729	Unknown	
9			625.2133	479.1588; 471.1501; 325.0932; 163.0398	Acteoside isomer	Jia et al. (2017)
10	623.1965	461.1653; 161.0242	625.2156	471.1509; 479.1508; 325.0930; 163.0394	Acteoside isomer	Li et al. (2008; Jia et al. (2017); Guo et al. (2019); Xue et al. (2019)

11	623.197	461.1658; 161.0242	625.2148	325.0925; 163.0396	Acteoside isomer	Li et al. (2008; Jia et al. (2017); Guo et al. (2019); Xue et al. (2019)
12	623.1967	461.1652; 161.0244			Acteoside isomer	Li et al. (2008); Guo et al. (2019); Xue et al. ('2019)
13	623.1969	461.1652; 161.0241			Acteoside isomer	Li et al. (2008); Guo et al. (2019); Xue et al. ('2019)
14	623.1974	461.1649; 161,0242			Acteoside isomer	Li et al. (2008); Guo et al. (2019); Xue et al. ('2019)
15			191.0698		Unknown	
16			597.2106	435.1689; 318.0433; 279.0875; 261.0776; 165.0555	Aketrilignoside B	Qin et al. (2013)
17			219.1011	189.0903; 174.0694; 158.0047; 141.0709	Unknown	
18	665.2070	623.1972; 503.1733; 461,1651; 315.1066; 161.0241			Acetyl acteoside isomer	Li et al. (2008, 2016)
19	665.2083	623.1960; 503.1749; 461.1649; 161.0236	667.2376	521.1694; 503.1547; 367.1035; 163.0392	Acetyl acteoside isomer	Li et al. (2008, 2016)
20	665.2077	623.1974; 503.1757; 461.1643; 161.0235			Acetyl acteoside isomer	Li et al. (2008, 2016)
21	665.2073	623.1973; 503.1759; 461,1631; 161.0239			Acetyl acteoside isomer	Li et al. (2008, 2016)
22	665.2079	623.1978; 503.1764; 461,1654; 161.0241			Acetyl acteoside isomer	Li et al. (2008, 2016)

23	527.1768	181.0505; 151.0396				Tecosid	Verma et al. (1979)
24	665.2079	623.1943; 503.1751; 461.1642; 161.0239				Acetyl acteoside isomer	Li et al. (2008, 2016)
25				357.1360	339.1257; 321.1125; 219.0603; 191.0682; 165.0548; 137.0599	Balanophonin	Boldizsár et al. (2012)
26				687.2689	633.5009; 327.0742; 309.0254; 219.0595; 183.0332; 165.0224	Unknown	
27				405.1923	387.1788; 233.1175; 201.0911; 167.0727	Fragransin B2 isomer	The Human Metabolome Database
28				393.1521	297.0976	Unknown	
29				393.1497	319.0651; 297.0951	Unknown	
30				225.1988		Unknown	
31				405.1895	387.1806; 251.1218; 233.1217; 201.0360; 181.0513; 167.0726	Fragransin B2 isomer	The Human Metabolome Database
32				345.1735	327.1606; 221.1190; 181.0866; 165.0896; 151.0741; 137.0605	Fragransin A2	Rédei et al. (2018)
33	693.39	647.3837; 617.3413; 441.3338;	629.3470; 495.3428;			Unknown	
34				489.3620	471.3487; 455.3535; 453.3378; 423.3277; 405.3110; 245.1541;	Arjunolic acid / Asiatic acid	The Human Metabolome Database

35			473.3641	455.3521; 409.3379; 203.1739; 201.1641; 191.1801; 189.1627	Corosolic acid / Maslinic acid	Zou et al. (2015)
36			487.3432	469.3615; 423.3770; 407.3049; 395.2157; 203.1481; 191.1801; 189.1627	Quillaic acid	Gevrenova et al. (2019)
37			435.2981	419.2409; 317.1971; 207.1396	Unknown	
38	485.3271	441.3377; 423.3218			Gypsogenic acid	Gevrenova et al. (2019)
39	355.3207	309.3171			Hydroxy-docosanoic acid isomer	Lipid Maps
40	355.3225	309.3144			Hydroxy-docosanoic acid isomer	Lipid Maps
41	369.3393	323.3326			Hydroxy-tricosanoic acid	Lipid Maps
42	383.3541	337.3480			Hydroxy-tetracosanoic acid	Lipid Maps
43	397.3686	351.3627			Hydroxy-pentacosanoic acid	Lipid Maps
44	467.4479	421.386			Hydroxy-triacontanoic acid	Lipid Maps
45	411.3855	365.3322			Hydroxy- hexacosanoic acid	Lipid Maps

7.5 SUPPLEMENTARY MATERIAL

FIGURE S1. EFFECT OF 5-FLUOROURACIL AND CISPLATIN AND ON CELL VIABILITY OF CACO-2 (A) AND MCF-7 (B), RESPECTIVELY.

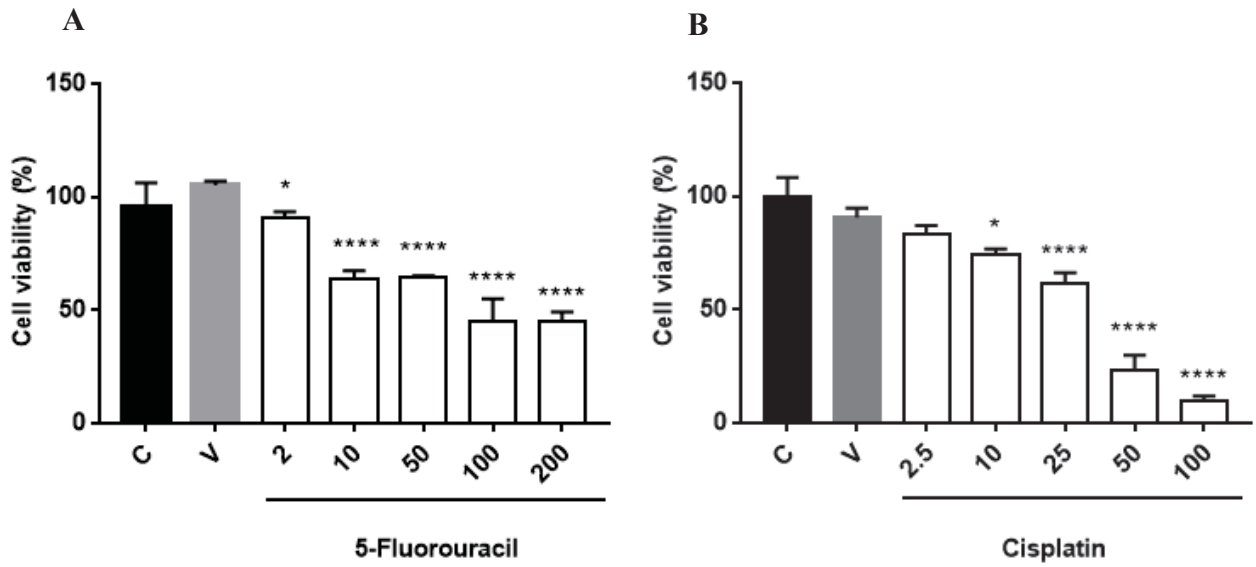

The cells were treated with medium (C: Dulbecco´s Modified Eagle Medium), vehicle (V: water 1%), cisplatin (2.5-100 µg/mL) or 5-fluorouracil (2-200 µg/mL) for 48 h before MTT assay. The results are expressed as mean ± S.E.M. *P <0.05 and ****P < 0.0001 when compared to vehicle group (V).

8 CONCLUSÃO

- Todas as frações polissacarídicas apresentaram-se constituídas majoritariamente por arabinogalactanas do tipo II, arabinanas e ramnogalacturonanas do tipo I e, ainda, HHBSF e HABSF apresentam glucomananas em sua composição;

- HHSF apresentou efeito antiulcerogênico, tanto preventivo como curativo da lesão gástrica, em ensaios *in vivo* agudos e crônicos, fato que pode estar relacionado à inibição da depleção de muco e GSH;

- HASP foi capaz de promover efeito analgésico na fase tardia da nocicepção induzida por formalina (dor inflamatória), além de mostrar atividade anti-edematogênica, diminuindo a alodinia mecânica e a atividade de mieloperoxidase no edema de pata induzido por carragenina;

- HABSF apresentou efeito citotóxico dose-dependente em células Caco-2 e MCF-7, enquanto que HHBSF não promoveu citotoxicidade; pequenas alterações estruturais poderiam explicar a diferença na atividade apresentada, uma vez que a AG II presente em HABSF possui uma maior proporção de cadeias de (1→6)-β-D-galactana do que HHBSF, além de RG I constituída por unidades de Gal*p*A não acetiladas e não metil-esterificadas, enquanto que a RGI em HHBSF apresentou-se constituída por unidades de Gal*p*A metil e não metil-esterificadas, acetiladas nas posições O-2 e/ou O-3;

- Extratos orgânicos contendo metabólitos secundários de cascas de *H. heptaphyllus* mostraram efeito antitumoral dose-dependente em células Caco-2 e MCF-7; a fração clorofórmica HHE-C, majoritariamente constituída por triterpenoides, ácidos graxos hidroxilados de cadeia longa, ácido 4-metoxibenzoico, ácido 3,4-dimetoxibenzoico e lignanas, concentrou os compostos citotóxicos; o ácido 4-metoxibenzoico foi identificado como responsável pela ação citotóxica contra as células tumorais testadas.

9 REFERÊNCIAS

ANANTHI, S. et al. In vitro antioxidant and in vivo anti-inflammatory potential of crude polysaccharide from *Turbinaria ornata* (Marine Brown Alga). **Food and Chemical Toxicology**, v. 48, n. 1, p. 187–192, 2010.

ASPINALL, G. O. CARBOHYDRATE POLYMERS OF PLANT CELL WALLS. **Biogenesis of Plant Cell Wall Polysaccharides**, p. 95–115, 1 jan. 1973.

AVIGAD, G. Carbohydrate Metabolism: Storage Carbohydrates. **Plant Biochemistry**, p. 143–204, 1 jan. 1997.

BAGGIO, C. H. et al. In vivo/in vitro studies of the effects of the type II arabinogalactan isolated from *Maytenus ilicifolia* Mart. ex Reissek on the gastrointestinal tract of rats. **Zeitschrift fur Naturforschung - Section C Journal of Biosciences**, v. 67 C, n. 7–8, p. 405–410, 2012.

BALASSIANO, I. T. et al. Demonstration of the lapachol as a potential drug for reducing cancer metastasis. **Oncology Reports**, v. 13, n. 2, p. 329–333, 2005.

BARBIERI, S. F. et al. Extraction, purification and structural characterization of a galactoglucomannan from the gabiroba fruit (*Campomanesia xanthocarpa* Berg), Myrtaceae family. **Carbohydrate Polymers**, v. 174, p. 887–895, 15 out. 2017.

BASTOS, D. H. M. et al. Phenolic antioxidants identified by ESI-MS from yerba maté (*Ilex paraguariensis*) and green tea (*Camelia sinensis*) extracts. **Molecules**, v. 12, n. 3, p. 423–432, 2007.

BEG, M. S. et al. Using a novel NQO1 bioactivatable drug, beta-lapachone (ARQ761), to enhance chemotherapeutic effects by metabolic modulation in pancreatic cancer. **Journal of Surgical Oncology**, v. 116, n. 1, p. 83–88, 2017.

BEIRITH, A.; SANTOS, A. R. S.; CALIXTO, J. B. Mechanisms underlying the nociception and paw oedema caused by injection of glutamate into the mouse paw. **Brain Research**, v. 924, n. 2, p. 219–228, 2002.

BI, W. P.; MAN, H. Bin; MAN, M. Q. Efficacy and safety of herbal medicines in treating gastric ulcer: A review. **World Journal of Gastroenterology**, v. 20, n. 45, p. 17020–17028, 2014.

BOLDIZSÁR, I. et al. The role of harmonized, gas and liquid chromatography mass spectrometry in the discovery of the neolignan balanophonin in the fruit wall of *Cirsium vulgare*. **Journal of Chromatography A**, v. 1264, p. 143–147, 2012.

BORGES, J. C. M. et al. Mosquiticidal and repellent potential of formulations containing wood residue extracts of a Neotropical plant, *Tabebuia heptaphylla*. **Industrial Crops and Products**, v. 129, n. December 2018, p. 424–433, 2019.

BRADFORD, M. M. A rapid and sensitive method for the quantitation of microgram quantities of protein utilizing the principle of protein-dye binding. **Analytical**

Biochemistry, v. 72, n. 1–2, p. 248–254, 7 maio 1976.

BRADLEY, P. P. et al. Measurement of cutaneous inflammation: Estimation of neutrophil content with an enzyme marker. **Journal of Investigative Dermatology**, v. 78, n. 3, p. 206–209, 1982.

BRAGA DE OLIVEIRA, A. et al. Lignans and naphthoquinones from *Tabebuia incana*. **Phytochemistry**, v. 34, n. 5, p. 1409–1412, 1993.

BRAVO, L. Polyphenols: Chemistry, Dietary Sources, Metabolism, and Nutritional Significance. **Nutrition Reviews**, v. 56, n. 11, p. 317–333, 2009.

BUCHANAN, B.; GRUISSEM, W.; JONES, R. Biochemistry and Molecular Biology of Plants - Google Books. 2000.

BYEON, S. E. et al. In vitro and in vivo anti-inflammatory effects of taheebo, a water extract from the inner bark of *Tabebuia avellanedae*. **Journal of Ethnopharmacology**, v. 119, n. 1, p. 145–152, 2008.

CAFFALL, K. H.; MOHNEN, D. The structure, function, and biosynthesis of plant cell wall pectic polysaccharides. **Carbohydrate Research**, v. 344, n. 14, p. 1879–1900, 28 set. 2009.

CANTU-JUNGLES, T. M. et al. Extraction and characterization of pectins from primary cell walls of edible açaí (*Euterpe oleraceae*) berries, fruits of a monocotyledon palm. **Carbohydrate Polymers**, v. 158, p. 37–43, 2017.

CARBONERO, E. R. et al. Lentinus edodes heterogalactan: Antinociceptive and anti-inflammatory effects. **Food Chemistry**, v. 111, n. 3, p. 531–537, 2008.

CARLOTTO, J. et al. A polysaccharide fraction from “ipê-roxo” (*Handroanthus heptaphyllus*) leaves with gastroprotective activity. **Carbohydrate Polymers**, v. 226, p. 115239, 15 dez. 2019.

_____. Polysaccharides from *Arctium lappa* L.: Chemical structure and biological activity. **International Journal of Biological Macromolecules**, v. 91, p. 954–960, 2016.

CARPITA, N. C.; GIBEAUT, D. M. Structural models of primary cell walls in flowering plants: Consistency of molecular structure with the physical properties of the walls during growth. **Plant Journal**, v. 3, n. 1, p. 1–30, 1993.

CHAPLAN, S. R. et al. Quantitative assessment of tactile allodynia in the rat paw. **Journal of Neuroscience Methods**, v. 53, n. 1, p. 55–63, 1994.

CHATTERJEE, A. et al. Polysaccharide-rich fraction of Termitomyces eurhizus accelerate healing of indomethacin induced gastric ulcer in mice. **Glycoconjugate Journal**, v. 30, n. 8, p. 759–768, 2013.

CHEN, G. et al. Analysis of flavonoids in *Rhamnus davurica* and its antiproliferative

activities. **Molecules**, v. 21, n. 10, p. 1–14, 2016.

CIPRIANI, T. R. et al. A polysaccharide from a tea (infusion) of *Maytenus ilicifolia* leaves with anti-ulcer protective effects. **Journal of Natural Products**, v. 69, n. 7, p. 1018–1021, 2006.

_____. Acidic heteroxylans from medicinal plants and their anti-ulcer activity. **Carbohydrate Polymers**, v. 74, n. 2, p. 274–278, 2008.

_____. Gastroprotective effect of a type I arabinogalactan from soybean meal. **Food Chemistry**, v. 115, n. 2, p. 687–690, 15 jul. 2009.

CIUCANU, I.; KEREK, F. A simple and rapid method for the permethylation of carbohydrates. **Carbohydrate Research**, v. 131, n. 2, p. 209–217, 15 ago. 1984.

CORDEIRO, L. M. C. et al. Arabinan and arabinan-rich pectic polysaccharides from quinoa (*Chenopodium quinoa*) seeds: Structure and gastroprotective activity. **Food Chemistry**, v. 130, n. 4, p. 937–944, 2012.

CÓRDOVA, M. M. et al. Polysaccharide glucomannan isolated from *Heterodermia obscurata* attenuates acute and chronic pain in mice. **Carbohydrate Polymers**, v. 92, n. 2, p. 2058–2064, 15 fev. 2013.

CORRÊA-FERREIRA, M. L. et al. Gastroprotective effects and structural characterization of a pectic fraction isolated from *Artemisia campestris* subsp maritima. **International Journal of Biological Macromolecules**, v. 107, p. 2395–2403, 2018.

D'ARCHIVIO, M. et al. Polyphenols, dietary sources and bioavailability. **Annali dell'Istituto Superiore di Sanita**, v. 43, n. 4, p. 348–361, 2007.

DA SILVA LOPES, L. et al. Mechanisms of the antinociceptive action of (-) Epicatechin obtained from the hydroalcoholic fraction of *Combretum leprosum* Mart & Eic in rodents. **Journal of Biomedical Science**, v. 19, n. 1, p. 68, 2012.

DALLAZEN, J. L. et al. Pharmacological potential of alkylamides from *Acmella oleracea* flowers and synthetic isobutylalkyl amide to treat inflammatory pain. **Inflammopharmacology**, 2019.

DE ABREU, M. B. et al. Phenolic glycosides from *Tabebuia argentea* and *Catalpa bignonioides*. **Phytochemistry Letters**, v. 7, n. 1, p. 85–88, 2014.

DE MELO, J. G. et al. Medicinal plants used as antitumor agents in Brazil: An ethnobotanical approach. **Evidence-based Complementary and Alternative Medicine**, v. 2011, 2011.

DE OLIVEIRA, A. J. B. et al. Structure and antiviral activity of arabinogalactan with (1→6)-β-d-galactan core from *Stevia rebaudiana* leaves. **Carbohydrate Polymers**, v. 94, n. 1, p. 179–184, 2013.

DE YOUNG, L. M. et al. Edema and cell infiltration in the phorbol ester-treated mouse

ear are temporally separate and can be differentially modulated by pharmacologic agents. **Agents and Actions**, v. 26, n. 3–4, p. 335–341, 1989.

DIXON, W. J. Experimental Observations. **Annu. Rev. Pharmacol. Toxicol.**, v. 20, p. 441–462, 1980.

DO NASCIMENTO, G. E. et al. Structure of an arabinogalactan from the edible tropical fruit tamarillo (*Solanum betaceum*) and its antinociceptive activity. **Carbohydrate Polymers**, v. 116, p. 300–306, 2015.

DO NASCIMENTO, G. E.; IACOMINI, M.; CORDEIRO, L. M. C. New findings on green sweet pepper (*Capsicum annum*) pectins: Rhamnogalacturonan and type I and II arabinogalactans. **Carbohydrate Polymers**, v. 171, p. 292–299, 2017.

DONG, Q.; FANG, J. N. Structural elucidation of a new arabinogalactan from the leaves of *Nerium indicum*. **Carbohydrate Research**, v. 332, n. 1, p. 109–114, 2001.

DUAN, J. et al. Structural features of a pectic arabinogalactan with immunological activity from the leaves of *Diospyros kaki*. **Carbohydrate Research**, v. 338, n. 12, p. 1291–1297, 2003.

DUTRA, R. C. et al. Medicinal plants in Brazil: Pharmacological studies, drug discovery, challenges and perspectives. **Pharmacological Research**, v. 112, p. 4–29, 2016.

BRASIL. Ministério do Meio Ambiente**. Espécies nativas da flora brasileira de valor econômico atual ou potencial plantas para o futuro - Região Sul**. Brasília: 2011.

FILISETTI-COZZI, T. M. C. C.; CARPITA, N. C. Measurement of uronic acids without interference from neutral sugars. **Analytical Biochemistry**, v. 197, n. 1, p. 157–162, 15 ago. 1991.

FIORITO, S. et al. Growth inhibitory activity for cancer cell lines of lapachol and its natural and semi-synthetic derivatives. **Bioorganic and Medicinal Chemistry Letters**, v. 24, n. 2, p. 454–457, 2014.

FREITAS, A. E. et al. Antidepressant-like action of the bark ethanolic extract from *Tabebuia avellanedae* in the olfactory bulbectomized mice. **Journal of Ethnopharmacology**, v. 145, n. 3, p. 737–745, 2013.

FRIŠČIĆ, M.; BUCAR, F.; HAZLER PILEPIĆ, K. LC-PDA-ESI-MSnanalysis of phenolic and iridoid compounds from *Globularia* spp. **Journal of Mass Spectrometry**, v. 51, n. 12, p. 1211–1236, 2016.

GAN, L. et al. Immunomodulation and antitumor activity by a polysaccharide–protein complex from *Lycium barbarum*. **International Immunopharmacology**, v. 4, n. 4, p. 563–569, 1 abr. 2004.

GARCEZ, F. R. et al. Novos constituintes químicos das cascas do caule de *Tabebuia heptaphylla*. **Quimica Nova**, v. 30, n. 8, p. 1887–1891, 2007.

GE, L. et al. Nine phenylethanoid glycosides from *Magnolia officinalis* var. biloba fruits and their protective effects against free radical-induced oxidative damage. **Scientific Reports**, v. 7, n. November 2016, p. 2–13, 2017.

GERBER, D. E. et al. Phase 1 study of ARQ 761, a β-lapachone analogue that promotes NQO1-mediated programmed cancer cell necrosis. **British Journal of Cancer**, v. 119, n. 8, p. 928–936, 2018.

GEVRENOVA, R. et al. A new liquid chromatography-high resolution Orbitrap mass spectrometry-based strategy to characterize glucuronide oleanane-type triterpenoid carboxylic acid 3, 28-O-bidesmosides (GOTCAB) saponins.A case study of *Gypsophila glomerata* Pall ex M. B. (Caryoph. **Journal of Pharmaceutical and Biomedical Analysis**, v. 159, p. 567–581, 2018.

_____. In-depth characterization of the GOTCAB saponins in seven cultivated *Gypsophila* L. species (Caryophyllaceae) by liquid chromatography coupled with quadrupole-Orbitrap mass spectrometer. **Biochemical Systematics and Ecology**, v. 83, n. December 2018, p. 91–102, 2019.

GHALEHSHAHI, H. G.; MADSEN, R. Silver-Catalyzed Dehydrogenative Synthesis of Carboxylic Acids from Primary Alcohols. **Chemistry - A European Journal**, v. 23, n. 49, p. 11920–11926, 2017.

GOEL, R. K. et al. Effect of lapachol, a naphthaquinone isolated from *Tectona grandis*, on experimental peptic ulcer and gastric secretion. **Journal of Pharmacy and Pharmacology**, v. 39, n. 2, p. 138–140, 1987.

GORIN, P. A. J.; IACOMINI, M. Polysaccharides of the lichens *Cetraria islandica* and *Ramalina usnea*. **Carbohydrate Research**, v. 128, n. 1, p. 119–132, 15 maio 1984.

GRAZZIOTINV, J. D. et al. Phytochemical and analgesic investigation of *Tabebuia chrysotricha*. **Journal of Ethnopharmacology**, v. 36, n. 3, p. 249–251, 1992.

GUIRAUD, P. et al. Comparison of antibacterial and antifungal activities of lapachol and beta-lapachone. **Planta medica**, v. 60, n. 4, p. 373–374, 1994.

GUO, K. et al. Identification of minor lignans, alkaloids, and phenylpropanoid glycosides in *Magnolia officinalis* by HPLC–DAD–QTOF-MS/MS. **Journal of Pharmaceutical and Biomedical Analysis**, v. 170, p. 153–160, 2019.

GUO, Q. et al. Structural characterization of a low-molecular-weight heteropolysaccharide (glucomannan) isolated from *Artemisia sphaerocephala* Krasch. **Carbohydrate Research**, v. 350, p. 31–39, 2012.

Handroanthus in Flora do Brasil 2020 em construção. Jardim Botânico do Rio de Janeiro.Disponível em: <http://reflora.jbrj.gov.br/reflora/floradobrasil/FB114085>. Acesso em: 09 set. 2019.

HARRIS, P. J. Primary and secondary plant cell walls: A comparative overview. **New Zealand Journal of Forestry Science**, v. 36, n. 1, p. 36–53, 2006.

HU, X. et al. Hpyerglycemic and anti-diabetic nephritis activities of polysaccharides separated from *Auricularia auricular* in diet-streptozotocin-induced diabetic rats. **Experimental and Therapeutic Medicine**, v. 13, n. 1, p. 352–358, 2017.

HUNSKAAR, S.; HOLE, K. The formalin test in mice: dissociation between inflammatory and non-inflammatory pain. **Pain**, v. 30, n. 1, p. 103–114, 1987.

Instituto de Pesquisas e Estudos Florestais. Disponível em: <http://www.ipef.br/identificacao/tabebuia.heptaphylla.asp>. Acesso em: 05 set. 2019a.

Instituto de Pesquisas e Estudos Florestais. Disponível em: <http://www.ipef.br/identificacao/tabebuia.alba.asp>.Acesso em: 05 set. 2019b.

IQBAL, J. et al. Plant-derived anticancer agents: A green anticancer approach. **Asian Pacific Journal of Tropical Biomedicine**, v. 7, n. 12, p. 1129–1150, 2017.

IWAMOTO, K. et al. The anti-obesity effect of Taheebo (*Tabebuia avellanedae* Lorentz ex Griseb) extract in ovariectomized mice and the identification of a potential anti-obesity compound. **Biochemical and Biophysical Research Communications**, v. 478, n. 3, p. 1136–1140, 2016.

JIA, C. et al. Identification of glycoside compounds from tobacco by high performance liquid chromatography/electrospray ionization linear ion-trap tandem mass spectrometry coupled with electrospray ionization orbitrap mass spectrometry. **Journal of the Brazilian Chemical Society**, v. 28, n. 4, p. 629–640, 2017.

JOUINI, M. et al. Physico-chemical characterization and pharmacological activities of polysaccharides from *Opuntia microdasys* var. rufida cladodes. **International Journal of Biological Macromolecules**, v. 107, n. PartA, p. 1330–1338, 2018.

KE, M. et al. Extraction, purification of *Lycium barbarum* polysaccharides and bioactivity of purified fraction. **Carbohydrate Polymers**, v. 86, n. 1, p. 136–141, 1 ago. 2011.

KLOSTERHOFF, R. R. et al. Structure and intracellular antioxidant activity of pectic polysaccharide from acerola (*Malpighia emarginata*). **International Journal of Biological Macromolecules**, v. 106, p. 473–480, 2018.

KREHER, B. et al. New furanonaphthoquinones and other constituents of *Tabebuia avellanedae* and their immunomodulating activities *in vitro* . **Planta Medica**, v. 54, n. 06, p. 562–563, 1988.

LI, L. et al. Isolation and purification of phenylethanoid glycosides from *Cistanche deserticola* by high-speed counter-current chromatography. **Food Chemistry**, v. 108, n. 2, p. 702–710, 2008.

LI, Q. et al. Kaempferol protects ethanol-induced gastric ulcers in mice via pro-inflammatory cytokines and NO. **Acta Biochimica et Biophysica Sinica**, v. 50, n. 3, p. 246–253, 2018.

LI, R. et al. Extraction, characterization of *Astragalus* polysaccharides and its immune modulating activities in rats with gastric cancer. **Carbohydrate Polymers**, v. 78, n. 4, p. 738–742, 17 nov. 2009.

LI, Y. et al. Screening and identification of three typical phenylethanoid glycosides metabolites from *Cistanches Herba* by human intestinal bacteria using UPLC/Q-TOF-MS. **Journal of Pharmaceutical and Biomedical Analysis**, v. 118, p. 167–176, 2016.

LIU, C.-J.; LIN, J.-Y. Anti-inflammatory and anti-apoptotic effects of strawberry and mulberry fruit polysaccharides on lipopolysaccharide-stimulated macrophages through modulating pro-/anti-inflammatory cytokines secretion and Bcl-2/Bak protein ratio. **Food and Chemical Toxicology**, v. 50, n. 9, p. 3032–3039, 1 set. 2012.

LIU, J.; WILLFÖR, S.; XU, C. A review of bioactive plant polysaccharides: Biological activities, functionalization, and biomedical applications. **Bioactive Carbohydrates and Dietary Fibre**, v. 5, n. 1, p. 31–61, 2015.

MAEDA, J. A.; MATTHES, L. A. F. Conservação de sementes de ipê. **Bragantia**, v. 43, n. 1, p. 51–61, 1984.

MALANGE, K. F. et al. Tabebuia aurea decreases hyperalgesia and neuronal injury induced by snake venom. **Journal of Ethnopharmacology**, v. 233, p. 131–140, 2019.

MARIA-FERREIRA, D. et al. Rhamnogalacturonan from *Acmella oleracea* (L.) R.K. Jansen: Gastroprotective and ulcer healing properties in rats. **PLoS ONE**, v. 9, n. 1, 2014.

MELLINGER-SILVA, C. et al. Isolation of a gastroprotective arabinoxylan from sugarcane bagasse. **Bioresource Technology**, 2011.

MELO, L. E. S. **Estudo químico de resíduos madeireiros de *Tabebuia serratifolia* (Vahl) G. Nicholson, *Acacia mangium* Willd. e *Dipteryx polyphylla* Hube**r. Tese (Doutorado em Química). Universidade Federal do Amazonas, 2016.

MENG, X.; LIANG, H.; LUO, L. Antitumor polysaccharides from mushrooms: A review on the structural characteristics, antitumor mechanisms and immunomodulating activities. **Carbohydrate Research**, v. 424, p. 30–41, 2016.

MOHNEN, D. Pectin structure and biosynthesis. **Current Opinion in Plant Biology**, v. 11, n. 3, p. 266–277, 2008.

MOTEA, E. A. et al. NQO1-dependent, tumor-selective radiosensitization of non-small cell lung cancers. **Clinical Cancer Research**, v. 25, n. 8, p. 2601–2609, 2019.

MULEY, M. M.; KRUSTEV, E.; MCDOUGALL, J. J. Preclinical assessment of inflammatory pain. **CNS Neuroscience and Therapeutics**, v. 22, n. 2, p. 88–101, 2016.

MZOUGHI, Z. et al. Optimized extraction of pectin-like polysaccharide from *Suaeda fruticosa* leaves: Characterization, antioxidant, anti-inflammatory and analgesic

activities. **Carbohydrate Polymers**, v. 185, n. January, p. 127–137, 2018.

NAKANISHI, T. et al. Triterpenes and flavonol glucuronides from *Oenothera cheiranthifolia*. **Chemical and Pharmaceutical Bulletin**, v. 55, n. 2, p. 334–336, 2007.

NARA, K. et al. Isolation of galactoglucomannan from apple hemicellulosic polysaccharides with binding capacity to cellulose. **Journal of Applied Glycoscience**, v. 51, n. 4, p. 321–325, 2004.

NASCIMENTO, A. M. et al. Gastroprotective effect and chemical characterization of a polysaccharide fraction from leaves of *Croton cajucara*. **International Journal of Biological Macromolecules**, v. 95, p. 153–159, 2017.

_____. Gastroprotective effect and structure of a rhamnogalacturonan from *Acmella oleracea*. **Phytochemistry**, v. 85, p. 137–142, 2013.

NEHRA, A. K. et al. Proton Pump Inhibitors: Review of Emerging Concerns. **Mayo Clinic Proceedings**, v. 93, n. 2, p. 240–246, 2018.

NERGARD, C. S. et al. Medicinal use of *Cochlospermum tinctorium* in Mali: Anti-ulcer, radical scavenging- and immunomodulating activities of polymers in the aqueous extract of the roots. **Journal of Ethnopharmacology**, v. 96, n. 1–2, p. 255–269, 2005.

NEWMAN, D. J. The influence of brazilian biodiversity on searching for human use pharmaceuticals. **Journal of the Brazilian Chemical Society**, v. 28, n. 3, p. 402–414, 2017.

OVODOVA, R. G. et al. Chemical composition and anti-inflammatory activity of pectic polysaccharide isolated from celery stalks. **Food Chemistry**, v. 114, n. 2, p. 610–615, 2009.

PAN, L. H. et al. Preventive effect of a galactoglucomannan (GGM) from *Dendrobium huoshanense* on selenium-induced liver injury and fibrosis in rats. **Experimental and Toxicologic Pathology**, v. 64, n. 7–8, p. 899–904, 2012.

PANDA, S. P. et al. Stem extract of *Tabebuia chrysantha* induces apoptosis by targeting sEGFR in Ehrlich ascites carcinoma. **Journal of Ethnopharmacology**, v. 235, p. 219–226, 2019.

PARK, B. S. et al. Antioxidant activity and characterization of volatile constituents of taheebo (*Tabebuia impetiginosa* martius ex DC). **Journal of Agricultural and Food Chemistry**, v. 51, n. 1, p. 295–300, 2003.

PEREIRA, I. T. et al. Antiulcer effect of bark extract of *Tabebuia avellanedae*: Activation of cell proliferation in gastric mucosa during the healing process. **Phytotherapy Research**, v. 27, n. 7, p. 1067–1073, 2013.

PETTOLINO, F. A. et al. Determining the polysaccharide composition of plant cell walls. **Nature Protocols**, v. 7, n. 9, p. 1590–1607, 2012.

PINK, J. J.; WUERZBERGER-DAVIS, S.; et al. Activation of a cysteine protease in MCF-7 and T47D breast cancer cells during β-lapachone-mediated apoptosis. **Experimental Cell Research**, v. 255, n. 2, p. 144–155, 2000.

PINK, J. J.; PLANCHON, S. M.; et al. NAD(P)H:quinone oxidoreductase activity is the principal determinant of β-lapachone cytotoxicity. **Journal of Biological Chemistry**, v. 275, n. 8, p. 5416–5424, 2000.

PLANCHON, S. M. et al. β-Lapachone-induced apoptosis in human prostate cancer cells: Involvement of NQO1/xip3. **Experimental Cell Research**, v. 267, n. 1, p. 95–106, 2001.

POPOV, S. V. et al. Chemical composition and anti-inflammatory activity of a pectic polysaccharide isolated from sweet pepper using a simulated gastric medium. **Food Chemistry**, v. 124, n. 1, p. 309–315, 2011.

PRABHU, V.; SHIVANI, A. An overview of history, pathogenesis and treatment of perforated peptic ulcer disease with evaluation of prognostic scoring in adults. **Annals of Medical and Health Sciences Research**, v. 4, n. 1, p. 22, 2014.

QIN, Y.; YIN, C.; CHENG, Z. A new tetrahydrofuran lignan diglycoside from *Viola tianshanica* maxim. **Molecules**, v. 18, n. 11, p. 13636–13644, 2013.

QUEIROZ, M. L. S. et al. Comparative studies of the effects of *Tabebuia avellanedae* bark extract and β-lapachone on the hematopoietic response of tumour-bearing mice. **Journal of Ethnopharmacology**, v. 117, n. 2, p. 228–235, 2008.

RAO, K. V.; MCBRIDE, T. J.; OLESON, J. J. Recognition and evaluation of lapachol as an antitumor agent. **Cancer Research**, v. 28, n. 10, p. 1952–1954, 1968.

RÉDEI, D. et al. Bioactivity-guided investigation of the anti-inflammatory activity of *Hippophae rhamnoides* Fruits. **Planta Medica**, v. 84, n. 1, p. 26–33, 2018.

REID, J. S. G. Carbohydrate Metabolism: Structural Carbohydrates. **Plant Biochemistry**, p. 205–236, 1 jan. 1997.

RIDLEY, B. L.; NEILL, M. A. O.; MOHNEN, D. Pectins: structure, biosynthesis, and oligogalacturonide-related signaling. **Phytochemistry,** v. 57, p. 929–967, 2001.

ROBERTS-THOMSON, I. C. THE RISE AND FALL OF PEPTIC ULCERATION: A DISEASE OF CIVILIZATION ?. **Journal of Gastroenterology and Hepatology**, p. 1–6, 2018.

RODRIGUES, M. R. A. et al. Antinociceptive and anti-inflammatory potential of extract and isolated compounds from the leaves of *Salvia officinalis* in mice. **Journal of Ethnopharmacology**, v. 139, n. 2, p. 519–526, 2012.

ROSSATO, M. F. et al. Structural improvement of compounds with analgesic activity: AC-MPF4, a compound with mixed anti-inflammatory and antinociceptive activity via opioid receptor. **Pharmacology Biochemistry and Behavior**, v. 129, p. 72–78, 2015.

SASSAKI, G. L. et al. Rapid synthesis of partially *O*-methylated alditol acetate standards for GC-MS: Some relative activities of hydroxyl groups of methyl glycopyranosides on Purdie methylation. **Carbohydrate Research**, v. 340, n. 4, p. 731–739, 2005.

SCALLY, B. et al. Effects of gastroprotectant drugs for the prevention and treatment of peptic ulcer disease and its complications: meta-analysis of randomised trials. **Lancet Gastroenterol Hepatol**, v. tbd, n. 4, p. 231–241, 2018.

SCHMEDA-HIRSCHMANNA, G.; PAPASTERGIOUB, F. Naphthoquinone derivatives and lignans from the Paraguayan Crude Drug “Tayï Pyta” (*Tabebuia heptaphylla*, Bignoniaceae). **Zeitschrift fur Naturforschung - Section C Journal of Biosciences**, v. 58, n. 7–8, p. 495–501, 2003.

SCOPARO, C. T. et al. Chemical characterization of heteropolysaccharides from green and black teas (*Camellia sinensis*) and their anti-ulcer effect. **International Journal of Biological Macromolecules**, v. 86, p. 772–781, 1 maio 2016.

_____. Gastroprotective bio-guiding fractionation of hydro-alcoholic extracts from green- and black-teas (*Camellia sinensis*). **Food Research International**, v. 64, p. 577–586, 2014.

SEDLAK, J.; LINDSAY, R. H. Estimation of total, protein-bound, and nonprotein sulfhydryl groups in tissue with Ellman’s reagent. **Analytical Biochemistry**, v. 25, p. 192–205, 1968.

SERHAN, C. N.; CHIANG, N.; DALLI, J. New pro-resolving n-3 mediators bridge resolution of infectious inflammation to tissue regeneration. **Molecular Aspects of Medicine**, 2017.

SICHAEM, J. et al. Tabebuialdehydes A-C, cyclopentene dialdehyde derivatives from the roots of *Tabebuia rosea*. **Fitoterapia**, v. 83, n. 8, p. 1456–1459, 2012.

SIMAS-TOSIN, F. F. et al. Glucuronoarabinoxylan from coconut palm gum exudate: Chemical structure and gastroprotective effect. **Carbohydrate Polymers**, 2014.

SINGLETON, V. L.; ROSSI, J. A.; JR, J. Colorimetry of Total Phenolics With Phosphomolybdic-Phosphotungstic Acid Reagents. **American Journal of Enology and Viticulture**, v. 16, n. 3, p. 144–158, 1965.

SMIDERLE, F. R. et al. Anti-inflammatory and analgesic properties in a rodent model of a (1→3),(1→6)-linked β-glucan isolated from Pleurotus pulmonarius. **European Journal of Pharmacology**, 2008.

SOUSA, S. G. et al. Chemical structure and anti-inflammatory effect of polysaccharide extracted from *Morinda citrifolia* Linn (Noni). **Carbohydrate Polymers**, v. 197, n. 2819, p. 515–523, 2018.

SRIKANTA, B. M.; SIDDARAJU, M. N.; DHARMESH, S. M. A novel phenol-bound pectic polysaccharide from *Decalepis hamiltonii* with multi-step ulcer preventive

activity. **World Journal of Gastroenterology**, v. 13, n. 39, p. 5196–5207, 2007.

SRIKANTA, Belagihally M.; SATHISHA, U. V.; DHARMESH, S. M. Alterations of matrix metalloproteinases, gastric mucin and prostaglandin E2 levels by pectic polysaccharide of swallow root (*Decalepis hamiltonii*) during ulcer healing. **Biochimie**, v. 92, n. 2, p. 194–203, 2010.

SU, J. et al. Anti-tumor and anti-virus activity of polysaccharides extracted from *Sipunculus nudus* (SNP) on Hepg2.2.15. **International Journal of Biological Macromolecules**, v. 87, p. 597–602, 2016.

SUNASSEE, S. N. et al. Cytotoxicity of lapachol, β-lapachone and related synthetic 1,4-naphthoquinones against oesophageal cancer cells. **European Journal of Medicinal Chemistry**, v. 62, p. 98–110, 2013.

SUO, M. et al. Bioactive phenylpropanoid glycosides from *Tabebuia avellanedae*. **Molecules**, v. 18, n. 7, p. 7336–7345, 2013.

TAMIELLO, C. S. et al. Structural features of polysaccharides from edible jambo (*Syzygium jambos*) fruits and antitumor activity of extracted pectins. **International Journal of Biological Macromolecules**, v. 118, p. 1414–1421, 2018.

TANAKA, L. Y. A.; DE OLIVEIRA, A. J. B.; GONALVES, J. E.; et al. An arabinogalactan with anti-ulcer protective effects isolated from *Cereus peruvianus*. **Carbohydrate Polymers**, v. 82, n. 3, p. 714–721, 2010.

TAYLOR, R. L.; CONRAD, H. E. Stoichiometric Depolymerization of Polyuronides and Glycosaminoglycuronans to Monosaccharides following Reduction of Their Carbodiimide-Activated Carboxyl Groups. **Biochemistry**, v. 11, n. 8, p. 1383–1388, 1972.

THAMBIRA, S. R. et al. Yellow lupin (*Lupinus luteus* L.) polysaccharides: Antioxidant, immunomodulatory and prebiotic activities and their structural characterisation. **Food Chemistry**, v. 267, n. March 2017, p. 319–328, 2018.

THE INTERNATIONAL AGENCY FOR RESEARCH ON CANCER (IARC) REPORT, W. Latest global cancer data: Cancer burden rises to 18.1 million new cases and 9.6 million cancer deaths in 2018. **International Agency for Research on Cancer**, n. September, p. 13–15, 2018.

TIJANI, S. A.; OLALEYE, S. B.; FAROMBI, E. O. Anti-ulcerogenic effect of the methanol extract of *Chasmanthera dependens* (Hochst) stem on male Wistar rats. 2018.

TJØLSEN, A. et al. The formalin test: an evaluation of the method. **Pain**, v. 51, n. 1, p. 5–17, 1992.

TORTORA, L. et al. Oleanolic and ursolic acid in dammar and mastic resin: isomer discrimination by using ToF-SIMS and multivariate statistics. **Surface and Interface Analysis**, v. 48, n. 7, p. 398–403, 2016.

UEDA, S. et al. Production of anti-tumour-promoting furano-naphthoquinones in *Tabebuia avellanedae* cell cultures. **Phytochemistry**, v. 36, n. 2, p. 323–325, 1 maio 1994.

WANG, C. et al. Antitumor and Immunomodulatory Activities of *Ganoderma lucidum* Polysaccharides in Glioma-Bearing Rats. **Integrative Cancer Therapies**, n. 29, p. 153473541876253, 2018.

WANG, J. et al. Antidepressant-like effects of the active acidic polysaccharide portion of ginseng in mice. **Journal of Ethnopharmacology**, v. 132, n. 1, p. 65–69, 2010.

WANG, L. et al. Antitumor activities and immunomodulatory of rice bran polysaccharides and its sulfates in vitro. **International Journal of Biological Macromolecules**, v. 88, p. 424–432, 1 jul. 2016.

WARASHINA, T.; NAGATANI, Y.; NORO, T. Constituents from the bark of *Tabebuia impetiginosa*. **Phytochemistry**, v. 65, n. 13, p. 2003–2011, 2004.

_____. Further constituents from the bark of *Tabebuia impetiginosa*. **Phytochemistry**, v. 66, n. 5, p. 589–597, 1 mar. 2005.

WONGRAKPANICH, S. et al. A Comprehensive Review of Non-Steroidal Anti-Inflammatory Drug Use in The Elderly. **Aging and Disease**, v. 9, n. 1, p. 143, 2018.

WOO, H. J. et al. HepG2 Hepatoma Cell Line Through Induction of Bax and Activation of Caspase. **Journal of medicinal food**, v. 9, n. 2, p. 161–168, 2006.

WOZNIAK, K. et al. The Role of Glutamate Signaling in Pain Processes and its Regulation by GCP II Inhibition. **Current Medicinal Chemistry**, v. 19, n. 9, p. 1323–1334, 2012.

WU, M. et al. Chemical characterization and in vitro antitumor activity of a single-component polysaccharide from *Taxus chinensis* var. mairei. **Carbohydrate Polymers**, v. 133, p. 294–301, 2015.

XUE, Z. et al. Profiling and isomer recognition of phenylethanoid glycosides from *Magnolia officinalis* based on diagnostic/holistic fragment ions analysis coupled with chemometrics. **Journal of Chromatography A**, p. 460583, 2019.

XUE, Z.; LI, H.; YANG, B. Positional isomerization of phenylethanoid glycosides from *Magnolia officinalis*. **Natural Product Communications**, v. 11, n. 12, p. 1861–1863, 2016.

YAMASHITA, M. et al. Stereoselective synthesis and cytotoxicity of a cancer chemopreventive naphthoquinone from *Tabebuia avellanedae*. **Bioorganic and Medicinal Chemistry Letters**, v. 17, n. 23, p. 6417–6420, 2007.

_____. Synthesis and evaluation of bioactive naphthoquinones from the Brazilian medicinal plant, *Tabebuia avellanedae*. **Bioorganic and Medicinal Chemistry**, v. 17, n. 17, p. 6286–6291, 2009.

YANG, L. C. et al. Natural killer cell–mediated anticancer effects of an arabinogalactan derived from rice hull in CT26 colon cancer–bearing mice. **International Journal of Biological Macromolecules**, v. 124, p. 368–376, 2019.
YU, Y. et al. Biological activities and pharmaceutical applications of polysaccharide from natural resources: A review. **Carbohydrate Polymers**, v. 183, p. 91–101, 1 mar. 2018.

YVONNE, K. et al. Galactoglucomannan-rich hemicellulose extract from Norway spruce (*Picea abies*) exerts benefeffects on chronic prostatic inflammation and lower urinary tract symptoms in vivo. **International Journal of Biological Macromolecules**, v. 101, p. 222–229, 2017.

ZHANG, L. et al. Furanonaphthoquinones from *Tabebuia avellanedae* induce cell cycle arrest and apoptosis in the human non-small cell lung cancer cell line A549. **Phytochemistry Letters**, v. 11, p. 9–17, 2015.

ZHANG, L.; HASEGAWA, I.; OHTA, T. Anti-inflammatory cyclopentene derivatives from the inner bark of *Tabebuia avellanedae*. **Fitoterapia**, v. 109, p. 217–223, 2016.
ZHANG, Y. et al. Advances in lentinan: Isolation, structure, chain conformation and bioactivities. **Food Hydrocolloids**, v. 25, n. 2, p. 196–206, 2011.

ZHU, Y. Y. et al. New approaches to the structural modification of olean-type pentacylic triterpenes via microbial oxidation and glycosylation. **Tetrahedron**, v. 67, n. 23, p. 4206–4211, 2011.

ZHU, Z. Y. et al. Effects of extraction methods on the yield, chemical structure and anti-tumor activity of polysaccharides from *Cordyceps gunnii* mycelia. **Carbohydrate Polymers**, v. 140, p. 461–471, 2016.

ZOU, D. et al. Analysis of chemical constituents in Wuzi-Yanzong-Wan by UPLC-ESI-LTQ-Orbitrap-MS. **Molecules**, v. 20, n. 12, p. 21373–21404, 2015.